GEC 90

43rd Annual
Gaseous Electronics Conference
16-19 October, 1990
Champaign-Urbana, Illinois

Conference Abstracts

"Learning and Labor"

The Alma Mater
on the campus of the
University of Illinois
at Urbana-Champaign

PROGRAM AND ABSTRACTS

43rd Annual Gaseous Electronics Conference

GEC 90

16 –19 October 1990
Champaign–Urbana, IL

A Topical Conference of the American Physical Society
Division of Atomic, Molecular and Optical Physics

Hosted by:
Department of Electrical and Computer Engineering,
University of Illinois

ACKNOWLEDGEMENTS

The Gaseous Electronics Conference gratefully acknowledges the support of the Department of Electrical and Computer Engineering and its business office, the Center for Compound Semiconductor Microelectronics, Conference and Institutes Department and the Administration of the University of Illinois for assistance with the local arrangements. Financial support for the Gaseous Electronics Conference has been provided by:

The Air Force Office of Scientific Research

The Army Research Office

The National Science Foundation

The General Electric Company

GTE Incorporated

IBM-E. Fishkill

The Gaseous Electronics Conference is a Topical Conference of the American Physical Society with sponsorship by the Division of Atomic, Molecular and Optical Physics.

CONTENTS

TECHNICAL PROGRAM

FORTY THIRD ANNUAL
GASEOUS ELECTRONICS CONFERENCE

REGISTRATION AND RECEPTION
6:30 PM - 9:30 PM, Monday, October 15, 1990
Convention Center, Chancellor Hotel, Alumni Room

SESSION AA. DISCHARGE MODELING

8:00 AM - 9:40 AM, Tuesday, October 16, Illiniwek Room
Chair: T. Sommerer, University of Illinois

8:00 - 8:25	AA-1(L)	USING NEURAL NETWORKS TO OBTAIN CROSS SECTIONS FROM ELECTRON SWARM DATA W. L. Morgan
8:25 - 8:40	AA-2	SWARM PARAMETERS IN MERCURY VAPOR G. R. Govinda Raju and Jane Liu
8:40 - 8:55	AA-3	DRIFT VELOCITIES OF ELECTRON SWARMS DEFINED BY THE ARRIVAL TIME SPECTRA IN METHANE H. Date, S. Yachi, K. Kondo, and H. Tagashira
8:55 - 9:10	AA-4	MODELING OF ELECTRON ENERGY DISTRIBUTIONS IN LOW PRESSURE WALL STABILIZED DISCHARGES IN THE NONLOCAL LOCAL FIELD REGIME M. J. Hartig and M. J. Kushner
9:10 - 9:25	AA-5	COMPARISONS OF COMPUTATIONAL METHODS TO REPRESENT ELECTRON TRANSPORT IN NONEQUILIBRIUM PLASMA SWITCHES H. Pak and M. J. Kushner
9:25 - 9:40	AA-6	PSEUDO-SPARK DISCHARGES VIA COMPUTER SIMULATION J.-P. Boeuf and L. C. Pitchford

SESSION AB. NOVEL SOURCES: CLUSTERS AND EXCITED STATES

8:00 AM - 9:30 AM, Tuesday, October 16, Grange Room
Chair: J. H. Moore, University of Maryland

8:00 - 8:30	AB-1(IV)	PREPARATION AND IR SPECTROSCOPIC CHARACTERIZATION OF MOLECULAR CLUSTER BEAMS G. Scoles
8:30 - 9:00	AB-2(IV)	ELECTRON COLLISIONS WITH EXCITED ATOMS AND MOLECULES S. Trajmar and J. C. Nickel

9:00 - 9:15 AB-3 AN INVESTIGATION OF LASER INDUCED FLUORESCENCE ON THE H_α AND H_β TRANSITIONS IN A SMALL TOKAMAK AND ITS RELATION TO EXCITATION CROSS-SECTIONS FOR HYDROGEN
I. S. Falconer, N. Finn, J. M. Wilson, and W. Wright

9:15 - 9:30 AB-4 ELECTRON EXCITATION FROM HELIUM METASTABLE LEVELS INTO EXCITED SINGLET LEVELS
C. C. Lin, L. W. Anderson, R. B. Lockwood, and F. A. Sharpton

SESSION BA. MODELS OF RF AND MICROWAVE PLASMAS

10:05 AM - 11:50 AM, Tuesday, October 16, Illiniwek Room
Chair: S. Bobbio, Microelectronics Center of North Carolina

10:05 - 10:20 BA-1 A SELF-CONSISTENT KINETIC CALCULATION OF HELIUM RF DISCHARGE PROPERTIES
W. N. G. Hitchon, T. J. Sommerer, and J. E. Lawler

10:20 - 10:35 BA-2 SELF-CONSISTENT RF SHEATH PROPERTIES AND STOCHASTIC HEATING FOR ARBITRARY SHEATH VOLTAGE WAVEFORM
S. E. Savas

10:35 - 10:50 BA-3 A SELF-CONSISTENT BOLTZMANN EQUATION MODEL OF RF PLASMA DISCHARGES
M. E. Riley and P. J. Drallos

10:50 - 11:05 BA-4 MODELING OF RF PLASMA DISCHARGES IN ARGON
P. J. Drallos and M. E. Riley

11:05 - 11:20 BA-5 MODELING OF LOW-PRESSURE MICROWAVE DISCHARGES IN Ar, He, and O_2
C. M. Ferreira, L. L. Alves, M. Pinheiro and A. B. Sa

11:20 - 11:35 BA-6 NUMERICAL ANALYSIS OF RF AND DC GLOW DISCHARGES USING A CONTINUUM MODEL
S.-K. Park

11:35 - 11:50 BA-7 A WKB/SWKB APPROACH TO ELECTRON THERMALIZATION AND ATTACHMENT
B. Shizgal

SESSION BB. BASIC PROCESSES IN COLLISION PHYSICS

10:05 AM - 11:55 AM, Tuesday, October 16, Grange Room
Chair: M. Dillon, Argonne National Lab

10:05 - 10:35 BB-1(IV) CORRELATION EFFECTS ON COLLISIONS
R. S. Berry and S. Ceraulo

10:35 - 11:00 BB-2(L) ELECTRON-IMPACT DOUBLE-IONIZATION AS A PROBE OF ELECTRON CORRELATION
J. H. Moore, M. A. Coplan, J. W. Cooper, and J. P. Doering

11:00 - 11:30 BB-3(IV) SUBEXCITATION ELECTRONS, A TOPIC IN GASEOUS ELECTRONICS
M. Inokuti

11:30 - 11:55 BB-4(L) NEAR THRESHOLD RO-VIBRATIONAL EXCITATION OF H_2
S. J. Buckman, M. J. Brunger, and D. S. Newman

SESSION CA. HEAVY-PARTICLE COLLISIONS

1:30 PM - 3:30 PM, Tuesday, October 16, Illiniwek Room
Chair: R. J. Van Brunt, NIST

1:30 - 2:00 CA-1(IV) ION-NEUTRAL COLLISIONS: INTERNAL ENERGY TRANSFER
W. Lindinger

2:00 - 2:15 CA-2 EXOTHERMIC REACTIVE COLLISIONS OF N^+, N_2^+ and H_2O^+ WITH H_2O AND CO_2 AT SUPRATHERMAL ENERGIES
J. A. Gardner, R. A. Dressler, R. H. Salter, C. R. Lishawa, and E. Murad

2:15 - 2:45 CA-3(IV) DISSOCIATIVE RECOMBINATION IN COMPLEX SYSTEMS
E. Herbst

2:45 - 3:15 CA-4(IV) RESONANCES IN MOLECULAR PHOTODISSOCIATION
K. C. Kulander, C. J. Cerjan, J. L. Krause, and A. E. Orel

3:15 - 3:30 CA-5 THE EXCITATION OF $N_2(B)$ IN THE REACTION BETWEEN $N_2(A)$ AND $N_2(X,v)$
L. G. Piper

SESSION CB. PLASMA SURFACE INTERACTIONS

1:30 PM - 3:35 PM, Tuesday, October 16, Grange Room
Chair: H. H. Sawin, MIT

1:30 - 2:05 CB-1(IV) SURFACE PROCESSES IN PLASMA ETCHING ENVIRONMENTS
H. F. Winters

2:05 - 2:20 CB-2 QUANTIFICATION OF PLASMA-SURFACE INTERACTIONS IN FLUOROCARBON ETCHING OF Si AND SiO_2
H. H. Sawin and D. C. Gray

2:20 - 2:35 CB-3 REAL-TIME MONITORING OF III-V MULTI-LAYER STRUCTURES DURING PLASMA ETCHING AND PASSIVATION
R. A. Gottscho, K. P. Giapis, and M. F. Vernon

2:35 - 2:50 CB-4 ION BOMBARDMENT ANGLE AND ENERGY IN ARGON RF DISCHARGES
Joanne Liu, G. L. Huppert, and H. H. Sawin

2:50 - 3:05 CB-5 DIAMOND FILM DEPOSITION BY PLASMAS GENERATED IN A MICROWAVE CAVITY RESONATOR
W. L. Hsu, E. A. Fuchs, and K. F. McCarty

3:05 - 3:20 CB-6 ENERGY TRANSFER FROM NOBLE GAS IONS TO SURFACES: COLLISIONS WITH CARBON, SILICON, COPPER, SILVER, AND GOLD IN THE RANGE 100-4000 eV
H. F. Winters, H. Coufal, H. L. Bay, and W. Eckstein

3:20 - 3:35 CB-7 INTERACTION OF SPUTTERED ATOMS WITH THE FILLING GAS IN MAGNETRON SPUTTERING DISCHARGES
I. S. Falconer, G. M. Turner, B. W. James and D. R. McKenzie

SESSION D. POSTERS
3:30 PM - 5:30 PM, Tuesday, October 16, Brundage and Zuppke Rooms
(Authors should post their material before the start of the session, preferably by 1:30 PM)

LASERS

D-1 A TIME-DEPENDENT TWO-ELECTRON-GROUP MODEL FOR A PULSED HELIUM/METAL-VAPOUR GLOW DISCHARGE
R. J. Carman

D-2 CHARACTERIZATION OF MICROWAVE STIMULATED LASER EMISSION IN XENON GAS MIXTURES
G. A. Hebner

D-3 EFFECTS OF LOCALIZED HEATING ON THE OPTICAL STABILITY IN AN E-BEAM PUMPED ATOMIC XENON LASER
E. L. Patterson, M. J. Hurst, and D. Wick

ELECTRON AND HEAVY PARTICLE COLLISIONS

D-4 $NH(^3\Sigma^-,v=1\text{-}3)$ FORMATION AND COLLISIONAL RELAXATION IN ELECTRON-IRRADIATED $Ar/N_2/H_2$ MIXTURES
J. A. Dodd, S. J. Lipson, D. J. Flanagan, W. A. M. Blumberg, B. D. Green, and J. C. Person

D-5 ENERGY TRANSFER IN FAST OXYGEN ATOM COLLISIONS
B. L. Upschulte, G. E. Caledonia, B. D. Green, and R. H. Krech

D-6 A RF ION SOURCE FOR THE PRODUCTION OF He^+ BEAMS
R. B. Lockwood, J. B. Boffard, M. Lagus, L. W. Anderson, and C. C. Lin

D-7 ELECTRON-ATOM COLLISIONS IN A LASER FIELD
P. H. G. Smith and M. R. Flannery

D-8 ANGULAR MOMENTUM CHANGES IN COLLISIONAL IONIZATION
A. Haffad and M. R. Flannery

RF GLOWS

D-23 SELF-CONSISTENT KINETIC CALCULATIONS OF LOW PRESSURE RF DISCHARGES IN Ar
R. P. Harvey, T. J. Sommerer and W. N. G. Hitchon

D-24 NUMERICAL ANALYSIS OF THE ELECTRICAL AND OPTICAL CHARACTERISTICS OF AN AC PLASMA DISPLAY PANEL CELL
A. Rabehi, J. P. Boeuf, and L. C. Pitchford

D-25 AN IMPROVED SPIRAL LOOP ANTENNA FOR INDUCTIVELY COUPLED PLASMA SOURCES
J. Menard and T. Intrator

D-26 EFFECT OF HOLE GEOMETRY ON A HOLLOW CATHODE PLUME
S. J. Mahajan and V. J. Gandhi

D-27 LIF, PIE, AND ACTINOMETRIC AXIAL PROFILES OF CF IN A SYMMETRIC PARALLEL-PLATE RF DISCHARGE IN CF_4 PLUS 5% Ar
W. T. Conner and H. H. Sawin

D-28 LANGMUIR PROBE MEASUREMENTS IN A 13.56 MHz RF DISCHARGE
J. V. Scanlan and M. B. Hopkins

D-29 SPATIALLY RESOLVED ION VELOCITY DISTRIBUTIONS IN A DIVERGING FIELD ELECTRON CYCLOTRON RESONANCE REACTOR
D. J. Trevor, T. Nakano, N. Sadeghi, J. Derouard, R. A. Gottscho, and P. D. Foo

D-30 APERTURE EFFECT OF CHARGED PARTICLES IN A MAGNETIZED PLASMA
E. Y. Wang, W. Q. Li, S. W. Lam, and N. Hershkowitz

D-31 THE VOLUME AVERAGED NATURE OF MICROWAVE INTERFEROMETRIC MEASUREMENTS
L. J. Overzet, J. C. Miller, T. J. Morel, and B. E. Cherrington

D-32 LASER-INDUCED FLUORESCENCE DOPPLER WIDTH DETERMINATION OF ION TEMPERATURE IN AN ELECTRON CYCLOTRON RESONANCE PLASMA
E. A. Den Hartog, H. Persing, and R. C. Woods

D-33 GAS KINETIC TEMPERATURE MEASUREMENTS IN A CH_4-H_2 DISCHARGES
H. N. Chu, E. A. Den Hartog, J. Jacobs, A. Salzberg, K. Bell, J. E. Lawler, and L. W. Anderson

D-34 SPATIALLY AND TEMPORALLY DEPENDENT EEDF MEASUREMENTS IN AN RF DISCHARGE
C. A. Anderson and W. G. Graham

D-35 OBSERVATION OF THE RADIAL MOTION OF THE SHEATH IN RF GLOW DISCHARGES
J. Derouard, M. P. Alberta and N. Sadeghi

D-36 A SELF-CONSISTENT SIMULATION OF RF GLOW PLASMA
K. Kitamori, A. Date, and H. Tagashira

SESSION E. POSTERS

7:00 PM - 9:00 PM, Tuesday, October 16, Brundage and Zuppke Rooms
(Authors should post the material at least one hour before the start of the session)

LAMPS AND RELATED PHENOMENA

E-1 TIME EVOLUTION OF THE CATHODE SPOT PLASMA IN METAL VAPOUR VACUUM ARCS
I. S. Falconer, A. J. Studer, P. D. Swift, B. W. James, D. R. McKenzie, I. G. Brown, and X. Godechet

E-2 DEPENDENCE OF ELECTRON ENERGY DISTRIBUTION ON THE Ar PRESSURE IN POSITIVE COLUMN OF LOW DIAMETER Hg-Ar LAMP DISCHARGES
G. Zissis, M. Yousfi, A. Alkaa, and J. J. Damelincourt

E-3 ENERGY BALANCE IN LOW PRESSURE Hg-Ar ELECTRIC DISCHARGE POSITIVE COLUMN
G. Zissis, P. Benetruy, and J. J. Damelincourt

E-4 OBSERVATIONS OF LOW PRESSURE DC BREAKDOWNS IN WEAK MAGNETIC FIELDS
S. Popovic, E. Kunhardt, and M. Margulies

E-5 ANALYSIS OF THE STREAMER TO ARC TRANSITION
S. K. Dhali and A. Rajabooshanam

ATOMIC PROPERTIES

E-6 DETECTION OF ATOMIC OXYGEN BY RESONANT THREE PHOTON IONIZATION AND TWO PHOTON LASER INDUCED FLUORESCENCE
G. Sultan, G. Baravian, and J. Jolly

E-7 ATOMIC DATA FOR TITANIUM
R. E. H. Clark and J. Abdallah, Jr.

E-8 AN ATOMIC ENERGY LEVEL SHIFT IN OXYGEN BY A LONG RANGE ION-ATOM INTERACTION
N. Kwon, M. Bohomolec, M. J. Colgan, and D. E. Murnick

LASER PRODUCED PLASMAS

E-9 NITROGEN ATOMS IN Ar-N_2 FLOWING MICROWAVE DISCHARGES FOR STEEL SURFACE NITRIDING
A. Ricard, J. Deschamps, J. L. Godard, L. Falk, and H. Michel

E-10 INVESTIGATIONS OF EFFICIENT PHOTOIONIZATION METHODS FOR CREATING HIGHLY COLLISIONAL PLASMAS
K. R. Stalder, D. J. Eckstrom and R. J. Vidmar

E-11 EMISSION STUDIES OF YBaCuO LASER INDUCED PLUMES
H. F. Sakeek, W. G. Graham, M. Higgins, T. Morrow, and D. G. Walmsley

E-12 UV AND VUV FLUORESCENCE OF HIGH PRESSURE ARGON EXCITED BY FLASH X-RAY SOURCE
J. M. Pouvesle, C. Cachoncinlle, F. Davanloo, J. J. Coogan, C. B. Collins, and F. Spiegelmann

E-13 PLASMA CREATED BY TEA CO_2 LASER BEAM ON A Ti TARGET WITH He AS BUFFER GAS
C. Boulmer-Leborgne, J. Hermann, and B. Dubreuil

E-14 BOUND-BOUND AND FREE-FREE RADIATION FROM RECOMBINING OXYGEN PLASMAS
L. S. Dzelzkalns, W. A. M. Blumberg, P. C. F. Ip, and R. A. Armstrong

DC AND HIGH PRESSURE

E-15 ARCING AND DISCHARGE FROM HIGH VOLTAGE SPACE POWER SYSTEMS
G. B. Hillard

E-16 A SPIN-DEPENDENT, OPTOGALVANIC EFFECT IN ^4He
L. D. Schearer and P. Tin

E-17 DC GLOW DISCHARGE MODELING APPLIED TO DIAMOND FILM GROWTH PLASMA REACTORS
M. Surendra, D. B. Graves, and L. S. Plano

E-18 LASER STARK SPECTROSCOPIC MEASUREMENTS OF PROBE PERTURBATIONS IN A DC DISCHARGE
T. Intrator, M. P. Alberta, H. Debontride, J. Derouard, and N. Sadeghi

E-19 ELECTRIC FIELD MEASUREMENT IN THE CATHODE SHEATH OF A GLOW DISCHARGE IN HYDROGEN
C. Barbeau and J. Jolly

E-20 A NEW EMISSION SPECTROSCOPIC SET-UP FOR NON-LTE PLASMA STUDIES
K. Etemadi and S. Akbar

E-21 IN-SITU GAS CONVERSION OF TRIMETHYLARSINE INTO HOMOLOGS USING A DOWNSTREAM NEAR AFTERGLOW PLASMA
B. G. Pihlstrom, T. Sheng, Z. Yu, and G. J. Collins

E-22 DIAMOND SYNTHESIS IN A 50 kW INDUCTIVELY COUPLED ATMOSPHERIC PRESSURE PLASMA TORCH
T. G. Owano, C. H. Kruger, and M. A. Cappelli

E-23 INFLUENCE OF THE ENERGY SPECTRUM OF ELECTRONS EJECTED FROM THE CATHODE ON ELECTRON BEHAVIOUR IN THE CATHODE SHEATH OF GLOW DISCHARGES IN HELIUM AND IN ARGON
R. J. Carman

E-24 INSTANTANEOUS ETCH RATE MEASUREMENT OF THIN TRANSPARENT FILMS BY INTERFEROMETRY FOR USE IN AN ALGORITHM TO CONTROL PLASMA ETCHER
H. L. Mishurda and N. Hershkowitz

GEC REFERENCE CELL

(An open discussion of these posters and any Post-Deadline papers will start at 8:00 PM in the Illiniwek Room - Session F)

E-25 COMPARISON OF ELECTRICAL CHARACTERISTICS OF GEC RF REFERENCE CELL
H. M. Anderson, P. Bletzinger, M. L. Brake, J. W. Butterbaugh, M. Dalvie, M. E. Elta, A. Garscadden, J. B. Gerardo, R. A. Gottscho, D. B. Graves, K. E. Greenberg, P. J. Hargis, Jr., R. Horwath, M. J. Kushner, J. L. Mock, P. A. Miller, J. K. Olthoff, M. L. Passow, J. R. Roberts, H. H. Sawin, G. Selwyn, M. Splichal, T. R. Turner, R. J. Van Brunt, J. T. Verdeyen, and J. R. Whetstone

E-26 NIST GEC REFERENCE CELL MEASUREMENTS
J. R. Roberts, J. K. Olthoff, R. J. Van Brunt, and J. R. Whetstone

Post-Deadline papers on GEC Reference Cell

SESSION F. GEC REFERENCE CELL - WORKSHOP

8:00 PM - 9:00 PM, Tuesday, October 16, Illiniwek Room
Chair: R. Gottscho, Bell Labs

F-1 SUMMARY OF MEASUREMENTS ON THE GEC REFERENCE CELL BY VARIOUS GROUPS
A. Garscadden

F-2 UPDATE ON HARDWARE AND MODIFICATIONS
P. Hargis

F-3 RF NIGHTMARES - PITFALLS AND SOLUTIONS
P. Miller

F-4 MODELERS' NEEDS: PHYSICS AND CELL DATA
D. GRAVES

An open discussion is encouraged on the above topics and any other relevant issues, but the key to a workshop success lies in the contributions from the floor. Spirited and free flowing interjections from the floor are encouraged, as are contributed insights and suggestions. Topics that should be raised include: What constitutes enough calibration? Is the harmonic content of the current meaningful and is it important for model evaluation? Is it important for process control? What are some ideas for future direction?

SESSION GA. PLASMA CHEMISTRY

8:00 AM - 9:55 AM, Wednesday, October 17, Illiniwek Room
Chair: J. Goree, University of Iowa

8:00 - 8:25 GA-1(L) RF DISCHARGE DEPOSITION OF SiO_2 IN N_2O-SiH_4 MIXTURES
L. E. Kline, W. D. Partlow, R. M. Young, R. R. Mitchell, and T. V. Congedo

8:25 - 8:40 GA-2 DIAGNOSTICS AND MODELING OF REACTIVE RF GLOW DISCHARGES IN SiH_4
T. Makabe, F. Tochikubo, and S. Kakuta

8:40 - 8:55	GA-3	MODELING AND OPTICAL DIAGNOSTICS OF REACTIVE RF GLOW DISCHARGES IN CH_4 AT 13.56 MHz T. Makabe, N. Nakano, A. Suzuki, F. Tochikubo,and Y. Yamaguchi
8:55 - 9:10	GA-4	SIMULATION OF REMOTE AND DIRECT PLASMA CVD OF SILICON ALLOYS M. J. Kushner, T. J. Sommerer, and Y. Weng
9:10 - 9:25	GA-5	IN-SITU GENERATION OF ARSINE BY USING ELEMENTAL ARSENIC SOURCE T. Sheng, Z. Yu, and G. J. Collins
9:25 - 9:40	GA-6	TRANSLATIONALLY HOT NEUTRALS IN CF_4 DISCHARGES FOR PLASMA PROCESSING T. J. Sommerer and M. J. Kushner
9:40 - 9:55	GA-7	PARTICLE GENERATION IN BORON TRICHLORIDE/METHANE/HYDROGEN RF DISCHARGES H. M. Anderson and J. L. Mock

SESSION GB. MODELING AND DIAGNOSTICS OF LAMP-LIKE DISCHARGES

8:00 AM - 10:00 AM, Wednesday, October 17, Grange Room
Chair: P. Vicharelli, GTE

8:00 - 8:25	GB-1(IV)	GENERATION AND DIAGNOSTICS OF SURFACE WAVE (SW) PLASMAS M. Moisan
8:25 - 8:50	GB-2(IV)	SURFACE WAVE DISCHARGES AS FLUORESCENT LAMPS D. Levy
8:50 - 9:05	GB-3	OPTICAL RADIATION EFFICIENCY OF SURFACE WAVE PRODUCED PLASMAS AS COMPARED TO DC POSITIVE COLUMNS J. Margot-Chaker, M. Moisan, and A. Ricard
9:05 - 9:30	GB-4(L)	AMBIPOLAR DIFFUSION THEORY OF THE HOT CATHODE NEGATIVE GLOW J. Ingold
9:30 - 9:45	GB-5	QUANTITATIVE SPECTROSCOPY ON Hg^+ J. E. Lawler, R. C. Wamsley, J. H. Ingold, L. Bigio, and V. D. Roberts
9:45 - 10:00	GB-6	SPATIAL MAPS OF Hg^+ AND Hg^* DENSITIES IN THE CATHODE REGION R. C. Wamsley, J. E. Lawler, J. H. Ingold, L. Bigio, and V. D. Roberts

WELCOME

10:20 AM - 10:30 AM, Wednesday, October 17
Illiniwek and Grange Rooms

William R. Schowalter
Dean, College of Engineering
University of Illinois

SESSION H. ALLIS PRIZE LECTURE

10:30 AM - 11:30 AM, Wednesday, October 17, Illiniwek and Grange Rooms
Chair: J. Gerardo, Sandia Laboratories

10:30 - 11:30 H-1 THE DIFFUSION OF CHARGED PARTICLES IN COLLISIONAL PLASMAS: FREE TO AMBIPOLAR DIFFUSION AND LOW TO HIGH PRESSURES
A. V. Phelps

SESSION J. BUSINESS MEETING

11:30 AM - 12:00 Noon, Wednesday, October 17, Illiniwek and Grange Rooms

SESSION K POSTERS

1:30 PM - 3:30 PM, Wednesday, October 17, Brundage and Zuppke Rooms
(Authors should post the material at least one hour before the start of the session)

GLOWS

K-1 AN IMPROVED STRING MODEL FOR PROFILE EVOLUTION WITH REDEPOSITION
T. J. Dalton, S. C. Jackson, and H. H. Sawin

K-2 VOLTAGE AND CURRENT CHARACTERIZATION FOR MEASURING RF POWER DELIVERED TO A PROCESS CHAMBER
J. F. Rupert, Keith J. Brankner, and L. J. Overzet

K-3 IMAGING OF THE DENSITY DISTRIBUTION OF VIBRATIONALLY EXCITED OXYGEN VIA LASER INDUCED PREDISSOCIATIVE FLUORESCENCE
L. M. Hitchcock, G. Kim, G. P. Reck, and E. W. Rothe

K-4 TWO ELECTRONS GROUP MODEL OF A RF GLOW DISCHARGE IN ARGON. COMPARISON WITH EXPERIMENTAL RESULTS
J. Derouard, H. Debontride, N. Sadeghi, P. Belenguer, and J. P. Boeuf

K-5 SIMULATION OF AN ECR MICROWAVE PLASMA ETCHING REACTOR
M. Hussein and G. A. Emmert

K-6 COMPARISON OF FLUID AND PARTICLE SIMULATIONS OF RF GLOW DISCHARGES
T. E. Nitschke, M. Surendra, and D. B. Graves

K-7 MAGNETRON PLASMA TRANSPORT SIMULATIONS
J. Goree, M. J. Goeckner, and T. E. Sheridan

K-8 DOSE UNIFORMITY OF PLASMA SOURCE ION IMPLANTATION APPLIED TO A WEDGE SHAPED TARGET
M. Shamim, J. T. Scheuer, and J. R. Conrad

K-9 MEASUREMENT OF BIMAXWELLIAN ELECTRON DISTRIBUTIONS IN RF DIFFUSION PLASMAS OPERATED NEAR ECR
R. W. Boswell and C. Cui

K-10 INVESTIGATION OF SEGMENTED HOLLOW CATHODE DISCHARGES
D. Bruno, H. Kirkici, and B. R. Cheo

K-11 PARTICULATES IN LOW PRESSURE DISCHARGES
G. M. Jellum, J. E. Daugherty, M. D. Kilgore, and D. B. Graves

K-12 SIMULATION OF ION MASS MEASUREMENT WITH FOURIER TRANSFORM MASS SPECTROMETRY IN A BOUNDED 1-D PLASMA
J. B. Friedmann, A. T. Johnson, and J. L. Shohet

K-13 NEGATIVE ION MEASUREMENTS FROM MODULATED RF DISCHARGES
L. J. Overzet and L. Luo

K-14 INVESTIGATION OF OXYGEN DISCHARGES BY CARS
C. Boisse-Laporte, G. Gousset, A. Granier, M. Lefebvre, J. Marec, M. Pealat, R. Safari, M. Touzeau, and M. Vialle

K-15 ENERGY ANALYSIS OF THE DIFFUSION PLASMA FROM AN INDUCTIVELY EXCITED DISCHARGE
P. Bletzinger

K-16 TRANSITION TO THE COLLISIONAL PLASMA SHEATH
T. E. Sheridan and J. Goree

K-17 STABLE OPERATING CONDITIONS FOR CATHODE-FALL DOMINATED DISCHARGES IN H_2, N_2, and Ar
Z. Lj. Petrovic and A. V. Phelps

ELECTRON COLLISIONS

K-18 SMALL-ANGLE ELECTRON-SODIUM ABSOLUTE DIFFERENTIAL CROSS SECTIONS, 3-20 eV
C. H. Ying, F. Perales, L. Vuskovic, and B. Bederson

K-19 CRITICAL EVALUATION OF ELECTRON CROSS SECTIONS FOR MOLECULES OF INTEREST IN PLASMA PROCESSING
W. L. Morgan

K-20 METASTABLE PRODUCTION FOLLOWING ELECTRON IMPACT DISSOCIATION OF O_2
L. LeClair, J. J. Corr, and J. W. McConkey

K-21 HIGH-RESOLUTION V.U.V. POLARIZATION STUDIES OF RARE GAS RESONANCE RADIATION FOLLOWING ELECTRON-IMPACT EXCITATION
C. Noren and J. W. McConkey

LAMP PHENOMENA

K-36 MEASUREMENT OF THE POWER DENSITY DISTRIBUTION WITHIN AN OPERATING SURFACE WAVE DISCHARGE LAMP
A. T. Rowley

K-37 SURFACE WAVES IN HIGHLY COLLISIONAL PLASMAS
G. G. Lister and T. Robinson

SESSION LA. ALTERNATIVE CONFIGURATIONS FOR PLASMA PROCESSING

3:30 PM - 5:35 PM, Wednesday, October 17, Illiniwek Room
Chair: A. Garscadden, Wright-Patterson Air Force Base

3:30 - 3:55	LA-1(IV)	RF DIFFUSION PLASMA ETCHING SYSTEMS R. W. Boswell and A. J. Perry
3:55 - 4:20	LA-2(IV)	MULTIPOLAR CONFINED REACTOR CONFIGURATIONS T. D. Mantei
4:20 - 4:45	LA-3(IV)	MAGNETRON ETCH REACTOR CONFIGURATIONS S. Bobbio
4:45 - 5:10	LA-4(IV)	STUDIES OF VOLUME AND SURFACE REACTIONS IN LOW PRESSURE REACTORS BY MODULATED EXCITATION J. Derouard, J. P. Booth, A. Bouchoule, P. Ranson, and N. Sadeghi
5:10 - 5:35	LA-5(IV)	ELECTRON CYCLOTRON RESONANCE SOURCES FOR PLASMA PROCESSING R. C. Myer

SESSION LB. LAMPS AND HIGH PRESSURE DISCHARGES

3:30 PM - 5:15 PM, Wednesday, October 17
Grange Room
Chair: J. Dakin, GE Lighting

3:30 - 3:45	LB-1	NEAR-RESONANCE ELECTRONIC RAMAN SCATTERING MEASUREMENTS OF $Hg(6^3P_1)$ IN A LOW-PRESSURE Hg-Ar DISCHARGE L. Bigio
3:45 - 4:00	LB-2	OPTICALLY-THICK DIAGNOSTICS OF ARC LAMPS USING A RETROREFLECTIVE ARRAY S. Couris, T. Fohl, and P. A. Vicharelli
4:00 - 4:15	LB-3	THE DETECTION OF GROUND STATE SCANDIUM IONS IN A HIGH PRESSURE METAL HALIDE DISCHARGE BY SATURATED LASER INDUCED FLUORESCENCE J. Kramer

4:15 - 4:30	LB-4	DIELECTRIC-BARRIER DISCHARGES AS A SOURCE OF NARROW-BAND VUV, UV OR VISIBLE EXCIMER RADIATION B. Gellert, B. Eliasson, and U. Kogelschatz
4:30 - 4:45	LB-5	ELECTRONIC QUENCHING EFFECTS OF ATOM-MOLECULE INTERACTIONS IN A NON-EQUILIBRIUM PLASMA AT ATMOSPHERIC PRESSURE M. Gordon and C. H. Kruger
4:45 - 5:00	LB-6	BREAKDOWN OF A WIRE-TO-PLANE DISCHARGE M. A. Jog, I. M. Cohen, and P. S. Ayyaswamy
5:00 - 5:15	LB-7	COMPARISON OF THE AWA LUMPED-CIRCUIT MODEL OF ELECTRICAL DISCHARGES WITH EMPIRICAL DATA W. B. Maier II, A. Kadish, and R. T. Robiscoe

SOCIAL HOUR AND BANQUET, WEDNESDAY, OCTOBER 17

Social Hour: Alumni Room 6:30 PM - 7:30 PM
Banquet: Midwest Ball Room 7:30 PM

SESSION NA. HIGH DENSITY PLASMA PROCESSING

8:00 AM - 9:45 AM, Thursday, October 18, Illiniwek Room
Chair: M. S. Barnes, IBM - East Fishkill

8:00 - 8:35	NA-1(IV)	HIGH ETCH RATE MODES IN MICROWAVE PLASMA ETCHING OF SILICON IN HIGH MAGNETIC FIELDS Y. Horiike and H. Shindo
8:35 - 8:50	NA-2	INVESTIGATION OF LIMITERS IN ECR PLASMAS FOR APPLICATIONS IN PLASMA PROCESSING B. G. Lane, D. L. Smatlak, G. Gibson, H. H. Sawin, L. Bourget, and R. S. Post
8:50 - 9:05	NA-3	MODELING REMOTE PLASMA SOURCES FOR MATERIALS PROCESSING USING A HYBRID MONTE CARLO-FLUID SIMULATION Y. Weng and M. J. Kushner
9:05 - 9:20	NA-4	LAMINAR PLASMA PRODUCTION WITH ECR R. Itatani and A. Hatta
9:20 - 9:45	NA-5(IV)	LOW PRESSURE HIGH DENSITY INDUCTIVE PLASMA FOR PLASMA PROCESSING-THEORY AND EXPERIMENT J. H. Keller, M. S. Barnes, and J. C. Forster

SESSION NB. ELECTRON EXCITATION AND DISSOCIATION

8:00 AM - 9:40 AM, Thursday, October 18, Grange Room
Chair: B. Bederson, New York University

8:00 - 8:30	NB-1(IV)	THEORY OF ELECTRON-MOLECULE COLLISIONS B. I. Schneider

8:30 - 8:45 NB-2 RANGE OF VALIDITY OF SECOND ORDER PERTURBATION SERIES FOR ELECTRON-HYDROGEN COLLISIONS
D. H. Madison

8:45 - 9:00 NB-3 ELECTRON-H_2O COLLISIONS IN AN EXACT EXCHANGE PLUS PARAMETER-FREE POLARIZATION MODEL
A. Jain, D. G. Thompson, and F. A. Gianturco

9:00 - 9:25 NB-4(L) CROSS SECTIONS FOR THE ELECTRON-IMPACT DOMINATED PROCESSES IN ETCHING PLASMAS
K. Becker

9:25 - 9:40 NB-5 MEASUREMENTS OF ELECTRON-IMPACT CROSS SECTION FOR DISSOCIATION FROM CH_4 INTO CH_3 AND CH_2
H. Sugai, T. Nakano, and H. Toyoda

SESSION PA. HIGH DENSITY PLASMA PROCESSING AND DIAGNOSTICS

10:05 AM - 12:00 Noon, Thursday, October 18, Illiniwek Room
Chair: J. Keller, IBM-E. Fishkill

10:05 - 10:40 PA-1(IV) LOW PRESSURE ETCHING USING HELICAL RESONATOR DISCHARGES
D. E. Ibbotson

10:40 - 11:05 PA-2(L) RF OR MICROWAVE PLASMA REACTORS? FACTORS DETERMINING THE OPTIMUM FREQUENCY OF OPERATION
M. Moisan, C. Barbeau, R. Claude, C. M. Ferreira, J. Margot-Chaker, J. Paraszczak, A. B. Sa, G. Sauve, and M. R. Wertheimer

11:05 - 11:20 PA-3 EXPERIMENT AND MODELING OF HELICON RF DIFFUSION PLASMAS
C. Charles, R. W. Boswell, P. Ranson, C. Laure, and A. Bouchoule

11:20 - 11:45 PA-4(L) EEDF EVOLUTION IN A LOW PRESSURE CAPACITIVE ARGON RF DISCHARGES AT 13.56 MHz
V. A. Godyak, R. B. Piejak, and B. M. Alexandrovich

11:45 - 12:00 PA-5 LANGMUIR PROBE STUDIES OF He, O_2 AND Cl_2 IN A 13.56 MHz PLASMA REACTOR
K. F. Al-Assadi and N. M. D. Brown

SESSION PB. ELECTRON IMPACT AND HEAVY PARTICLE COLLISIONS

10:10 AM - 11:50 AM, Thursday, October 18
Grange Room
Chair: S. Chung, University of Wisconsin

10:10 - 10:35 PB-1(L) METAL ATOM DIFFERENTIAL CROSS SECTIONS
L. Vuskovic

10:35 - 10:50 PB-2 ELECTRON-POLARIZED PHOTON COINCIDENCE STUDY OF THE HEAVY NOBLE GASES
K. Martus, S. Zheng and K. Becker

10:50 - 11:05 PB-3 RATES FOR THE VIBRATIONAL EXCITATION OF O_3, CO_2, AND N_2O BY ELECTRON IMPACT
K. Holtzclaw, B. L. Upschulte, B. D. Green, W. A. M. Blumberg, and S. J. Lipson

11:05 - 11:20 PB-4 ELECTRON ENERGY DISTRIBUTION FUNCTIONS AND KINETICS OF EXCITED ELECTRONIC STATES IN NITROGEN AFTERGLOW
R. Nagpal and P. K. Ghosh

11:20 - 11:35 PB-5 CALCULATIONS OF FINE-STRUCTURE CHANGING COLLISIONS OF EXCITED Xe
A. P. Hickman, D. L. Huestis, and R. P. Saxon

11:35 - 11:50 PB-6 STATE-TO-STATE QUENCHING OF XENON 6p LEVELS BY RARE GASES
W. J. Alford

SESSION QA. PLASMA DIAGNOSTICS

1:30 PM - 3:30 PM, Thursday, October 18, Illiniwek Room
Chair: B. G. Lane, MIT

1:30 - 1:45 QA-1 COMPUTER-CONTROLLED LANGMUIR PROBE AND OPTICAL EMISSION SPECTROMETER FOR A DC DISCHARGE
I. D. Sudit and R. C. Woods

1:45 - 2:00 QA-2 DIAGNOSTICS AND MODELING OF RADICAL DENSITY PROFILES IN A METHANE RF DISCHARGE
H. Sugai, H. Toyoda, and Y. Hikosaka

2:00 - 2:15 QA-3 PHOTODETACHMENT MEASUREMENT OF D^- DENSITY IN A HOT CATHODE TRIODE DISCHARGE
B. N. Ganguly and A. Garscadden

2:15 - 2:30 QA-4 DETERMINATION OF NEGATIVE ION DENSITIES IN A CF_4 RF PLASMA
F. J. De Hoog, J. L. Jauberteau, G. J. Meeusen, M. Haverlag, G. M. W. Kroesen

2:30 - 2:45 QA-5 CALIBRATED SPATIAL AND TEMPORAL PROFILES OF H-ATOMS IN HYDROGEN DISCHARGES
B. L. Preppernau, T. M. Cerny, J. R. Dunlop, A. D. Tserepi, and T. A. Miller

2:45 - 3:00 QA-6 TIME DEPENDENT PROCESSES IN AN ARGON RF GLOW DISCHARGE
M. Colgan, N. Kwon, Y. Li, and D. E. Murnick

3:00 - 3:15 QA-7 LINESHAPE MEASUREMENTS IN PROCESSING GAS DISCHARGES
J. R. Dunlop, T. M. Cerny, B. L. Preppernau, A. D. Tserepi, and T. A. Miller

3:15 - 3:30 QA-8 EXPERIMENTAL STUDIES OF PLASMA DYNAMICS AND EMISSIONS IN DENSE PINCH PLASMA
M. Yokoyama, Y. Kitagawa, and Y. Yamada

SESSION QB. ATOMIC Xe AND OTHER LASERS

1:30 PM - 3:15 PM, Thursday, October 18, Grange Room
Chair: J. Crane, Lawrence Livermore Laboratory

1:30 - 1:45 QB-1 GAIN MEASUREMENTS IN FISSION-FRAGMENT EXCITED XENON GAS MIXTURES
G. A. Hebner and G. N. Hays

1:45 - 2:00 QB-2 GAIN AT 2.03 μm IN THE FISSION FRAGMENT EXCITED Xe LASER: MODEL COMPARISONS WITH EXPERIMENTS
J. W. Shon and M. J. Kushner, G. A. Hebner, and G. N. Hays

2:00 - 2:15 QB-3 LONG PULSE, 100 μs FLAT TOP, ELECTRON BEAM PUMPED, Ar/Xe LASER
T. T. Perkins, X. Chen, S. M. Freshman, and J. H. Jacob

2:15 - 2:30 QB-4 VIBRATIONAL AUTOIONIZATION IN Ne_2^* NEAR THE ADIABATIC IONIZATION THRESHOLD
S. B. Kim, D. J. Kane, and J. G. Eden

2:30 - 2:45 QB-5 ROTATIONALLY RESOLVED EXCITATION SPECTROSCOPY OF $nf(^3\Sigma_g^+, ^3\Pi_g)$ AND $np^1\Pi_g$ OF Ne_2
S. B. Kim, D. J. Kane, and J. G. Eden

2:45 - 3:00 QB-6 OBSERVATION AND SIMULATION OF BOUND→FREE EMISSION FROM Zn_2 AND Cd_2 EXCIMERS
G. Rodriguez and J. G. Eden

3:00 - 3:15 QB-7 SPECTROSCOPY AND KINETICS OF PHOTODISSOCIATED PbI_2
G. Rodriguez and J. G. Eden

SESSION R. POSTERS

3:30 PM - 5:30 PM, Thursday, October 18, Brundage and Zuppke Rooms
(Authors should posted their material 1 hour before the start of the session)

DISCHARGES

R-1 ION-SURFACE INTERACTIONS IN REACTIVE ION ETCHING
R. Mouncey, W. G. Graham, and A. McKinley

R-2 POWER DEPOSITION IN PARALLEL PLATE DISCHARGES
J. P. Verboncoeur, V. Vahedi, and C. K. Birdsall

R-3 STANDING WAVE DISCHARGE (SWD) IN A MIXTURE OF HELIUM-NEON GAS AND AT 433 MHz FREQUENCY
Z. Rakem and P. LePrince

R-4 CHAOS IN ELECTRICAL DISCHARGES IN GASES
D. F. Hudson

R-5 HYBRID FLUID-PARTICLE MODEL OF TRANSIENT HOLLOW CATHODE DISCHARGES
L. C. Pitchford and J.-P. Boeuf

R-6 CHARACTERISATION OF A PULSED MULTICUSP ION SOURCE
A. A. Mullan, W. G. Graham, and M. B. Hopkins

R-7 CYLINDRICAL MAGNETRON EMPLOYING A NON-HOMOGENEOUS PERIODIC MAGNETIC FIELD FOR DEPOSITING HERMETIC COATINGS ON FLUORIDE GLASS FIBERS
Z. Yu, G. J. Collins, B. Haribson, and I. Aggarwal

R-8 GENERATION OF ELECTRON BEAMS BY A HELICON ANTENNA
R. W. Boswell and P. Zhu

R-9 HELICAL RESONATOR PLASMA SOURCE
M. A. Lieberman, A. J. Lichtenberg, D. L. Flamm, and K. Niazi

R-10 MEASUREMENT OF THE DENSITY AND TRANSLATIONAL TEMPERATURE OF Si($3p^2\ ^1D_2$) ATOMS IN RF SILANE PLASMA USING UV LASER ABSORPTION SPECTROSCOPY
T. Goto, M. Sakakibara, and M. Hiramatsu

TRANSPORT CALCULATIONS

R-11 RF DISCHARGE MODELING
R. T. McGrath

R-12 EXAMINATION OF TEMPORAL RELAXATIONS OF TRANSPORT PARAMETERS AND RATE COEFFICIENTS
P. Hui and E. Kunhardt

R-13 ELECTRON MACROKINETICS
E. E. Kunhardt

R-14 MODELING OF MAGNETIC MULTICUSP HYDROGEN PLASMAS FOR NEGATIVE ION PRODUCTION: AN IMPROVEMENT
C. Gorse, R. Celiberto, M. Caccicatore, M. Bacal, and M. Capitelli

R-15 INFLUENCE OF ELECTRON-ELECTRON COLLISIONS ON ELECTRON DISTRIBUTION FUNCTIONS IN N_2 DISCHARGES FROM MONTE CARLO METHOD
M. Yousfi, A. Alkaa, O. Lamrous, and A. Himoudi

PLASMA CHEMISTRY

TRANSPORT OF ELECTRONS AND IONS

ETCHING DISCHARGES

R-29 LIF CHARACTERIZATION OF A De MULTIDIPOLE DISCHARGE
M. J. Goeckner, J. Goree, and T. E. Sheridan

R-30 PLASMA CHARACTERIZATION OF A DOWNSTREAM MICROWAVE SOURCE
D. L. Smatlak and C. C. Pao

R-31 THICKNESS OF THE ION SHEATH AROUND A CYLINDRICAL ELECTRODE IMMERSED IN A PLASMA
M. Nachman and J. Montreuil

R-32 ION KINETICS IN LOW PRESSURE RF MODULATED SHEATHS
M. S. Barnes, J. C. Forster, and J. H. Keller

SESSION S. CROSS SECTION WORKSHOP

7:00 PM - 9:00 PM, Thursday, October 18, Illiniwek and Grange Rooms
Chair: K. H. Becker, CCNY

7:00 - 7:10 S-1 MCHF ATOMIC STRUCTURE CALCULATIONS
C. F. Fischer

7:10 - 7:20 S-2 ELECTRON EXCITATION OF EXCITED TARGET ATOMS
C. C. Lin

7:20 - 7:30 S-3 STUDIES OF ELECTRON-MOLECULE COLLISIONS ON HIGHLY PARALLEL COMPUTERS
C. Winstead, Q. Sun, P. G. Hipes, V. McKoy, and M. A. P. Lima

7:30 - 7:40 S-4 ELECTRON-IMPACT DISSOCIATION OF MOLECULES
P. C. Cosby

7:40 - 7:50 S-5 FUTURE OPPORTUNITIES FOR RESEARCH
R. A. Phaneuf

7:50 - 9:00 OPEN DISCUSSION

SESSION TA. SHEATHS, GLOWS AND CHEMISTRY

8:00 AM - 9:40 AM, Friday, October 19, Illiniwek Room
Chair: K. Greenberg, Sandia National Laboratory

8:00 - 8:25 TA-1(L) THE BOHM CRITERION AND SHEATH FORMATION
K.-U. Riemann

8:25 - 8:40 TA-2 STUDIES OF TEMPERATURE PROFILES OF N_2 IN A LOW-PRESSURE, DC GLOW DISCHARGE USING HIGH RESOLUTION CARS
P. P. Yaney, J. Cirillo, and M. Millard

8:40 - 8:55 TA-3 EXCITATION OF BALMER ALPHA IN H_2 - Ar MIXTURES AT LOW VOLTAGES AND HIGH E/n
B. M. Jelenkovic, Z. Lj. Petrovic, and A. V. Phelps

8:55 - 9:10 TA-4 ENERGY BALANCE OF COLD NEGATIVE GLOW ELECTRONS
J. E. Lawler, T. J. Sommerer, and W. N. G. Hitchon

9:10 - 9:25 TA-5 REMOVAL OF SULFUR DIOXIDE FROM GAS STREAMS USING DIELECTRIC BARRIER DISCHARGE
M. B. Chang, J. Balbach, M. J. Kushner, and M. J. Rood

9:25 - 9:40 TA-6 PROCESSING FLUE GASES TO REMOVE SO_2 AND NO_x USING 60Hz PLASMA EXCITATION AND PHOTOLYSIS
J. H. Balbach, M. B. Chang, M. J. Rood, and M. J. Kushner

SESSION TB. NOVEL TECHNIQUES IN COLLISION PHYSICS

8:00 AM - 9:40 AM, Friday, October 19, Grange Room
Chair: T. W. Shyn, University of Michigan

8:00 - 8:30 TB-1(IV) ATOMIC OXYGEN AND NITROGEN SOURCES
J. P. Doering

8:30 - 8:55 TB-2(L) FAST OXYGEN ATOM STUDIES
G. E. Caledonia, B. L. Upschulte, R. H. Krech, and K. W. Holtzclaw

8:55 - 9:10 TB-3 LASER INDUCED FLUORESCENCE DETECTION OF GROUND-STATE MOLECULAR FRAGMENTS FOLLOWING ELECTRON-IMPACT DISSOCIATION OF COOLED TARGETS
M. Darrach and J. W. McConkey

9:10 - 9:40 TB-4(IV) THE USE OF ELECTRON CYCLOTRON RESONANCE ION SOURCES FOR MULTICHARGED ION COLLISION STUDIES
F. W. Meyer

SESSION VA. LASERS AND PHOTOPHYSICS

10:00 AM - 12:00 Noon, Friday, October 19, Illiniwek Room
Chair: G. Hebner, Sandia National Laboratory

10:00 - 10:15 VA-1 VACUUM ULTRAVIOLET TIME-RESOLVED LASER-INDUCED FLUORESCENCE FOR RADIATIVE LIFETIME MEASUREMENTS
T. R. O'Brian and J. E. Lawler

10:15 - 10:30 VA-2 MEASUREMENT OF COLLISIONAL BROADENING OF THE INTERCOMBINATION RESONANT TRANSITIONS IN Sr AND Ca
J. Crane, R. Presta, J. Christensen, J. Cooke, and M. Shaw

10:30 - 10:45 VA-3 OPTICAL GAIN IN Hg AT 5461Å VIA RECOMBINATION PUMPING
R. L. Rhoades and J. T. Verdeyen

10:45 - 11:00 VA-4 THE EFFECT OF CF_4 IMPURITIES ON OPERATION OF THE ELECTRON-BEAM EXCITED KrF LASER
R. Hui, H. Hwang, K. James, and M. J. Kushner

11:00 - 11:15 VA-5 PHOTOASSOCIATION OF KRYPTON-FLUORINE COLLISION PAIRS
R. B. Jones, J. S. Schloss, and J. G. Eden

11:15 - 11:30 VA-6 KINETICS AND SPECTROSCOPY OF $ArKr^+$ and Kr_2^+
R. B. Jones and J. G. Eden

11:30 - 11:45 VA-7 UV $XeBr(^2\Sigma \rightarrow {}^2\Sigma)$ PULSED FLASHLAMP AND BREAKDOWN VOLTAGE CHARACTERISTICS OF Xe/Br_2 MIXTURES
P. B. Keating, G. Black, and L. A. Schlie

11:45 - 12:00 VA-8 TRANSVERSE EXCITATION OF LARGE VOLUME HYDROGEN AZIDE (HN_3) GAS MIXTURES
M. W. Wright, L. A. Schlie, and E. A. Dunkle

SESSION VB. SIMULATIONS

10:00 AM - 12:00 PM, Friday, October 19, Grange Room
Chair: J. Scheuer, University of Wisconsin

10:00 - 10:30 VB-1(IV) PARTICLE-IN-CELL COMBINED WITH MONTE CARLO COLLISIONS–IN LIVING COLOR
C. K. Birdsall

10:30 - 10:45 VB-2 PARTICLE SIMULATIONS OF RF GLOW DISCHARGES: ELECTRON POWER DEPOSITION AND ELECTRON ENERGY DISTRIBUTION FUNCTIONS
M. Surendra and D. B. Graves

10:45 - 11:00 VB-3 PIC MODELLING OF ELECTROPOSITIVE AND ELECTRONEGATIVE RIE SYSTEMS WITH VARYING AREA RATIOS
R. W. Boswell, D. S. Vender, and H. B. Smith

11:00 - 11:15 VB-4 MODELING AND SIMULATION OF MAGNETICALLY CONFINED, LOW PRESSURE PLASMAS IN TWO DIMENSIONS
R. K. Porteous and D. B. Graves

11:15 - 11:30 VB-5 STABILITY OF PARTICULATE-CONTAMINATED LOW PRESSURE ELECTRIC DISCHARGES
M. J. McCaughey and M. J. Kushner

11:30 - 11:45 VB-6 SIMULATION OF NANOCRYSTAL PARTICLE GENERATION IN SPUTTER DEPOSITION DISCHARGES
S. J. Choi, R. S. Averback, and M. J. Kushner

11:45 - 12:00 VB-7 THE INFLUENCE OF NON-LINEAR VOLUMETRIC PROCESSES ON THE DIFFUSION OF CHARGED PARTICLES IN AN ELECTRONEGATIVE DISCHARGE
D. E. Bell and W. F. Bailey

SESSION AA

8:00 AM - 9:40 AM, Tuesday, October 16

Convention Center, Chancellor Hotel - Illiniwek Room

DISCHARGE MODELING

Chair: T. Sommerer, University of Illinois

AA-1 Using Neural Networks to Obtain Cross Sections from Electron Swarm Data. W.L. MORGAN, Kinema Research, 18720 Autumn Way, Monument, CO 80132—Although still more a curiosity than an accepted technique in computational modeling, the very new field of neural computing is beginning to find applications in physics. I will present some background on neural computing and will discuss the use of neural networks to obtain electron impact cross sections from measured drift velocities, characteristic energies, and other swarm data. This is what is known as an "inverse problem", which is a class of problems for which neural networks may be frequently superior to other numerical algorithms. Cross section results for a model problem and for Xe obtained using a neural network will be presented. In order to illustrate what may be possible, results for He, Ar, and CH_4 obtained using a different optimization algorithm will be discussed. I will discuss possible further development of these algorithms and potential applications to other areas of interest in gaseous electronics.

Research supported by the Wright Research and Development Center, Wright–Patterson AFB, OH.

AA-2 Swarm Parameters In Mercury Vapour, * G.R. GOVINDA RAJU and JANE LIU, U. of Windsor - Swarm parameters i.e., electron drift velocity, characteristic and mean energy and Townsend's first ionization coefficients in mercury vapour are calculated using a Monte Carlo Simulation technique and a rigorous solution of the Boltzmann Equation. The range of E/N covered is 20-1400 Td. Four excitation cross sections $^3P_0$, $^3P_2$, $^3P_1$, $^1P_1$ are evaluated to obtain good agreement between the experimental and theoretical values of swarm parameters by the mean collision time approach of the Monte Carlo Simulation technique. Using the same collision cross sections the Boltzmann Equation has been solved numerically and the swarm parameters are calculated. If the Holstein form of solution is used the agreement with experimental results of mean energy and drift velocity is within 12% over a limited range of $240 < E/N < 540$ Td. To obtain good agreement with measured ionization efficients also over the entire range a rigorous solution is required adopting which very good agreement between the two methods are obtained. Data on excitation and total collision frequency are also presented.

AA-3 Drift velocities of electron swarms defined by the arrival time spectra in methane, H.DATE, S.YACHI, K.KONDO and H.TAGASHIRA, Hokkaido Univ., Mitsubishi Ele.Corp., Anan Tech. Col. and Hokkaido Univ. - Drift velocities defined by the arrival time spectra of electron swarms in methane have been calculated by a new method[1] of Boltzmann equation analysis using the time derivative expansion of the distribution function. With focusing on the mean arrival time drift velocity W_m which is directly estimated from the experiment for the arrival time spectra and by the present method, the calculation was made for the E/p_0 values from 1 to 300 $Vcm^{-1}Torr^{-1}$. In the high E/p_0 above 50 $Vcm^{-1}Torr^{-1}$, the results show the differences of the values of the drift velocities defined by various principles[1] because of the considerable ionization in a swarm. The difference of the values between W_m and the center of mass drift velocity W_r at E/p_0=300 $Vcm^{-1}Torr^{-1}$ amounts to about 30 %.

1 K.Kondo and H.Tagashira, to appear in J.Phys.D(1990)

AA-4 Modeling of Electron Energy Distributions in Low Pressure Wall Stabilized Discharges in the Nonlocal Local Field Regime.* Michael J. Hartig and Mark J. Kushner, University of Illinois, 607 E. Healey, Champaign, IL 61820. In glow discharges having radius-pressure products of r•p < 1 Torr-cm, electron mean free paths are commensurate with the radius of the discharge tube. Arc-like discharges may have gas densities which are depleted on the axis and therefore have an E/N which is a function of radius. Because of the "mixing" of electron populations at different radial points due to their long diffusion lengths, the Local Field Approximation cannot be used to obtain the electron energy distribution (EED) as a function of radius using E/N(r). In this respect we have developed a computer model that solves Boltzmann's equation for the spatially dependent EED, while taking into account mixing of radial components of the EED by drift and diffusion. At small r•p, the EED is nearly uniform as a function of radius due to the high rate of mixing of high energy electrons and the insulating nature of the sheaths. The EED may, in fact, be cut off at the sheath potential. This model is coupled to a plasma-hydro simulation for heavy particle kinetics and results will be presented for He/Hg discharges.

*Work supported by Sandia National Laboratory and the National Science Foundation (ECS88-15781 and CBT88-03170).

AA-5 Comparisons of Computational Methods to Represent Electron Transport in Nonequilibrium Plasma Switches.* Hoyoung Pak and Mark J. Kushner, University of Illinois, 607 E. Healey, Champaign, IL 61820. Low pressure optically triggered pseudosparks, or Back-Lit-Thyratrons (BLT) are inherently multidimensional transient devices. The method which should be used to model electron transport in such devices is therefore problemmatic. In this respect, we have developed a versatile model for these switches with which to compare different modeling approaches. In our 2-dimensional time dependent model, fluid equations are solved to obtain the electron and ion densities, and Poisson's equation is solved for the electric potential. These equations can be solved using the local field approximation, employing conservation equations for the bulk electron energy and momentum, or adding multiple beam components to the electron distribution. Combinations of these methods can also be employed. We will discuss the parameter space (gas pressure, voltage, electrode gaps) in which each of these methods can be reliably used. Due to the induction time required to achieve quasi-equilibrium conditions, employing the energy equation and beam components slow the response of the switch compared to the LFA approach.

*Work supported by the Office of Naval Research and the National Science Foundation (ECS88-15781 and CBT88-03170).

AA-6 Pseudo-spark discharges via Computer Simulation: J.-P. BOEUF and L.C. PITCHFORD, CNRS, Centre de Physique Atomique, Toulouse, FRANCE - Pseudo-spark discharges are transient hollow cathode discharges on the left hand side of the Paschen curve which are characterized by an extremely rapid transition, often accompanied by a high-brightness electron beam, to a relatively long-lived, high-current-density, diffuse discharge. We have developed a model of the initiation of pseudo-spark discharges based on a 2-D hybrid fluid - Monte Carlo approach. Based on these numerical results, a picture has emerged which helps in clarifying the basic mechanisms of the pseudo-spark discharges. A necessary condition is the existence of a large and localized source of ionization due to the hollow cathode effect which develops as a result of plasma formation in the main anode-cathode gap. The space and time dependent electric field and electron and ion densities calculated from our model will be presented for typical pseudo-spark conditions, and we will discuss the phases leading to the onset of this discharge mode.

SESSION AB

8:00 AM - 9:30 AM, Tuesday, October 16

Convention Center, Chancellor Hotel - Grange Room

NOVEL SOURCES: CLUSTERS AND EXCITED STATES

Chair: J. H. Moore, University of Maryland

AB-1 Preparation and IR Spectroscopic Characterization of Molecular Cluster Beams, G. SCOLES*, Chemistry Department, Princeton University–Methods will be described for the formation and (IR spectroscopic) characterization of molecular clusters. For small clusters (up to tetramers and pentamers) the detailed structure can be obtained via the resolution of their rovibrational spectrum. These clusters are presently delivering useful information on nonadditivity in molecular interactions and are being used in several laboratories as starting material in reactions in which the mutual orientation of the reactants is known. For larger clusters ($n = 10^{2\pm1}$) other "structural" and "dynamical" questions can be addressed such as the location of chromophores in inert gas clusters, their mobility, their use as temperature probes, the sticking probability in molecule-cluster collisions and the probability of dimer formation of two chromophores coexisting in a cluster.

*Work supported by the NSF via grant CHE-87-09572.

AB-2 Electron Collisions with Excited Atoms and Molecules,* S. TRAJMAR and J. C. NICKEL, Jet Propulsion Laboratory, California Institute of Technology and University of California, Riverside.–Experimental methods for producing excited species suitable for electron collision studies and techniques for cross section measurements will be described. A brief summary of available cross section data will also be given. General principles related to cross section measurements for excited species and some details on works in our laboratory concerning laser-excited atoms and metastable rare gases will be presented.

* Work supported by Los Alamos National Laboratory (DOE), The National Science Foundation and the National Aeronautics and Space Administration.

AB-3 An investigation of laser induced fluorescence on the Hα and Hβ transitions in a small tokamak and its relation to excitation cross-sections for hydrogen I.S. FALCONER, N. FINN, J.M. WILSON and W. WRIGHT, School of Physics, U. of Sydney, Australia. - When the Hα transition is pumped with a powerful dye laser beam enhanced emission is observed not only on the Hα transition, but also on the Hβ transition due to electron excitation to its upper level. from the upper level for the Hα transition. The ratio of the laser induced fluorescence signal on these transitions has been measured, and also calculated using a collisional-radiative model. The model shows that the ratio is only weakly dependent on electron temperature for 10 eV < Te < 1 000 eV, and electron density for densities > 10^{19} m^{-3}. The experimental results lie considerably below the calculated values over a wide range of plasma parameters. This suggests that the cross-sections used in the collisional-radiative model may be significantly in error.

AB-4 Electron Excitation from Helium Metastable Levels into Excited Singlet Levels. CHUN C. LIN, L. W. ANDERSON, R. B. LOCKWOOD, and FRANCIS A. SHARPTON, U. of Wisconsin--We have measured electron excitation cross sections of He to several singlet levels from both the 2^1S and 2^3S metastable levels. A hollow cathode discharge is used to form a He atomic beam containing about 10^{-4}-10^{-5} 2^3S metastables for each ground-level He atom. The ratio of 2^1S-level atoms to 2^3S-level atoms in this beam is measured to be 0.06. The metastables are excited to the various n^1L levels by an electron beam with energy below 20 eV so that excitation of the ground-level atoms is not possible. From the observed energy dependence of the absolute intensity of the $n^1L \rightarrow 2^1L'$ emission we determine the cross sections for exciting n^1L from each of the metastable species. The peak cross sections for the 2^3S-to-3^1D and 2^1S-to-3^1D excitations are about 4×10^{-16} and 2×10^{-15} cm^2 respectively. To measure cross sections above 20 eV, a different method for producing metastables will be discussed.

SESSION BA

10:05 AM - 11:50 AM, Tuesday, October 16

Convention Center, Chancellor Hotel - Illiniwek Room

MODELS OF RF AND MICROWAVE PLASMAS

Chair: S. Bobbio, Microelectronics Center of North Carolina

BA-1 A Self-Consistent Kinetic Calculation of Helium rf Discharge Properties W. N. G. HITCHON,† T. J. SOMMERER,‡ and J. E. LAWLER† †U of Wisconsin and ‡U of Illinois—A kinetic description of discharge plasmas based on the propagator (Green's function) for Boltzmann's equation has been used to describe the cathode fall of a helium dc glow discharge[1] and a helium rf discharge.[2] Poisson's equation is solved simultaneously to yield self-consistent kinetic results. This presentation will focus on three distinctly non-equilibrium aspects of the results for rf discharges: the existence of a weak bulk field out-of-phase with the strong sheath fields, calculated bulk electron energies much lower than found in other calculations, and the formation of double field reversals near the sheath-bulk interface. The latter feature may be a precursor to the observed gathering of macroparticles near sheath-bulk boundaries.

[1]T. J. Sommerer, W. N. G. Hitchon, and J. E. Lawler, Phys. Rev. A **39** 6356 (1989).

[2]T. J. Sommerer, W. N. G. Hitchon, and J. E. Lawler, Phys. Rev. Lett. **63** 2361 (1989).

BA-2 Self-Consistent rf Sheath Properties and Stochastic Heating for Arbitrary Sheath Voltage Waveform. STEPHEN E. SAVAS, Applied Materials, Santa Clara, Calif. 95054. We have calculated rf sheath properties analytically using realistic waveforms for the rf sheath voltage, and with a modified non-maxwellian electron energy distribution (EEDF). The purpose is to permit ion density, current density and stochastic electron heating rate to be obtained for any rf sheath voltage waveform.This work has two parts.The first uses a Fourier series expansion for the rf current and follows the method of Lieberman and Godyak to obtain the rf voltage Fourier coefficients (FC) for an arbitrary rf current waveform. The values for the FC of the current are then found for specified voltage waveform (SVW) by solving the simultaneous equations for the FC of voltage, each of which is a function of the FC of the current. The resulting solutions for the FC of the current are used to calculate the ion density, sheath edge velocity and the modified Child law relation beween ion current and sheath voltage. The second part of the work derives the modified EEDF and rate of Stochastic heating-using Chebyshev expansions for the EEDF-as functions of the sheath speed. The time-averaged power flow to electrons is then found by averaging the stochastic heating using the sheath edge velocity for each voltage waveform (SVW). We show results for ion densities, current densities and stochastic heating. The ion density depends very weakly on the SVW but the stochastic heating depends strongly on SVW. The modification to Child's Law is mainly by a constant multiplier different for each SVW.

BA-3 A Self-Consistent Boltzmann Equation Model of RF Plasma Discharges,* M. E. RILEY and P. J. DRALLOS, Sandia National Laboratories -- We are presenting a numerical model for calculating the time-dependent behavior of RF plasma discharges. The model includes three dimensions in phase-space, self-consistent electric fields, and treats ion motion with fluid equations. An important feature of the model is that the Vlasov operator is implemented using methods of characteristics instead of finite difference. This allows the particle moving algorithms to be free of the Courant condition time-step constraints. Here, the time-step is limited by the collision period or plasma frequency. The model is based on an exact Boltzmann solver[1] in a 2-D velocity-space. In the present model, we have represented the velocity distribution function with a separation of variables approximation. This effectively reduces the dimensionality of the present computation from three to two dimensions. We have tested a space-independent version of the present model against the 2-D exact code with good results. Our modeling efforts have thus far dealt with RF discharges for rare gases in GEC reference cell configurations.

*This work performed at Sandia National Laboratories, supported by the U.S. Department of Energy under Contract Number DE-AC04-76DP00789.

[1]P. J. Drallos and J. M. Wadehra, Phys. Rev. A 40, 1967 (1989).

BA-4 Modeling of RF Plasma Discharges in Argon,* P. J. DRALLOS and M. E. RILEY, Sandia National Laboratories -- We have developed a Boltzmann description of electrons in an RF plasma discharge. Our model includes two velocity space dimensions and one dimension in configuration space. Other features include self-consistent electric fields, electron motion along characteristic curves and a fluid description for the ion motion. We are presenting results from simulations of RF discharges in argon. Included among these results are the formation and steady state behavior of the plasma sheaths. Also included, are time and space resolved excitation and ionization profiles, electron and ion distributions, I-V characteristics, and electron velocity distribution functions. Theoretical details of the model are discussed in a companion paper at the conference.

*This work performed at Sandia National Laboratories, supported by the U.S. Department of Energy under Contract Number DE-AC04-76DP00789.

BA-5 Modeling of Low-Pressure Microwave Discharges in Ar, He, and O_2^*, C. M. Ferreira, L. L. Alves, M. Pinheiro and A. B. Sá, IST, Lisbon Tech. U. - A kinetic study of low-pressure microwave discharges in Ar, He, and O_2 is carried out using electron transport parameters and rate coefficients derived from solutions to the Boltzmann equation together with the continuity and transport equations for the charged particles, taking into account stepwise ionization processes. The Boltzmann equation is solved over a wide range of the applied frequency, $\omega/2\pi$, but assuming that $\omega > \tau_e^{-1}$, τ_e denoting the characteristic time for electron energy relaxation by collisions. The formulation provides discharge characteristics for the maintenance field and for the mean absorbed power per electron in the three gases which are shown to agree satisfactorily with experimental data obtained from surface wave discharges. It is shown that such an agreement would not be obtained without consideration of the role played by stepwise ionization processes in sustaining the discharge.

* Work Supported in part by JNICT and NATO

BA-6 Numerical Analysis of RF and DC Glow Discharges using a Continuum Model, S.-K. PARK, Motorola, Inc., APRDL - The governing equations of a continuum model were solved to investigate the collective behavior of charged particles and potential distribution in low-pressure RF/DC glow discharges. The method of lines with automatically variable time step and variable order, and orthogonal collocation on finite elements were found to be an efficient numerical technique for solving the stiff system of coupled parabolic and elliptic partial differential equations. Both electropositive (Argon-like) and electronegative (Chlorine) glow discharges were examined. The electronegative discharge exhibited much smaller electron density, much thinner sheath, much greater potential drop and electrical field strength in the bulk plasma, and severe modulation by applied RF of electron energy, ionization and excitation rates even in the bulk. In addition, the effect of system parameters including pressure, interelectrode spacing, RF/DC voltages, applied frequency, and secondary electron coefficient, was studied. Finally, the excitation rate profiles from a continuum model were employed as an input to a neutral transport and reaction model to predict etching rate, uniformity, and anisotropy. The ultimate goal is to develop a global plasma reactor model to combine the glow discharge model with the neutral transport and reaction model.

BA-7 A WKB/SWKB Approach to Electron Thermalization and Attachment,* B. SHIZGAL,Dept. of Chemistry, U. of British Columbia-The relaxation of a nonequilibrium distribution of electrons in gases is governed by a Fokker-Planck equation. The time evolution of the electron transport properties can be expressed as a sum of exponential terms with each term characterized by an eigenvalue of the Fokker-Planck operator. This eigenvalue problem can be transformed to a Schroedinger equation with a potential function parametrized by the electron-moderator cross section and the gas temperature. The eigenvalues and the eigenfunctions are calculated with a WKB semiclassical approximation and compared with exact numerical results. The application of the WKB approximation provides a useful interpretation and proves to be a very efficient method of studying electron transport processes when an attachment reaction is included. An alternate semiclassical approach (SWKB) based on supersymmetric quantum mechanics will also be discussed.

* Work supported by the Natural and Engineering Research Council of Canada.

SESSION BB

10:05 AM - 11:55 AM, Tuesday, October 16

Convention Center, Chancellor Hotel - Grange Room

BASIC PROCESSES IN COLLISION PHYSICS

Chair: M. Dillon, Argonne National Lab

BB-1 **Correlation Effects on Collisions.** R. Stephen Berry and Sandra Ceraulo, Department of Chemistry and The James Franck Institute, The Universtiy of Chicago, Chicago, Illinois 60637. Electron correlations in atoms may be probed by processes of two-electron ionization, particularly by study of the relative intensities of one-electron and two-electron ejection, and by angular correlation of the ejected electrons. Ionization may be accomplished by photons, in which case one studies the role of correlation on the transition amplitudes, and by electron impact, which, if done with fast electrons, probes the correlation in the initial state. Two-electron ionization becomes amenable to computation if the electronic wave functions represented by a collective- mode basis.

BB-2 Electron-Impact Double-Ionization as a Probe of Electron Correlation, J.H. MOORE, M.A. COPLAN, J.W. COOPER, University of Maryland, J.P. DOERING, Johns Hopkins University--Electron-impact double-ionization of atoms with coincident detection of the outgoing electrons--so-called (e,3e) experiments--are a sensitive probe of electron correlation. In a preliminary experiment we have investigated the double ionization of argon under conditions where a 205 eV Auger electron is detected in coincidence with a second (ejected or scattered) electron of the same energy.[1] The (e,3e)-like experiment (only two of the three electrons are detected) has demonstrated strong final-state electron correlation effects. An apparatus is being designed to carry out a true (e,3e) experiment for the investigation of initial-state correlation. The goal is to measure the distribution of relative momentum of a pair of atomic electrons. To permit a theoretically tractable separation of initial- and final-state correlation effects, this experiment must be carried out in a regime where the cross section is small. The design of the apparatus permits many triple-coincidence measurements to be performed simultaneously.

[1] Phys. Rev **A41**, 535 (1990).

BB-3 Subexcitation Electrons, a Topic in Gaseous Electronics,* MITIO INOKUTI, ANL--The term "subexcitation electrons" stems[1] from studies of the interactions of ionizing radiations with matter, in which electrons of kinetic energies T below many keVs are abundantly generated. Electrons with T above the first electronic-excitation threshold E_1 degrade rapidly, while subexcitation electrons, i.e., electrons with $T < E_1$, moderate gradually until they reach the thermal energy E_{th}. Transport of electrons in commonly occurring gases such as H_2, N_2, O_2, CO_2, and H_2O in the domain $E_{th} < T < E_1$ has been studied in detail in recent years.[2] Results for each gas illustrate a noteworthy point, e.g., the role of a resonance in causing stochastic aspects of electron transport in N_2.

1. R. L. Platzman, Radiat. Res. 2, 1 (1955).
2. M. Inokuti, in Molecular Processes in Space, edited by T. Watanabe et al., (Plenum, 1990) p. 65.

*Work supported in part by the U.S. Dept. of Energy, Assist. Sec. for Energy Research, OHER, under Contract W-31-109-ENG-38.

BB-4 Near Threshold Ro-Vibrational Excitation of H_2

S.J. Buckman, M.J. Brunger and D.S. Newman, Electron Physics Group, Australian National University - Absolute differential cross sections for ro-vibrational excitation of H_2 (v=0-1) have been measured at incident energies between 1.0 and 5.0 eV and over an angular range of 5-130°. The absolute scale has been established by use of the relative flow technique in conjunction with the known helium elastic cross section. The differential cross sections have been extrapolated and integrated to yield the total ro-vibrational cross section. The magnitude of this cross section below 2 eV has been the subject of considerable debate between the "beam"[1] and "swarm"[2] communities for over twenty years, and more recently between swarm measurements and theory[3]. The present results are in good agreement both with previous beam measurements and theory at energies below 2 eV, and lie well above (40-60%) the cross section derived from swarm experiments.

[1] H. Ehrhardt *et al. Phys. Rev.* **173**, 222 (1968)
F. Linder and H. Schmidt, *Z. Naturforsch.* **26a**, 1603 (1971)
[2] R.W. Crompton *et al. Aust. J. Phys.* **22**, 715 (1969)
[3] M.A. Morrison *et al. Aust. J. Phys.* **40**, 239 (1987)

SESSION CA

1:30 PM - 3:30 PM, Tuesday, October 16

Convention Center, Chancellor Hotel - Illiniwek Room

HEAVY-PARTICLE COLLISIONS

Chair: R. J. Van Brunt, NIST

CA-1 Ion-Neutral-Collisions: Internal Energy Transfer*, W. LINDINGER, Inst. Ionenphysik, Univ. Innsbruck, Austria - A substantial amount of data on the role of vibrational excitation of molecular ions in collisions with neutrals has been obtained over the past years using Selected Ion Flow Drift Tube (SIFDT) techniques: A model by Ferguson[1] explaining the quenching of vibrational ionic excitation via transient complex formation followed by vibrational predissociation is supported by a series of systematic data on $O_2^+(v)$ and $NO^+(v)$ ions. The excitation and de-excitation of molecular ions in collisions with helium buffer gas atoms has been investigated simultaneously and the influence of kinetic and vibrational energy, respectively, on the reactivity of molecular ions can be separated quantiatively for a variety ion/molecule reactions.

* Work supported by Fonds zur Förderung der wissenschaftlichen Forschung.

[1] E.E. Ferguson, J.Phys.Chem., 90 (1986) 731.

CA-2 Exothermic Reactive Collisions of N^+, N_2^+, and H_2O^+ with H_2O and CO_2 at Suprathermal Energies, J. A. GARDNER, R. A. DRESSLER, R. H. SALTER, C. R. LISHAWA,* and E. MURAD, Geophysics Lab, GL/PHK—Gas phase ion-neutral reactive collisions are being studied at suprathermal energies ($E_{c.m.}$ = 1 to 40 eV). Reaction cross sections are measured and product kinetic energies are determined for the exothermic collision systems: a) N^+, N_2^+, and H_2O^+ with H_2O, and b) N^+ and N_2^+ with CO_2. Charge exchange, hydrogen exchange, and collisional dissociation reactions have been observed. Charge exchange is the fastest process observed with cross sections above 7 $Å^2$ throughout this energy range in each case except the N_2^+—CO_2 collision pair. Charge exchange primarily proceeds via large impact parameter collisions in which little momentum is transferred; some small impact parameter charge exchange reactions involving high momentum transfer have also been observed. The hydrogen exchange reactions are consistent with the predictions of the spectator stripping model. The collisional ionization channels include small impact parameter collisions with high momentum transfer. We discuss here the methods used in these experiments, the results of these measurements, and the utilization of these results in modeling the environment of spacecraft in near-earth orbit (200 - 400 km altitude).

* Permanent Address: Deptartment of Physics and Engineering, Utica College of Syracuse University, Utica, NY 13502

CA-3 Dissociative Recombination in Complex Systems, * E. HERBST, Dept. of Physics, Duke University- Although many experimental studies of the rate coefficients for dissociative recombination reactions between polyatomic positive ions and electrons have been reported, it is only recently that studies of the neutral product branching ratios have appeared. To offer a comparison with these new experimental studies, we have reformulated a phase space theory for the calculation of neutral product branching ratios[1] and utilized the theory on selected reactions such as $H_3O^+ + e$ and $HOCO^+ + e$. The theory, which contains two adjustable parameters, is based on the premise that the parent neutral formed by the ion and electron loses its memory of the details of its formation as it comes apart. Both two-body and three-body channels are included. Our initial results show that most of the experimental results can be reproduced without constraining the adjustable parameters unduly.

*Work supported by the National Science Foundation.

[1] E. Herbst, Astrophys. J. **222**, 508 (1978).

CA-4 Resonances in Molecular Photodissociation, *K.C. KULANDER, C.J. CERJAN and J.L. KRAUSE, Lawrence Livermore National Laboratory A.E. OREL** Dept of Applied Science, UC Davis -- Structure in the absorption lineshape of dissociative bands of polyatomic molecules indicates the presence of scattering resonances on the final electronic state potential energy surface. We have employed the time-dependent wave packet method to study the dynamics of the dissociation process in order to understand the character of the particular resonances responsible. A single calculation for a wave packet corresponding to a particular initial vibrational state provides both the photodissociation cross section and the final state distributions for all wavelengths. Such resonances lead to appreciable enhancement of the absorption cross section and to rapid variations of product state distributions as functions of wavelength. The resonances are characterized according to the underlying classical periodic orbits. The periods of these orbits are correlated with the recurrences in time-dependent correlation function whose Fourier transform is the absorption spectrum.

* Work performed under the auspices of the U.S. Dept of Energy at Lawrence Livermore National Laboratory under contract W-7405-Eng-48

**Computer time supplied by the San Diego Supercomputing Center

CA-5 The Excitation of N_2 (B) in the Reaction Between N_2 (A) and N_2 (X,v), * L.G. PIPER, Physical Sciences Inc., Andover, MA 01810

We have studied the excitation of N_2 (B) from the interaction between N_2 (A) and N_2 (X,v) in a discharge-flow reactor. Spectroscopic observations between 200-400 nm and 560-900 nm, respectively, monitor the N_2 (A) and N_2 (B) while a metastable-helium Penning-ionization diagnostic determines N_2 (X,v) number densities. The energy-transfer process proceeds at a rate that is roughly tenth gas kinetic. When $^{15}N_2$ (X,v) interacts with $^{14}N_2$ (A), the observed product is $^{15}N_2$; (B), indicating that the process involves transfer of electronic rather than vibrational energy. The $^{15}N_2$ (B) emission shifts to $^{14}N_2$ (B) when excess $^{14}N_2$ (X) is added to the reactor. The rate of transfer from $^{15}N_2$ (B) to $^{14}N_2$ (B) is nearly gas kinetic.

* Work sponsored in part by the Air Force Weapons Laboratory.

SESSION CB

1:30 PM - 3:35 PM, Tuesday, October 16

Convention Center, Chancellor Hotel - Grange Room

PLASMA SURFACE INTERACTIONS

Chair: H. H. Sawin, MIT

CB-1 Surface Processes in Plasma Etching Environments, H. F. WINTERS, IBM Res. Ctr., San Jose, CA- An understanding of etching reactions requires a knowledge of: (1) the types of gas phase particles which react at the surface, (2) the types of product formed, and (3) the processes which lead from reactant to product. The capabilities and limitations of a state-of-the-art experimental system, which was designed to address these issues will be described. The state of our understanding (lack of) for surface processes in a plasma environment will be illustrated with new data for the etching of Si(111) with F-atoms. The large number of products formed during the etching of silicon with Cl-atoms, H-atoms, and F-atoms and mixtures thereof will used to illustrate the complexity of etching reactions. It will be shown that spontaneous etching Si(111) by F-atoms at room temperature produces the stable gases SiF_4, Si_2F_6, and Si_3F_8 with SiF_4 being the dominant product. As the surface temperature is increased, the relative contribution of the etch products SiF_4, Si_2F_6, and Si_3F_8 decrease while SiF_2 increases and eventually becomes the major species. Ion bombardment significantly enhances the production rate for all products but not proportionately and not by the same mechanisms. The influence of doping and surface conditions on the etch rate will also be discussed. A few comments will be made about the chemiluminescence associated with the reaction.

CB-2 Quantification of Plasma-Surface Interactions in Fluorocarbon Etching of Si and SiO_2, H. H. SAWIN and D. C. GRAY, MIT- A molecular beam apparatus has been constructed which allows the synthesis of dominant species fluxes to a wafer surface during fluorocarbon plasma etching. In this apparatus Si and SiO_2 etching kinetics have been studied as a function of independently variable fluxes of free radicals and ions, as well as ion energy and substrate temperature. These species include CF_2 as a polymer forming precursor, Ar^+ and CF_3^+ ions, and F as the primary etchant. Etching yields and product distributions were measured using interferometry and line-of-sight mass spectrometry. The ability of CF_2 to suppress Si etching through the formation of polymeric surface films has been quantified as a function of these parameters. In contrast, although CF_2 will not spontaneously etch SiO_2, Ar^+ sputtering rates may be enhanced by a factor of 3 over "clean" sputtering rates due to CF_2 gas phase sticking. In the presence of large fluxes of atomic fluorine characteristic of CF_4 etching, CF_2 was found to have no measurable effect on the total SiO_2 etching yields, verifying that CF_x type radicals are not critical for oxygen removal during silicon dioxide etching. Quantitative models for the ion-enhanced surface kinetics have been proposed for use in a PC-based etching profile simulator.

CB-3 Real-Time Monitoring of III-V Multi-Layer Structures During Plasma Etching and Passivation, R.A. GOTTSCHO, K. P. GIAPIS, and M. F. VERNON, AT&T Bell Laboratories - Plasma etching of III-V compound semiconductor multi-layer structures is necessary for microfabrication of high speed electronic and photonic devices such as heterojunction bipolar transistors, surface emitting lasers, and self-electro-optic effect (SEED) devices. Besides simple end-point detection and rate-monitoring, it is important to control wafer temperature and minimize plasma-induced damage. Using pulsed laser excitation, we monitor photoluminescence (PL) from both AlGaAs and GaAs simultaneously during etching of AlGaAs/AlAs/GaAs multi-layer structures. As the multi-layer structure is etched, PL yield from both materials oscillates due to thin film interference. However, before etching ends, AlGaAs PL intensity disappears because of plasma-induced damage. At the end-point, the GaAs surface also becomes damaged and the GaAs PL yield decreases. However, this damage can be neutralized by using hydrogen plasma treatments. In this case, PL is used to monitor the passivation end-point and efficiency.

CB-4 Ion Bombardment Angle and Energy in Argon rf Discharges, J. LIU, G.L. HUPPERT, and H.H. SAWIN, M.I.T. -- The effect of collisions on ion bombardment characteristics have been studied by varying the operating plasma pressure from 10 to 500 mtorr and peak-to-peak voltage from 80 to 140 V. Both rf modulation of the sheath voltage and charge-exchange collisions between argon ions and neutrals are necessary to produce multiple peaks in the energy distribution, as shown by experimental data and Monte Carlo simulations. As pressure increases, the number of mean free path in the plasma sheath increases; therefore, the fraction of ions with large incidence angles increases. At the same time, the ion energy distribution becomes fully-developed, that is, the shape of the distribution does not change with pressure or incident angle. At low pressures, a small fraction of ions still strike the electrode with large incident angles, but with low energies. Some effects of magnetic field on sheath width and ion characteristics will also be presented.

CB-5 Diamond Film Deposition by Plasmas Generated in a Microwave Cavity Resonator, W. L. Hsu, E. A. Fuchs, and K. F. McCarty, Sandia National Laboratories, Livermore, CA - Diamond, among its many unique properties, is the hardest material known to man and has five times the thermal conductivity of copper at room temperature. The ability to nucleate and grow thin films of diamond from gas phase radicals has generated tremendous commercial interests. In this paper we discuss our experience in depositing diamond films using a plasma which is heated by applying 2.45 GHz microwave power to a cylindrical cavity resonator. The quality of the films at various growth conditions, through analyses by Raman spectroscopy and scanning electron microscopy, will be presented. When the silicon substrates were maintained at 1000°C, films with high contents of diamond could be obtained with a methane to hydrogen ratios in the feed gas of up to 1%, as similarly reported by other researchers. Maximum growth rates of up to 0.8 μm/hr were obtained. More recently we have been able to deposit diamond at a significantly lower temperature of 500°C. This temperature was measured by a calibrated infrared camera. At this temperature, the diamond content of the films was significantly higher than that for the higher temperature case. Furthermore, the growth environment can tolerate a much higher methane ratio in the feed gas (up to 20%). This richer hydrocarbon mixture in effect translates to a higher film growth rate.

CB-6 Energy Transfer from Noble Gas Ions to Surfaces: Collisions with Carbon, Silicon, Copper, Silver, and gold in the Range 100-4000 eV, H.F. WINTERS, H. COUFAL, H.L. BAY, *W. ECKSTEIN, IBM Res. Ctr, San Jose, CA--Most surfaces in a plasma are bombarded by a flux of energetic ions; therefore, knowledge of the amount of energy that an incoming atom or ion transfers to a surface during a collision is essential for the accurate modeling of many technologically important processes, including glow discharge sputtering, plasma etching, and ion implantation. The amount of reflected energy is also crucial to the design of thermonuclear fusion reactors where energy losses from the plasma to the reactor walls have important consequences for the particle and energy balance of the system. The energy deposited into carbon, silicon, copper and silver surfaces by He^+, Ar^+ and Xe^+ ions impinging with kinetic energy in the range 100-4000 eV has been measured. The energy deposited into gold by the same ions has been measured from 10 eV to 4000 eV. This data allows one to understand the dependence of the energy reflection coefficient on ion mass, substrate mass and ion energy. Xe^+ deposits more than 95% of its energy between 500-4000 eV for all materials. The other ions deposit at least 80% of their energy in this range. The energy reflection from surfaces is also investigated by computer simulation using the TRIM.SP program. The experimental trends are semi-quantitatively reproduced by the simulation but there are some quantitative differences in the absolute results. The implication of these results for the understanding of collisional processes at solid surfaces will be discussed.

* Max-Planck-Institut fur Plasmaphysik, EURATOM Association, Garching, Federal Republic of Germany

CB-7 Interaction of sputtered atoms with the filling gas in magnetron sputtering discharges. I.S. FALCONER, G.M. TURNER, B.W.JAMES and D.R. McKENZIE, School of Physics, U. of Sydney, Australia - The characteristics of thin films produced in magnetron sputtering discharges are determined by the energy and angular distribution of the sputtered atoms as they strike the substrate. The effect of collisions with filling gas atoms on both the energy and angular distribution has been investigated using a Monte Carlo code: the relationship between the initial energy distribution of the sputtered atoms and the relative masses of the sputtered and filling gas atoms on the characteristics of the condensing atoms will be presented. A comparison of the calculated energy distribution and that deduced from an interferometric measurement of line shape of spectral emission lines of the sputtered atoms shows a large discrepancy, which is attributed to the heating of the filling gas by the energetic sputtered atoms. An extension of the Monte Carlo to give the temperature rise of the filing gas suggests that this is the case.

SESSION D

3:30 PM - 5:30 PM, Tuesday, October 16

Convention Center, Chancellor Hotel - Brundage and Zuppke Rooms

POSTERS

D-1 A Time–Dependent Two–Electron–Group Model for a Pulsed Helium/Metal–Vapour Glow Discharge, R.J.CARMAN, Macquarie University, Sydney, Australia. Two–electron–group models (2–EGM) have been developed* to consider deviations from a Maxwellian electron energy distribution function (EEDF) in various DC low–pressure glow discharges without solving the Boltzmann equation explicitly. This method has been extended to describe the EEDF in a high–current pulsed glow discharge in a helium/metal vapour mixture. Two groups of electrons are defined in energy space representing those comprising the bulk of the EEDF and those in the high–energy tail region. The electron energy balance equations between the two groups include energy transfer due to the electric field, coulomb collisions, and elastic and inelastic collisions involving the various atomic and ionic species. The 2–EGM model has been applied to an existing self–consistent 1–EGM model for a He–Sr laser discharge** which evaluates the radial and temporal development of the plasma parameters during the current pulse, recombination phase and afterglow periods. Failure to take into account the depletion of high–energy tail electrons is shown to lead to a serious overestimate of the calculated excitation and ionisation rates of the rare gas.

*W.L. Morgan and L. Vriens J.Appl.Phys. 51 5300 (1980).

**R.J.Carman I.E.E.E. J.Q.E. Sept. 1990.

D-2 Characterization of Microwave Stimulated Laser Emission in Xenon Gas Mixtures,* G. A. HEBNER, Sandia National Laboratories -- The characteristics of microwave stimulated laser emission in He/Xe and Ar/Xe gas mixtures at 1.73, 2.03 and 2.65 μm will be discussed. The microwave discharge system employs a "meander line" slow wave structure to generate an intense, nonradiating electric field at 2.45 GHz. In this particular system, the magnitron is capable of operating up to 3 KW in either a pulsed or CW mode and can produce a plasma in argon or helium at pressures of approximately 150 torr to less than a torr. The 1.73 and 2.65 μm laser emission were observed in pulsed mode operation of Ar/Xe gas mixtures at pressures of 100 to 40 torr while 2.03 μm laser emission was observed in both CW and pulsed operation of He/Xe gas mixtures at pressures of less than 20 torr. Operating parameters and the potential for high quality oscillator development will be discussed.

*This work was performed at Sandia National Laboratories, supported by the U.S. Department of Energy under Contract Number DE-AC04-76DP00789.

D-3 **Effects of Localized Heating on the Optical Stability in an E-Beam Pumped Atomic Xenon Laser,*** E. L. PATTERSON, M. J. HURST and DAVID WICK, Sandia National Laboratories--It has been found previously[1] that the e-beam pumped atomic xenon laser stops lasing when the energy loading reaches 180 mJ/cc. This laser termination could be caused either by a change in laser kinetics[2] or by lensing caused by gas motion driving the laser resonator unstable. Time resolved lensing due to non-uniform refractive index was investigated by recording the induced deflections on 13 Ar^+ laser beams after a double pass through the laser volume. The ABCD matrix for beam propagation through the system was then derived and the cavity stability investigated for various configurations. It was found that for the conditions where termination occurred that the cavity remained stable leading to the conclusion that termination was due to changes in the laser kinetics.

*This work supported by the U. S. Department of Energy under Contract No. DE-AC04-76-DP00789

[1]E. L. Patterson, G. E. Samlin, P. J. Brannon, and M. J. Hurst, Scheduled for publication in IEEE J. Quant. Elec., Sept. 1990.

[2]M. Ohwa and M. J. Kushner, Scheduled for publication in IEEE J. Quant. Elec., Sept. 1990.

D-4 $NH(^3\Sigma^-, v=1-3)$ Formation and Collisional Relaxation in Electron-Irradiated $Ar/N_2/H_2$ Mixtures,* J.A. DODD, S.J. LIPSON, D.J. FLANAGAN, W.A.M. BLUMBERG, Geophysics Laboratory (AFSC), B.D. GREEN and J.C.PERSON, Physical Sciences Inc.,-- The nascent distribution of $NH(v=1-3)$ resulting from the $N(^2D)+H_2$ reaction has been determined. Rate constants for the vibrational relaxation of NH(v=1,2) by Ar, N_2, and H_2 have also been measured. Vibrationally excited $NH(v\leq 3)$ was produced in $Ar/N_2/H_2$ mixtures irradiated by a pulsed 35 kV electron beam in the GL LABCEDE facility. Time-resolved Fourier spectroscopy was used to observe NH(v) vibrational fundamental band emission. NH(v=1-3) populations were obtained using a synthetic spectral fitting code, and then analyzed using a single-quantum relaxation model. A detailed kinetic model was used to predict the effects of N and H atoms in the gas mixture on the kinetics of NH(v). These results are important for predicting the IR spectra of NH produced by combustion processes.

*Supported by the Air Force Office of Scientific Research.

D-5 Energy Transfer in Fast Oxygen Atom Collisions,
B.L. Upschulte, G.E. Caledonia, B.D. Green, R.H. Krech
Physical Sciences Inc.

Translational to vibrational energy transfer cross sections have been measured using a crossed molecular beam apparatus. The target beam, a pulsed free jet expansion of molecular species, collides at right angles with a source of fast oxygen atoms. The pulsed high flux source of translationally fast, atomic oxygen generates an instantaneous flux up to 5 x 10^{22} atoms sr^{-1} s^{-1} at controllable velocities throughout the 5 to 12 x 10^5 cm s^{-1} range. By viewing the resulting infrared fluorescence with selected 0.5 μm bandpass filters and an InSb detector, we evaluate band integrated cross sections through the 2.0 to 5.5 μm wavelength region. A circular variable filter radiometer is used to provide spectral bandshapes. Target molecules include N_2, NO, H_2O, CO, CO_2, and CH_4. In two instances chemical reactions which are inaccessible at thermal velocities lead to the production of $OH^*(v)$ and $CO^*(v)$ from H_2O and CO_2 respectively. The cross section for production of $CO^*(v)$ from O-atom collisions with CO_2 is a large value, 6 x 10^{-17} cm^2. Collisions involving the target molecule CO show long lasting emissions in the fundamental band. Cross sections, reaction paths, energetics, and comparisons with available experimental and theoretical literature will be presented.

D-6 A RF Ion Source for the Production of He^+ Beams.
R. B. LOCKWOOD, JOHN B. BOFFARD, MARK LAGUS, L. W. ANDERSON, and CHUN C. LIN, UNIVERSITY OF WISCONSIN--The operating characteristics of a capacitively-coupled, RF ion source for producing He^+ ions has been studied.[1] The discharge is confined in a quartz bottle capped at the ends by a metal electrode and an extractor canal. The He^+ ions are pushed out of the discharge by a 1-3 kV voltage across the electrode and the extractor canal. A magnetic field of about 100 G along the axis of extraction helps to confine the electrons to the center of the discharge column. The extractor uses a Pierce-type geometry followed by an einzel lens and deflecting plates. Because of Penning ionization, high purity is essential; therefore research grade He gas is passed through a liquid N_2 trap. Ion currents of 5-15 μA are routinely obtained with energies of 1-3 keV. The energy spread of the ion beam will be discussed.

[1]The ion source operation has been aided by private communications with H. T. Richards.

D-7 **Electron-Atom Collisions in a Laser Field.*** Philip.H.G. Smith and M.R.Flannery, **Georgia Institute of Technology.** A semi-classical Floquet approach is used to solve exactly, the Schrodinger equation for the laser/hydrogen interaction in a soft photon weak-field limit, to give dressed states of the atom in the laser field. Perturbative dressing is shown to provide an incomplete description, and cannot predict the distinctive features of the Floquet approach. Electron-hydrogen collisions in a laser field are then described via a multichannel eikonal treatment, in which the dressed states are closely coupled. Cross sections for 1S-2S and 1S-$2P_0$ excitations are presented as a function of field strength and impact energy, and compared with the Born-wave result.

* Research supported by AFOSR-89-0426.

D-8 Angular Momentum Changes in Collisional Ionization*, A. Haffad and M. R. Flannery, Georgia Institue of Technology - Single and Double Differential cross sections for ionization in e - H(nl) and H(1s) - H(nl) collisions are reported as a function of impact energy E, final energy ϵ and angular momentum l′ of the ejected electron. This process is assumed to occur via an energy-changing and angular momentum-changing binary collision between the Rydberg electron in state nl and the projectile e or H(1s). The atomic projectile can also be excited. Systematic trends in the variation of the classical cross sections with final angular momentum l′ are discussed and are in accord with a previous quantal treatment[1].

*Research supported by U.S. Air Force Office of Scientific Reasearch under Grant No. AFOSR-89-0426.

[1]M. R. Flannery and K. McCann, Phys. Rev. **19** (1979) 2206.

D-9 Electron- Impact Excitation of Molecular Ions* A. E. OREL, Dept. of Applied Science, UC Davis, T. N. RESCIGNO, Lawrence Livermore National Laboratory--The complex Kohn variational method, which has been very successful in treating the scattering of electrons from neutral polyatomic molecules, can also be used for studying electron collisions with molecular ions. We will discuss our modification of this method to deal with Coulomb boundary conditions. We treat the additional complication of electron-impact excitation of states which are optically allowed from the ground state. We will also discuss a new method for the cut-off of the irregular outgoing wave continuum functions near the origin. This involves a more physical choice for this function that improves convergence. We illustrate our method on a study of electron-impact excitation of N_2^+, H_2^+, and HeH^+.

* Work performed under the auspices of the U.S. Dept of Energy at Lawrence Livermore National Laboratory under contract W-7405-Eng-48

D-10 Possible Applications of the Pais Variational Phase Shift Approximation, *S.R. Valluri,U. of Western Ontario, Ed Mansky, School of Physics, GA Tech and W.J. Romo, Ottawa-Carleton Inst. of Physics, Carleton University, Canada.
The Pais variational phase shifts have been computed from convenient analytic expressions. Partial derivatives of these analytic expressions forphase shifts with respect to l, the angular momentum, and k, the wave number, are obtained and evaluated for a variety of potentials including the Woods-Saxon potential which is of relevance in stability of metal clusters. The partial derivative with respect to l facilitates the calculation of the differential cross section in the semi classical limit. The derivative with respect to k is useful in obtaining time delay coefficients etc. The Pais method gives more accurate phase shifts than the WKB for low energies and gives good results for large l and k like the WKB. It is a viable alternative to the WKB in a variety of calculations.
1. W.J. Romo and S. R. Valluri. J. Phys B (Submitted for publication).

D-11 Calculation of Radiative Recombination Cross Sections of Oxygen Atom.* S. CHUNG and CHUN C. LIN, U. of Wisc., and E. T. P. LEE, Geophysics Laboratory (AFSC).--Radiative recombination cross sections have been calculated for the process $e^- + O^+ \rightarrow O[(^4S)n\ell]^{3,5}L$. The wave functions of both the bound and continuum states were computed by the Hartree-Fock method with the exchange and orthogonality constraints included via Lagrange's undetermined multipliers. Compared with the hydrogenic counterparts, the cross sections $\sigma_{n\ell}$ for $\ell \geq 3$ are virtually identical, but for $\ell=0,1$ the two sets of cross sections are totally different. For $\ell=2$, the agreement is quite good at low energy of electron, but the discrepancy becomes larger at high energies. The agreement/disagreement is readily traced to the corresponding agreement/disagreement of the wave functions between H and O, as we find that for $\ell \geq 2$ the wave functions of O and H are virtually identical for both the bound and continuum states, but for $\ell=0,1$, the two sets are markedly phase-shifted from each other. The radiative recombination rate coefficients are obtained by averaging these cross sections over the Maxwell-Boltzmann distribution of electron speed.

*Supported by Geophysics Laboratory (AFSC).

D-12 Triple Differential Cross Sections for Electron-Atom Collisions Near Threshold, *S. JONES and D. H. MADISON, LAMR, U. of Missouri-Rolla -- Recently, Schlemmer et al.[1] measured triple differential cross sections for electron-hydrogen and electron-helium collisions near threshold. Angular distributions were measured with one electron detector being rotated relative to the beam direction, and the second detector being maintained at 180° relative to the first detector. These measurements revealed that equal velocity electrons ejected at 90°, relative to the beam direction, exhibit totally different behavior for hydrogen and helium. For hydrogen the cross section is a minimum, and for helium there is a maximum at 90°, whereas standard theories would predict a minimum for both atoms. We are investigating several possible mechanisms which could lead to this difference. The effects of electron capture plus double ionization, correlation in the atomic wavefunctions, correlation between the two final state electrons and post-collision interactions will be discussed, and our results will be compared with the experimental data.

*Work supported by the NSF.

[1]P. Schlemmer, T. Rosel, K. Jung, and H. Ehrhardt, Phys. Rev. Lett. 63, 252, 1989.

D-13 Measurement of Stokes Vectors in Electron-Atom or Ion-Atom Impacts, R. ANDERSON, U of MO-Rolla--This paper will discuss some new techniques to determine Stokes vector components in coincident electron impact studies where optical emission produced by the electron involves a definite set of known density matrix elements. This discussion also applies to coincident ion-atom coincident measurements. The described techniques may be used over a spectral region from 0.11 to 2 μm with the apparatus tailored to the wavelength region of the emission from the experiment. In the vacuum UV the radiation detector which must be used is the PMT. Polarization effects have been noted in the measured signal for PMTs but this can be reduced for light at near normal incidence. It can be shown that polarization effects can be corrected in the division-of-amplitude photopolarimeter.

D-14 Coincident Electron Impact Ionization Experiment for Atoms and Molecules.* J. P. DOERING and L. GOEMBEL, Johns Hopkins U. -- We have constructed an coplanar, asymmetric (e,2e) experiment to study ionization-excitation branching ratios for atoms and molecules. A standard variable-angle electron energy loss spectrometer has been modified by placing an additional electron energy analyzer 70-90° to the incident electron direction. This arrangement allows a low energy (5-25 eV) secondary electron to be detected in coincidence with the scattered high-energy (200 eV) primary electron after an ionizing collision. Changing the primary electron scattering angle from +5° to -5° allows both binary and recoil lobes of secondary electron intensity to be sampled. In preliminary experiments, coincidences have been obtained for ionization of He and Ar to the ground state of the ion and for ionization of N_2 to produce the ground and excited A states of the ion.

*Work supported by NSF Grant ATM-8915375.

D-15 *Electron Energy Loss Spectroscopy of CF_4, SiF_4 and GeF_4,** M. Dillon and D. Spence, *ANL,* and K. Kuroki, *National Inst. of Police Science*, Tokyo, Japan

Electron energy loss spectra (eels) have been recorded for the isoelectronic series CF_4, SiF_4, and GeF_4 over an energy loss interval of 20 eV and an angular scattering range of 0^o to 9^o. In addition, optical oscillator strength distributions have been derived from eels recorded at zero-angle scattering. Whenever possible, these have been normalized to values taken from the literature.

Electronic transitions from lone pair orbitals analogous to those in CF_4 have been found in SiF_4 and GeF_4. Structured Rydberg transitions from orbitals of a predominantly X-F character (a_1) have also been found in the ionization continuum of all three molecules.

*Work supported by the U.S. Department of Energy,Assistant Secretary for Energy Research, Office of Health and Environmental Research, under contract w-31-109-ENG-38.

D-16 Subexcitation Electrons in Gaseous H_2 and D_2,* MINEO KIMURA, ANL and Rice U., I. KRAJCAR BRONIC, Ruder Boskovic Inst. and ANL, and MITIO INOKUTI, ANL--
Subexcitation electrons in isotope gases of H_2 and D_2 are investigated by using the Spencer-Fano theory and the continuous-slowing-down approximation. An elementary argument based on the Born approximation indicates that the moderation rate in H_2 is higher than that in D_2 by a factor of two. From a more rigorous treatment of cross sections, we find that the difference in the moderation rate is smaller with a value of 1.5-1.7 below 1 eV, but above thermal energy. This is so because cross sections for H_2 and D_2 are quite different near each threshold, and hence, so are degradation spectra.

*Work supported in part by the U.S. Department of Energy, Assistant Secretary for Energy Research, Office of Health and Environmental Research, under Contract W-31-109-ENG-38, and NSF project No. JF-802/NSF.

D-17 *Electron Elastic Scattering and Vibrational Excitation of GeH_4* ,* H. Tanaka and L. Boesten, *Sophia University, Tokyo, Japan*, M. Dillon , D. Spence, *ANL*
Absolute elastic differential cross sections for electron collisions with GeH_4 have been determined for incident electron energies of 1.5 to 100 eV. Angular and energy distributions as well as vibrational excitation functions obtained with low-energy electrons reveal the existence of a Ge-H σ^* shape resonance with a maximum at ~ 2 eV in the t_2 component of the scattered electron state.

Work supported in part by the U.S. Department of Energy, Office of Health and Environmental Research, under contract W-31-109-Eng-38 and by a Grant in Aid from the Ministry of Education, Science, and Culture, Japan.

D-18 Time Dependent Optical Emission and Electron Energy Distribution Function Measurements in RF Plasmas§, K. R. STALDER, SRI International, W. G. GRAHAM, Queen's University, and C. A. ANDERSON AND A. A. MULLAN, University of Ulster, Coleraine--We report on further measurements of the time-dependent optical emission using time resolved photon counting techniques and electron energy distribution functions (EEDF) using time resolved Langmuir probe techniques in rf plasmas. These experiments were carried out at frequencies ranging from 100-400-kHz and at 13.56-MHz. Experiments in H_2-CH_4 plasmas, pure argon plasmas, and nitrogen plasmas illustrate electron energy loss due to vibrational excitation in molecular gas plasmas. We obtained excellent agreement between the measured time dependent optical emission and the emission intensity calculated from the EEDF folded in with known optical emission cross sections at the lower frequencies. While probe measurements at 13.56-MHz are not yet possible, optical measurements show extremely high harmonic excitation processes, indicative of highly non-equilibrated EEDF's.

*Work supported in part by ARO Contract No. DAAL03-89-K-0157 and a NATO Research Grant.

D-19 Theoretical Analysis of Vibrational Excitations and Structures of CO Adsorbed on Ni(100) M. KIMURA, ANL and Rice U.--Vibrational excitations and structure of CO chemisorbed on the Ni(100) surface are investigated theoretically by using the continuum multiple-scattering method. Experimentally, Andersson[1] observed two peaks at 59.5 and 256.6 meV in the electron energy loss spectrum. The present analysis confirms that these peaks are due to vibrational excitations of the Ni-C and C-O stretching modes, respectively. In addition, the study clarifies the possible structure of adsorbed CO on Ni(100).

[1]S. Andersson, Solid St. Comm. 21, 75 (1977).

---

*Work supported in part by the U.S. Department of Energy, Assistant Secretary for Energy Research, Office of Health and Environmental Research, under Contract W-31-109-ENG-38.

D-20 Simulation of an ECR Magnetic-Mirror Plasma Processing System with a Bounded 1D Plasma,* J. L. Shohet, A.T. Johnson, J.B. Friedmann, and K.A. Ashtiani, Engineering Research Center for Plasma-Aided Manufacturing, U. of Wisconsin-Madison- The physical properties of processing plasmas confined in magnetic mirrors can be described with a kinetic simulation (PDP1)[1] in a bounded electrostatic plasma system in one planar dimension. This work calculates the electrostatic potentials produced in a processing plasma by an electron cyclotron resonance source and compares the results to experimental measurement. The ECR source is placed at one end of the processing region and potentials are calculated along the magnetic axis. The potentials are measured using emissive probes in an Argon plasma with T_e=3eV and n_e=10^9/cm^3.

*Work supported by the National Science Foundation under Grant No. ECD. 8721545

[1]W. S. Lawson, *Jour. of Comp. Phy.* 80, 253 (1989).

D-21 An Analytical Estimate of the Parameter Dependence of the Plasma Density in RF Discharges, M. F. TOUPS and D. W. ERNIE, U. of Minnesota—The sustaining mechanisms of a rf discharge are investigated and the relative contribution of each sustaining mechanism to the total energy deposition in the bulk region of the plasma is modelled analytically. The two sustaining mechanisms modelled include electron collisions with the time varying sheath potentials and secondary electron emission from the electrodes by ion bombardment. The chemical and kinetic energy lost from the bulk region of the plasma by ions and electrons which recombine at the electrode surface is also considered. Expressions are derived for the power contributed by each of the sustaining and loss mechanisms. Energy balance is used to solve for an estimate of the plasma density. Under the assumptions presented in this derivation, it is found that the plasma density is proportional to the square of the frequency of the applied rf potential for a fixed rf amplitude and gas composition. The plasma density is also found to be relatively insensitive to the gas pressure. These results will be compared with experimental measurements reported previously.[1]

[1]M. F. Toups, D. W. Ernie, and H. J. Oskam, *42nd Gaseous Electronics Conference*, Palo Alto, CA (1989), Paper E–8.

D-22 Modeling of Low Pressure Plasmas with Non-Uniform Magnetic Fields,* R. K. PORTEOUS and D.B. GRAVES, U.C. Berkeley - In order to treat ECR reactors with non-uniform magnetic fields and complex (axisymmetric) geometries, we have developed a model that incorporates a two-dimensional electron fluid coupled to particle ions. Electrons are allowed to diffuse across magnetic field lines depending on their collisions with neutrals. Power is deposited with both axial and radial spatial variation. Poisson's equation is solved globally to provide the self-consistent electric field. This formalism is sufficiently efficient computationally that industrial scale reactors can be simulated from the source region into the downstream region.

* Work supported in part by IBM T.J. Watson Research Center.

D-23 Self-Consistent Kinetic Calculations of Low Pressure rf Discharges in Ar,* R.P.HARVEY, T.J.SOMMERER, W.N.G.HITCHON, UW--Madison --One dimensional rf parallel-plate discharges in Ar have been studied with a self-consistent kinetic model, previously used on He discharges[1]. Calculations of the ion distribution function, $f(z,v_z,t)$, and the electron distribution function, $f(z,v_z,v,t)$ are done consistently with the electric field. The electron distribution function and average energy are studied as discharge parameters are varied for cases resembling the reference reactor.

*Work supported by NSF under grant number EDC8721545

[1]T.J.Sommerer, W.N.G.Hitchon, J.E.Lawler, Phys.Rev.Lett. 63 2361 (1990)

D-24 Numerical Analysis of the Electrical and Optical Characteristics of an AC Plasma Display Pannel Cell,* A. RABEHI, J.P. BOEUF and L.C. PITCHFORD, Univ. Paul Sabatier, CPAT, URA 277, Toulouse, FRANCE.- A one dimensional model of an AC plasma display pannel cell in neon argon mixtures has been developped. The model is based on self-consistent solutions of electron and ion transport equations (fluid model) coupled with Poisson's equation and with the excited species kinetics (Penning effect and light emission). The charging of the dielectric covering the electrodes is also taken into account. The model can reproduce well the succession of transient discharges which characterizes the "on state" of a plasma display cell. The fast growth of the current density during each transient discharge is related to the direct ionization of neon atoms by electon impact, while the slow decrease of the current density is related to Penning ionization. A study of the influence of gas mixture and pressure on electrical and optical characteristics of the cell will be presented. The results are in good agreement with experimental measurements of current density[1] and light output[2]. Discrepancies between experiment and model concerning the optimum gas composition for light output efficiency can probably be attributed to radial effects which are not taken into account in the model.

*Work supported in part by Thomson Tubes et Dispostifs Optoélectroniques.

[1]O.Sahni, C. Lanza and W.E. Howard, J. Appl. Phys. 49, 2365 (1978).

[2]M. Gay, Thomson Tubes et Dispostifs Optoélectroniques, Unpublished (1989).

D - 25 An Improved Spiral Loop Antenna for Inductively Coupled Plasma Sources,[1] J. MENARD and T. INTRATOR, Dept Nuclear Eng. & Eng. Physics, Univ. Wisconsin

We have developed and characterized a metal enamel coated spiral loop antenna that is useful as an inductively coupled plasma source. It has enhanced plasma confinement due to multi dipole magnetic cusp fields on the boundary, and is very efficient. Operation is possible at low neutral pressures, Ar, He, N_2 discharges at ($P_o > 6 \times 10^{-5}$Torr), with a range of background magnetic field from 0 - 150 Gauss. The hardware and a wideband tunable matching network will be described. The source uniformity and other characteristics over a range of operating parameters including power, pressure, and choice of gas will be shown.

[1]supported by NSF Grant ECS-8704529

D-26 Effect of Hole Geometry on a Hollow Cathode Plume, S. M. MAHAJAN and V. J. GANDHI, Tennessee Technological University—A small hole in the flat side of a hollow cathode is known to create a plasma plume on the outside of the cathode. Such a plasma plume has been used for the analysis of different materials[1]. The intensity of the plume depends strongly upon gas pressure, electrode spacing and the discharge current. In addition, geometry of the hole has been found to influence the intensity of the plume. A finite difference technique was used to simulate potential distribution in the vicinity of a hole in the hollow cathode. Four different hole geometries were based upon either a constant diameter or a linearly increasing/decreasing diameter. Results indicate that a hollow cathode with a linearly increasing hole diameter has a unique potential distribution. Therefore, a hollow cathode with such a hole geometry is expected to produce most intense plasma plume.

Experimental results of emission spectroscopy on hollow cathode plume in Argon (at 3 torr) with different geometries of holes will also be presented.

[1]R. K. Marcus and W. W. Harrison, "Analysis of Geological Samples by Hollow Cathode Plume Atomic Emission Spectrometry," *Analytical Chemistry*, Vol. 59, pp. 2369-2373, 1987.

D-27 LIF, PIE, and Actinometric Axial Profiles of CF in a Symmetric Parallel-Plate RF Discharge in CF_4 plus 5% Ar, W.T. CONNER and H.H. SAWIN, Massachusetts Institute of Technology - The on-axis spatial profiles of laser induced florescence (LIF) from CF, and plasma induced emission (PIE) from CF and from Ar, were measured in a symmetric, well-confined, parallel-plate (1 cm gap) 13.56 MHz RF glow discharge. The conditions used were: a 112 sccm flow rate of CF_4 plus 5% Ar at 500 mTorr and 70 W nominal plasma power. For LIF the ($A\,^2\Sigma^+$-$X\,^2\Pi$) 0-0 transition of CF was pumped and the 0-2 florescence was detected. For PIE the CF ($B\,^2\Delta$-$X\,^2\Pi$) 0-0 and the Ar 4s'(½)-4p'(½) transitions were used. The CF actinometric profile did not accurately follow the LIF profile, which should track the CF ground state concentration. If spatially averaged and axially centered data are used, however, then Ar is a good actinometer for CF (as a function of discharge power and pressure).[1] The LIF profile is consistent with a diffusion limited wall loss mechanism having a CF-wall sticking coefficient of approximately 0.2, in accordance with a separately developed model.[2]

[1]L.D.Baston Kiss, J.P. Nicolai, W.T. Conner, and H.H. Sawin, 42nd GEC J3, 1989.

[2]L.D.Baston Kiss and H.H. Sawin, to be published.

D-28 Langmuir probe measurements* in a 13.56 MHz rf discharge, J.V.SCANLAN,M.B.HOPKINS, Physics,DCU,Dublin 9, Ireland- The use of Langmuir probes in rf plasmas is hampered by the presence of a time dependent component in the local plasma potential, resulting in erroneous values for the electron temperature and density. The second derivative of the I-V characteristic, which is used to determine the eedf, is particularly sensitive to the presence of rf fluctuations. We have investigated the use of a tuned circuit whose impedance, at 13.56 MHz, is much greater than the probe-plasma impedance. The circuit has been shown to reduce the rf at the plasma-probe sheath by a factor of at least five. The rf potential imposed on the plasma potential has been measured as typical 50-100V (peak to peak) at ~300 mTorr but falls to 13-30V (peak to peak) at pressures of ~30 mTorr. The "tuned" probe has been shown to work reasonably well at the lower pressures giving electron temperatures in the range 1.5-3.0 eV for Argon. The second derivative shows that in all cases a significant rf component is still present. At the higher pressures (200-300mTorr) the tuned probe records temperatures of the order of 10-15eV which are completely erroneous.

* Supported by VG Quadrupoles, Middlewich, England

D-29 Spatially Resolved Ion Velocity Distributions in a Diverging Field Electron Cyclotron Resonance Reactor, DENNIS J. TREVOR, TOSHIKI NAKANO*, NADER SADEGHI#, JACQUES DEROUARD#, RICHARD A. GOTTSCHO, PANG DOW FOO, AT&T Bell Laboratories - Electron cyclotron resonance sources are gaining widespread use in plasma processing because they offer high ion flux with controllable energy and thereby high etching and deposition rates with minimal damage. To determine how ion energy distributions evolve from source to wafer as a function of plasma parameters we measured Doppler broadened and shifted laser-induced fluorescent line profiles from Ar^+ metastable ions. Spatially resolved distributions, measured at positions above and across a wafer platen, differ markedly from shifted Maxwell-Boltzman functions. Ions are accelerated along the magnetic field direction by a weak (~ 0.5 V/cm), ambipolar electrostatic field. The ion energy component perpendicular to the electric field corresponds to a temperature of only 0.39 ± 0.05 eV.

* National Defense Academy, Yokosuka, Japan
# Universite Joseph Fourier and CNRS, Grenoble, France

D-30 Aperture Effect of Charged Particles in a Magnetized Plasma.* E. Y. Wang**, W. Q. Li**, S.W. Lam, and N. Hershkowitz, University of Wisconsin-Madison— The nature of the charged particle flux through an aperture depends on the plasma conditions, geometry and electrostatic potential in the vicinity of the aperture. The presence of magnetic fields further complicates this problem. The distribution function may be distorted after passing through an aperture. Experimental conditions should be carefully handled for the purpose of diagnoses. In this paper we describe experimental investigations of the plasma potential profiles existing in front of an aperture, measured with emissive probes. The transmission of the entrance particles through a finite thickness aperture is experimently investigated and compared with the single particle orbit model. It is found that the measurement of transmission can be used as a diagnostic of plasma perpendicular temperature in the magnetic field.

*Work supported by Engineering NSF ATM-8611161.
**On leave from SWIP, P.O.Box 15, Leshan, Sichuan, China

D-31 The volume averaged nature of microwave interferometric measurements.* LAWRENCE J. OVERZET, JOHN C. MILLER, THOMAS J. MOREL AND BLAKE E. CHERRINGTON, University of Texas at Dallas, Richardson, TX 75083. — The use of microwave interferometry is spreading, particularly in the semiconductor processing industry where plasma densities tend to be low (most often below 10^{10} cm^{-3}) and the plasmas themselves can be small compared to several wavelengths at a sensitive microwave frequency. Microwave interferometry has been billed as a technique to measure the line integral of the electron density in these glow discharges.[1] In fact, microwave interferometers only measure the line integral of the electron density if a few rather restrictive assumptions can be applied. A more general set of assumptions shows the volume averaged nature of these measurements. The capabilities of the author's own interferometer will be outlined and the difficulties and advantages of the technique will be pointed out. In addition, the densities calculated from interferometric measurements of a CF_4 discharge will be presented.

* Work supported in part by Texas Instruments Inc.

[1] See for example: D.I.C. Pearson, G.A. Campbell, C.W. Domier, and P.C. Efthmion, Mat. Res. Soc. Symp. Proc. 117, 311–317 (1988).

D-32 Laser-Induced Fluorescence Doppler Width Determination of Ion Temperature in an Electron Cyclotron Resonance Plasma. E.A. DEN HARTOG, H. PERSING and R. CLAUDE WOODS. University of Wisconsin-Madison.---The transverse ion temperature ($T_{i\perp}$) is an important internal parameter of an etching plasma. If this temperature is an appreciable fraction of the axially directed energy of the ions, the anisotropy of an etch may be severely degraded. We have determined the transverse ion temperature in a nitrogen electron cyclotron resonance (ECR) plasma by measuring the Doppler broadened lineshape of a suitable N_2^+ transition using laser-induced fluorescence (LIF). LIF is a non-invasive means of measuring $T_{i\perp}$ with good spatial resolution. The ion velocity distribution is expected to vary with both radial and axial position because of known gradients in magnetic field and electric potential. $T_{i\perp}$ was measured on axis 30 cm downstream from the ECR region. Over a range of neutral pressures (0.5 mTorr $\leq P \leq$ 4 mTorr) $T_{i\perp}$ was found to vary from 0.25 eV to 0.12 eV. The axially directed ion energy is expected to be comparable to the decrease in plasma potential measured between the ECR source and downstream regions($\Delta\Phi$ = -10 eV). This results in ion pitch angles $\Theta \approx v_\perp/v_\parallel$ up to 8°.

* Work supported by NSF Grant #ECD-8721545

D - 33 Gas Kinetic Temperature Measurements in a Ch_4-H_2 Discharge,* H. N. CHU, E. A. DEN HARTOG, J. JACOBS, A. SALZBERG, K. BELL, J. E. LAWLER, L. W. ANDERSON, Engineering Research Center for Plasma-Aided Manufacturing, University of Wisconsin-Madison

We have measured the rotational temperature in a CH_4-H_2 gas discharge under diamond growth conditions using emission on both the R branch of the 3 d $^1\Sigma \Rightarrow$ 2 p $^1\Sigma$ band in H_2 and the R branch of the B $^2\Sigma \Rightarrow$ X $^2\Sigma$ band in CN. The rotational temperatures obtained from both H_2 and CN are the same. Because the collision rate for a CH_4-H_2 discharge at 30 Torr is large compared to the radiative decay rate for the excited levels in either H_2 or CN, we expect that the rotational temperature is identical to the gas kinetic temperature. The CN is observed due to impurity nitrogen in the CH_4 gas. Other bands that we have studied in the H_2 molecule are too perturbed to be useful for temperature measurements. We have observed laser induced fluorescence (LIF) using the B $^2\Sigma \Leftrightarrow$ X $^2\Sigma$ transition in CN and are studying the use of LIF for measuring the gas kinetic temperatures.

D-34 Spatially and temporally dependent EEDF measurements in an rf discharge. C.A. Anderson, University of Ulster, Coleraine, N. Ireland and W.G. Graham Queen's University, Belfast, N. Ireland - A time resolved Langmuir probe technique[1] has been used to measure plasma parameters, including the electrons energy distribution function (EEDF) in an rf driven, parallel-plate discharge, operating at frequencies of up to 1MHz. In the present discharge, except very close to the electrodes, the shape of the EEDF, at any given time during the rf cycle, is found to be quite constant throughout the discharge. The effects of changes in various operating parameters, such as rf power and gas pressure, on the EEDF have been studied. Changes in the EEDF are found to depend particularly on when the measurement is made during the rf cycle.

[1] C.A. Anderson, W.G. Graham and M.B. Hopkins. Appl. Phys. Lett. 52 783 (1988).

D-35 Observation of the Radial Motion ot the Sheath in RF Glow Discharges. J. DEROUARD, M.P ALBERTA AND N. SADEGHI, Univ. Grenoble I, France.--We present results concerning 3-dimensional spacially and time resolved electric field vector measurements in RF capacitive glow discharges through Ar,He-K mixtures. Discharges with frequency ranging from DC to several MHz were investigated using the laser Stark spectroscopy of NaK[1]. The field maps show the existence of large radial fields close to the small, powered electrode especially at the beginning of the anodic half cycle, in agreement with previous findings[2]. Also the potential distribution on the walls in DC discharges has been inferred from the comparison with numerical simulations.

[1] J. Derouard, N. Sadeghi, Opt. Comm. 57, 239 (1986)
[2] R.A. Gottscho *et al* , J. Appl. Phys. 66, 492 (1989)

D-36 A Self-Consistent Simulation of RF Glow Plasma* K.KITAMORI, Hokkaido Institute of Tech. and A.DATE and H.TAGASHIRA, Hokkaido University - The behavior of electrons, positive and negative ions and generation rate of radicals by electron collision are calculated by a Monte Carlo method allowing for the non-equilibrium of electron energy. The transport and reactions of radicals in the gas and at the electrodes are calculated by solving rate equations, using the radical generation profile obtained by the Monte Carlo model. A C-coupled SiH4 plasma for p=0.5Torr, d=2.0cm and Vrf=450V is simulated. The cross sections of SiH4 by Ohmori et al.[1] and the reaction rate constants of radicals and ions in Kushner[2] are used. The density of SiH3 radicals is found ~ 10^{12} cm^{-3} and the deposition rate of amorphous Si is estimated to be ~ 51 A/min.

*Suported in part by The Ministry of Education, Japan.

[1] Y.Ohmori,M.Simozuma and H.Tagashira, J.Phys.D,19,1029 (1986)

[2] M.J.Kushner, J.Appl.Phys.63,2332 (1988)

SESSION E

7:00 PM - 9:00 PM, Tuesday, October 16

Convention Center, Chancellor Hotel - Brundage and Zuppke Rooms

POSTERS

E-1 Time evolution of the cathode spot plasma in metal vapour vacuum arcs. I.S. FALCONER, A.J. STUDER, P.D. SWIFT, B.W.JAMES and D.R. McKENZIE, School of Physics, U. of Sydney, Australia, Ian G. BROWN and Xavier GODECHET, LBL, U. of California, Berkeley - The degree of ionization of the cathode spot of pulsed metal vapour vacuum arcs has been investigated using emission spectroscopy and time-resolved measurements of the charge-state fraction of ions extracted from the cathode spot. The intensity of emission lines from the doubly-ionised atoms relative to that of both singly-ionised and neutral atoms decreases throughout the life of the discharge, as does the fractional-charge-state of the extracted ions, for a number of cathode materials. Furthermore the current density per cathode spot is greater early in the life of the pulse. These results are significant in relation to the application of vacuum arcs to high-charge-state heavy ion sources.

E-2 Dependence of electron energy distribution on the Ar pressure in positive column of low diameter Hg-Ar lamp discharges , G. ZISSIS, M. YOUSFI, A. ALKAA, J.J. DAMELINCOURT, Univ. Paul Sabatier, CPAT, CNRS Toulouse, FRANCE.- The a priori knowledge of electron energy distribution is necessary for, in particular, discharge modeling of compact fluorescent lamps whose the study is recently again stimulated. The aim of this communication is simply to report the electron energy distribution, which is far to be a maxwellian distribution, in a positive column of a lamp discharge for super-narrow tube diameters (3 mm) under different Ar pressures (5 to 20 Torr). Electron energy distributions are calculated from a powerful and accurate two-term solution of Boltzmann equation including the most important collisional processes occurring in the gas (i.e.:elastic electron-atom collisions with energy exchange and thermal motion of atoms, inelastic electron-atom collisions including collisions with ground state and excited atoms, super-elastic electron-atom collisions, coulomb electron-electron collisions, atom-atom collisions leading to creation of new electrons in the gas). The method of calculation and the chosen collision cross sections in Ar and Hg are already described elsewhere.[1] Our results show a strong dependence on Ar pressures of the bulk of energy distribution and a more soft dependence of the tail. Such a dependence has therefore an important consequence on electron swarm parameters sensitive to the bulk distribution (electron temperature, electron mobility). The fraction of electron energy lost during elastic and inelastic collisions are also calculated. It is shown that elastic collision are the lowest (9 %) for the lowest Ar pressure (5 torr). Meanwhile the energy lost to excite the two first radiative Hg levels and also the energy lost to excite the two first Hg metastable levels remain practically unchanged during the pressure variation.

[1] M. Yousfi, G. Zissis, A. Alkaa, J.J. Damelincourt, Phys. Rev A , 1990, 42, 2

E-3 Energy Balance in Low Pressure Hg-Ar Electric Discharge Positive Column, G.Zissis, P. Bénétruy, J.J.Damelincourt, C.P.A.Toulouse France -- In this work we report the observed differences in the energy balance in the positive column of two different cases of Hg-Ar low pressure discharges. We have compared, on one hand, the "classical" discharge (radius 18mm, Ar pressure 400Pa and discharge current 400mA) and on the other one the special super narrow discharge (R=0.75mm, p=2000Pa, I=20mA). Our study has been carried out for two different partial pressures of Hg saturated vapor in the discharge plasma corresponding to two tube cold spot temperatures (0.17Pa at T_{cs}=20°C and 4.8Pa at 65°C). Energy balance has been calculated by using a self-consistent collisionnal radiative model and assuming a diffusion controlled positive column. Our main conclusions are: (a) Diffusion losses in the super narrow discharge (20% of the total power injected in the positive column) are greater than those in the classical discharge (1.4%). These losses remain almost constant (within ±15%) as a function of the cold spot temperature. (b) The evolution of the total radiation losses (UV+vis+IR, due to Hg only) as a function of the T_{cs} in the super narrow tube has been found to be faster than the classical discharge. Thus, for a classical tube we found 45% of radiation at 20°C and 80% at 65°C, for a super narrow tube we have obtained 10% and 72% respectively. (c) Elastic collision losses are more important in the case of classical tube at lower cold spot temperatures than the losses in super narrow tube at the same temperature, this is mainly due to the differences in the electron energy distribution function between the two discharges. (d) In our model the Ar ionization and Ar excitation have been included, we found that the radiation losses due to Ar, at the lower T_{cs} are more important in the case of super narrow tube (39%) than those in classical discharge (22%) but as expected they become negligible at higher cold spot temperatures (<0.5% in both cases).

E-4 Observations of Low Pressure DC Breakdowns in Weak Magnetic Fields,* S. POPOVIĆ, E. KUNHARDT, M. MARGULIES, Weber Research Institute, Polytechnic University, - We report observations of DC breakdowns around a spherical anode in Ar and N_2 at pressures between 10^{-4} and 0.1 Pa. Axial magnetic fields up to 1.8×10^{-3}T were applied. Pre-breakdown region of parameters showed an abundance of novel phenomena related to electron trapping in this electrical and magnetic field configuration. A stable toroidal volume of confined electrons could be observed as a light ring around the anode at electrical fields substantially below the DC-breakdown values. This plasma mode is stable enough to allow studies on chaotic behavior of electron trajectories and their relation to DC breakdown. The influence of external circuitry as well as space charge effects to breakdown characteristics were analyzed.

*Work supported by SDIO/IST.

E-5 Analysis of the Streamer to Arc Transition, S.K. DHALI and A. RAJABOOSHANAM, Southern Illinois University-We report the results of numerical simulations of a streamer to arc transition model for high-voltage and high-pressure discharges in nitrogen gas. Although streamers and steady-state arcs have been studied extensively, very little work has been done on the transition from streamer to the arc phase. The present model includes the important physical processes such as gas heating, neutral gas dynamics, electron-molecule, and molecule-molecule collisions that come into play in the transition of a streamer like discharge to an arc. The calculations were done in the radial direction until a quasi steady-state was reached. Our simulations indicate that the electron density, gas temperature and the arc current are all functions of the applied voltage: higher over-voltage produces a higher value of electron density, gas temperature, and nitrogen atom density. The simulation also suggests that for short duration discharge the gas heating is primarily due to the A-A quenching and the three body electron recombination.

E-6 Detection of atomic oxygen by resonant three photon ionization and two photon laser induced fluorescence,* G. SULTAN, G. BARAVIAN, J. JOLLY, L.P.G.P., (Associé CNRS), U. of PARIS-SUD 91405 ORSAY FRANCE - A method is presented which should allow the determination of absolute number density in discharge and post-discharge by simultaneous measurement of the number of photoions created by 2+1 resonant enhanced multiphotoionization (REMPI) of atomic oxygen and the laser induced fluorescence (LIF) following two photon excitation. For the first experiment [see 1], oxygen atoms are created in a dc discharge in O2 and are driven out by the gas flow to the detection chamber where a laser beam is focused, the wavelength is scanned around 226 nm. The atom density is obtained by REMPI. The LIF at 845 nm was simultaneously observed. Then the discharge was created in the interaction volume and the laser beam was focused directly into the plasma. The LIF signal previously calibrated allows the determination of O atoms density in the discharge.

*Work supported in part by DRET
[1] Chem. Phys. Letters 159, 361 (1989)
G. Baravian, J. Jolly, P. Persuy and G. Sultan

E-7 *Atomic Data for Titanium,* R.E.H. Clark and J. Abdallah, Jr., Los Alamos National Laboratory* - *In order to carry out a computer model of a non-LTE plasma, data for a variety of processes for several stages of ionization are needed. A recently developed set of computer codes has been used to calculate such data for all ionization stages of titanium. The types of data calculated are energies, oscillator strengths, electron impact excitation and ionization, photoionization, autoionization, and branching ratios for autoionization. All of the data are available in the ALADDIN system of atomic data used by the International Atomic Energy Agency.*

**This work was performed under the auspices of the U.S. Department of Energy.*

E-8 **An Atomic Energy Level Shift in Oxygen by a Long Range Ion-Atom Interaction,** N. Kwon, M. Bohomolec, M. J. Colgan, D. E. Murnick. **Department of Physics, Rutgers University - Newark, NJ 07102.** - The 3^3P-5^3S transition in atomic oxygen at 725.4 nm has been studied in a weak discharge using high resolution optogalvanic spectroscopy. The transition appears as a superposition of two components with different centroids and widths. The centroids of the two components differ by 226±28 MHz. The broader spectrum is believed due to long range interaction of ^3P neutral oxygen with $^4S_0$ ionic oxygen in the O_2^+ state($d^4\Sigma_g^+$)[1] at large internuclear separation, R. An order of magnitude estimation for R by the charge-quadrupole interaction yields 30 Å. The shifted broad spectrum explains previously puzzling asymmetric placement of oxygen laser oscillations[2] at 8445 Å originating from the ^3P level.

[1] N. Bjerre and S. R. Keiding, Phys. Rev. Lett. **56**, 1459 (1986)
[2] M. S. Feld, B. J. Feldman, A. Javan and L. H. Domash, Phys. Rev. **A7**, 257 (1973)

E-9 NITROGEN ATOMS IN Ar-N_2 FLOWING MICROWAVE DISCHARGES FOR STEEL SURFACE NITRIDING.

A.RICARD, J. DESCHAMPS, J.L. GODARD, L. FALK* AND H. MICHEL*

Plasma Phys. Lab. Bt 212. CNRS. Paris-Sud Univ. 91405 - - Orsay-(*)Science Genie Surf. Lab. CNRS - Ecole Mines - 54042 Nancy - France

High N-atom densities (10^{15}-10^{16} cm^{-3}) have been produced in high pressures (20-760 Torr) Ar-N_2 flowing post-discharges. Gas ionization is performed by 2.45GHz surfatron and surfaguide exciters with 100-200 watts transmitted power. N-atoms have been measured by NO titration and by absolute intensities of 1st positive system of N_2 in the afterglow. From kinetics analysis, the N-atom recombination rate has been found to decrease with gas temperature from $4(\pm1) \times 10^{-33}$ cm^6 sec^{-1} (T_o=296K) to 1.3×10^{-33} cm^6 sec^{-1} (T = 600K). The N-atom densities keep a value multiplied by 1 and 2 at the T = 840K nitriding temperature of steel surfaces. The growing of γ' - Fe_4N coating thickness with N atom densities in the post discharge reactor is reported.

E-10 Investigations of Efficient Photoionization Methods for Creating Highly Collisional Plasmas*, K. R. STALDER, D. J. ECKSTROM and R. J. VIDMAR, SRI International-We are beginning a program designed to investigate microwave absorption in highly collisional plasmas. Considerable effort will be placed on developing means for efficiently ionizing large volumes of high pressure gases. Our initial experiments will utilize two-dimensional, windowless spark-board arrays in helium. Two-step photoionization by resonance radiation will create a highly collisional plasma with a tailored electron density gradient which should absorb microwaves over a large bandwidth. Addition of low-ionization-potential additives will enhance the ionization yield. Plasma densities and collision frequencies will be determined from measurements using Langmuir probes and microwave interferometers. We will report our results for the spark-board experiments and on the plasma density profiles generated by these light sources.

*Work Supported by AFOSR under Contract No. F49620-90-C-0041.

E-11 Emission studies of YBaCuO laser induced plumes. H.F. Sakeek, W.G. Graham, M. Higgins, T. Morrow and D.G. Walmsley Queen's University, Belfast, N. Ireland - The laser induced plasma plume created above a YBCuO target during the production of a thin film using a KrF (248 nm) beam is being studied. The spatial and temporal distribution of emission lines, characteristic of the various atomic and molecular components of the target, is studied as a function of the lower fluence and oxygen concentration in the preparation chamber. The high resolution spectra are used to determine the velocity distribution of the different species. It is found that, in vacuum the elemental oxide emission lines are particularly sensitive to the laser fluence. The effect becomes more pronounced with the addition of oxygen. We are currently looking for a correlation of this oxide production with the thin film superconductor quality.

E-12 UV and VUV Fluorescence of High Pressure Argon Excited by Flash X-ray Source *, J.M. POUVESLE, C. CACHONCINLLE, F. DAVANLOO, J.J. COOGAN, C.B. COLLINS and F. SPIEGELMANN, GREMI, Orléans University, France, the University of Texas at Dallas, LPQ, Toulouse University, France-The fluorescence from high pressure argon plasmas (1-30 bars) has been excited with an intense flash X-ray device in this study. For the first time a UV-VUV spectrum has been recorded under such conditions of excitation. The dominant features were the so-called second and third continua of argon. The spectra[1] were very similar to the ones obtained with α particle excitation at equivalent pressures, but, in the present case, the very high levels of fluorescence were sufficient to allow time resolved spectroscopy by conventional means. In order to better understand the origin of the third continuum observed in argon, and other rare gases but He, precise calculations on ionic excimer potential curves have been performed, specially on Ar_2^{2+}. Data will be discussed at the light of these theoretical results.

* Work supported in part by NATO grant N° 890508, in part by CNRS, in part by SDIO/IST and directed by NRL.

[1] C. Cachoncinlle et al, J. Phys. D, pending.

E-13 Plasma created by TEA CO_2 laser beam on a Ti target with He as buffer gas. *C.BOULMER-LEBORGNE, J.HERMANN and B.DUBREUIL, GREMI -ORLEANS University -FRANCE- Time and spatially resolved spectroscopic study of the plasma plume created by the interaction of a TEA CO_2 laser beam with a Ti target in a cell containing He gas (0-760Torr) is achieved. The laser pulse duration is varied in the 0.1-5μs range, yielding different laser power densities. Electron density deduced from Stark broadening as well as neutral and ionic He and Ti line kinetics are measured for several gas pressures and deposited laser energies at different heigths from the target. At the beginning of the plasma pulse (0-200ns) the gas is almost completely ionised. A calculation assuming E.T.L. conditions leads to the determination of the electron temperature (5eV) at this time. Then the plasma is in recombination phasis, the electron temperature and density decrease with time. Ionisation and recombination phasis time evolution depends on gas pressure combined to laser pulse power density. From these results the experimental condition influence on the ablation process is dicussed.

* Work supported by L'AIR LIQUIDE - FRANCE

E-14 Bound-Bound and Free-Free Radiation from Recombining Oxygen Plasmas,* L.S. Dzelzkalns and W.A.M. Blumberg, Geophysics Laboratory (AFSC), P.C.F. Ip and R.A. Armstrong, Mission Research Corp. - The absolute intensity of line and continuum infrared emissions in laser-produced oxygen plasmas have been measured for gas pressures of 50-100 torr over the wavelength range of 2 to 9 microns. The oxygen atom line emission spectra were analysed using plasma line broadening theory. The plasma electron density and electron temperature were determined from fits of calculated spectra to the experimental data. The continuum infrared radiation has been measured for observation times of 2 to 20 microseconds following plasma formation. A significant component of this continuum radiation is interpreted as due to free-free scattering of electrons from neutral oxygen atoms. The wavelength dependence of the neutral Bremsstrahlung has been determined and compared with previous experimental and theoretical data.

*Work supported by the Air Force Office of Scientific Research and the Defense Nuclear Agency.

E-15 Arcing and Discharge From High Voltage Space Power Systems, *G. B. HILLARD, SVERDRUP TECHNOLOGY- The F2 region of the earth's ionosphere, through which the space shuttle, proposed space station, and many satellites operate, is characterized by an atomic oxygen plasma ($N_e = 10^6/cm^3$). As space power systems require increasingly high voltage, breakdown and arcing from negatively biased surfaces exposed to the plasma will pose severe problems. We will review the know facts about such arcing as well as the competing theoretical explanations of the breakdown process. We will argue that existing data suggests that these arcs are a special case of the classical vacuum arc and will describe laboratory experiments now underway to prove this hypothesis. We will describe an upcoming space experiment, to be flown on the shuttle in 1993, which will perform comprehensive investigations of high voltage surfaces with ionospheric plasma.
*Supported by NASA Lewis Research Center under contract NAS-25366

E-16 A Spin-dependent, Optogalvanic Effect in $^4He^*$. L.D. SCHEARER and PADETHA TIN, University of Missouri-Rolla.--We have observed changes in the electrical conductivity of a helium discharge when the metastable atoms are excited with a diode-pumped, LNA laser tuned to the helium resonance lines near 1083 nm. The plasma impedance is a function of the electron density in the cell which is controlled by either of two collisional processes: $He^m + e \rightarrow He^+ + 2e$ or $He^m + He^m \rightarrow He^+ + He + e$. The first case is the conventional optogalvanic effect which we observe by varying the intensity of the resonant laser light, thus varying the metastable density. In the second case we modify the cross section for the collision by varying the spin polarization of the metastable atoms. In a weak helium discharge metastable-metastable collisions are an important source of electrons in the plasma; consequently the plasma impedance can be controlled by modifying the collision cross-section. Since the reaction must conserve spin angular momentum the cross section for the process can be varied by optical pumping methods which orient the metastable spins. Using a diode-pumped LNA laser as the optical pumping source, we observe large impedance changes associated with the ensemble spin orientation. Orientations of nearly 100% are obtained.

*Work supported in part by The National Science Foundation.

E-17 DC Glow Discharge Modeling Applied to Diamond Film Growth Plasma Reactors, M. SURENDRA and D.B. GRAVES, U.C. Berkeley; and LINDA S. PLANO, Crystallume- We have applied a recently developed self-consistent dc glow discharge modeling and simulation technique[1] to the problem of the structure of hydrogen/hydrocarbon dc discharges used in the deposition of diamond carbon thin films. In this approach, equations for the spatial profile of electron and ion number density, electric field strength, charged particle flux and electron-impact inelastic collisions are solved numerically. Insight into the nature of molecular dissociation and energetic species densities and fluxes under conditions of interest for deposition of diamond carbon films is provided. Model results are compared to experimental measurements of optical emission; Langmuir probe estimates of ion density, electron temperature and plasma potential; and results from the application of pin-hole mass spectrometry through one electrode.

[1]M. Surendra, D.B. Graves and G.J. Jellum, Phys. Rev. A, 41, 1112, (1990).

E-18 Laser Stark Spectroscopic Measurements of Probe Perturbations in a DC Discharge, [1]T. INTRATOR, [2]M. P. ALBERTA, H. DEBONTRIDE, J. DEROUARD, and N. SADEGHI, University Grenoble I, FRANCE

We have mapped the local plasma potential in DC discharges, both with and without floating and emissive probes. Laser Stark spectroscopy of NaK was used to benchmark the electric field (integrated to give potential) measurement.[3] The potential perturbations were due to a small, movable, floating and/or current biased electrostatic probe that was positioned both inside and outside of the sheath region.[4,5] The parallel plate discharge was in He^+ and 2% K, at a neutral density of 1.2×10^{16} cm^{-3}, current density of 14 - 60 μ A cm^{-2}, with a breakdown voltage of 265 - 385 Volt.

---

[1]Partially supported by Univ. de Grenoble; and NSF Grant ECS-8704529
[2]Dept NEEP, Univ. Wisconsin
[3]J. Derouard and N. Sadeghi, Optical Communications 57, 239 (1986)
[4]D. Diebold *et al.*, Rev. Sci. Instrum. 59, 270 (1988)
[5]T. Intrator *et al.*, Journ. Appl. Phys. 64, 2927 (1988)

E-19 Electric Field Measurement in the Cathode Sheath of a Glow Discharge in Hydrogen, C. BARBEAU and J. JOLLY, LPGP (CNRS), U. Paris-Sud, 91405 Orsay France - Electric field intensity measurements have been performed in the cathode fall region of a DC hydrogen glow discharge. The technique, based on polarization dependent Stark broadening of plasma-induced emission of the Balmer lines, has a dynamic range from a few tens of volts/cm to kilovolts/cm. The theoretical Stark relative intensities of the π-components of the Hδ line were computed under dipolar electric approximation, using the method described by Lüders.[1] As hydrogen excited atoms may have high kinetic energies in the cathode fall region,[2] we use the observation of the Doppler broadened Hα emission profile to determine the velocity of the atoms, and afterwards to calculate a "synthetic profile" of the Hδ line. The experimental and calculated profiles are in very good agreement. The entire cathode fall region was investigated. The axial electric field variation is linear over most of the cathode sheath.

[1] Lüders G., Ann. Phys. 8, 301 (1951).
[2] Barbeau C., Jolly J., To be published in J. Phys. D. 23 (1990).

E-20 A NEW EMISION SPECTROSCOPIC SET-UP FOR NON-LTE PLASMA STUDIES,*K. ETEMADI, S. AKBAR, SUNY/BUFFALO, ECE DEPARTMENT-A new fully automated emission spectroscopic set-up is described for non-LTE plasma studies. The set-up consists of a 3/4 meter spectrograph with an OMA for recording molecular spectra or line broadening, 0.5 m monochromator with a specially designed exit slit for simultaneous measurements of a spectral line with its neighboring continuum, a computerized plasma scanning system and a spectrograph wavelength control system. For non-LTE studies the elctron number densities of an Ar+H(2%) free-burning arc at atmospheric pressure is determined by the broadening of H line and compared with the densities derived by the absolute line intensity measurements . The data acquisition time for measuring H , a spectral line and continuum of Ar at 10 axial and 50 radial locations in the arc was minimized to less than 10 second.

*work supported by NSF Grant # CTS8910685.

E-21 In-situ Gas Conversion of Trimethylarsine into Homologs using a Downstream Near Afterglow Plasma.* B. G. PIHLSTROM, T. SHENG, Z. YU, and G. J. COLLINS, Colorado State U.-The downstream near afterglow region of either a helium or hydrogen plasma, where the electron temperature is below 0.3 eV, has been used to decompose and convert trimethylarsine (TMAs) to arsenic and carbon bearing gas products analyzed using a mass spectrometer. Methylarsine homologs, $(CH_3)_nAsH_{3-n}$, including arsine, AsH_3, were generated with an upstream hydrogen plasma but not with a helium plasma. We employed an upstream deuterium plasma in order to verify via isotopic tagging that the major source of the arsenic hydrogenation was from the upstream plasma and not hydrogen fragmented from the trimethylarsine. In the near afterglow hydrogen plasma the major TMAs hydrocarbon gas conversion products created was methane with a hydrogen plasma whereas with a helium plasma ethane, ethylene and acetylene were formed.

*Work Supported by SERI, Contract # XM-0-19142-9

E-22 **Diamond Synthesis in a 50 kW Inductively Coupled Atmospheric Pressure Plasma Torch**, T.G. OWANO, C.H. KRUGER, and M.A. CAPPELLI, Stanford University- Polycrystalline diamond coatings have been deposited on molybdenum and silicon substrates using a 50 kW inductively coupled atmospheric pressure plasma torch. The argon-hydrogen-methane plasma generated has a free stream active area of 35 cm^2, with temperatures and electron densities of approximately 5000 K and 2×10^{14} cm^{-3}, respectively. Growth rates are on the order of 10 μm/hr. Growth morphology is found to be sensitive to reactor conditions such as surface temperature and hydrogen-to-carbon gas feed ratio. Spectroscopic analysis of the gas phase, as well as intrusive gas sampling is compared with models of the reacting environment. Scanning electron microscopy indicates that well facetted crystals are obtained with growth along the 100 and 111 planes. Nearly continuous films are also formed and found to be of lower quality. Raman scattering data is used to compare the bonding structure to that obtained by other various deposition techniques.

E-23 Influence of the Energy Spectrum of Electrons Ejected from the Cathode on Electron Behaviour in the Cathode Sheath of Glow Discharges in Helium and in Argon, R.J.CARMAN, Macquarie University, Sydney, Australia. The form of the energy distribution of electron flux (EDEF) at the cathode sheath/negative glow boundary of a low–pressure glow discharge has been evaluated to investigate the influence of the initial energy spectrum of electrons ejected from the cathode by secondary emission. The calculations have been carried out using a simple one–dimensional model* which assumes forward scattering of the electrons in the sheath during all elastic and inelastic collisions and a linearly decreasing electric field. Comparisons between the calculated results and measured** EDEF profiles at the sheath/negative glow boundary for a helium glow discharge with a cathode fall of ≈200V exhibit close agreement. Notably, the structure of the high energy "tail" region of the EDEF including the unscattered "beam" electrons agree well. The results also suggest that electrons are ejected from the cathode predominantly by He^+ ion bombardment under such conditions.

*R.J.Carman and A.Maitland J.Phys.D 20 1021 (1987).
**P.Gill and C.E.Webb J.Phys.D 10 299 (1977).

E-24 Instantaneous Etch Rate Measurement of Thin Transparent Films by Interferometry for use in an Algorithm to Control Plasma Etcher, H. L. Mishurda and N. Hershkowitz, Engineering Research Center for Plasma Aided Manufacturing, University of Wisconsin - Madison -- A goal of our ERC is to develop a feedback system to control a plasma etcher. A RIE plasma etcher is used to etch 1μm of thermally grown SiO_2 with a gas mixture of $CHF_3/CF_4/O_2$. The time constants of the plasma's response to changes in external variables which are critical to the operation of the feedback loop will be discussed. A thin-film interferometer is used to measure the change in film thickness and via a computer interface and algorithm computes the instantaneous etch rate. The etch rate will be used as feedback to optimize the etch process by changing the RF power, pressure, and gas flow. Results will be presented showing interferometric traces and the instantaneous etch rates computed from them. Optical emission data will also be presented and compared to the etch rate measurements.

* Work supported by NSF Grant No. ECD-8721545

E - 25 Comparison of Electrical Characteristics of GEC RF Reference Cells,
P. J. Hargis, Jr., K. E. Greenberg, P. A. Miller, and J. B. Gerardo, Sandia National Laboratories,
R. A. Gottscho, AT&T Bell Labs,
A. Garscadden and P. Bletzinger, Wright-Patterson,
J. R. Roberts, J. K. Olthoff, J. R. Whetstone, and R. J. Van Brunt, NIST,
H. M. Anderson, M. Splichal, J. L. Mock University of New Mexico,
M. L. Passow, M. L. Brake, and M. E. Elta, University of Michigan,
D. B. Graves, U. C. Berkeley,
M. J. Kushner and J. T. Verdeyen, University of Illinois,
G. Selwyn and M. Dalvie, IBM Yorktown,
J. W. Butterbaugh and H. H. Sawin, MIT,
T. R. Turner and R. Horwath, SEMATECH.

The design of a GEC rf Reference Cell was initiated at the 1988 Gaseous Electronics Conference workshop. The Reference Cell was developed to facilitate the comparison of experimental and theoretical rf discharge data obtained by different researchers. Measurements have been made to determine whether or not cells installed in various laboratories across the United States display the same electrical characteristics for a particular set of input parameters. In particular, voltage and current waveforms, dc bias, and discharge power were measured for argon discharges operating at pressures from 0.1 to 1.0 Torr and peak-to-peak driving voltages from 75 to 200 Volts. A simple model, which accounted for capacitance and inductance of the Reference Cell, was used to determine the actual plasma voltage and current from the measured voltage and current waveforms. A comparison of these initial data sets will be presented.

E-26 NIST GEC Reference Cell Measurements,* J. R. ROBERTS, J. K. OLTHOFF, R. J. VAN BRUNT and J. R. WHETSTONE, NIST-Measurements performed on the NIST GEC Reference Cell are presented. These measurements include base pressure, operating pressure, leak rate, gas flow rate, and current for various voltages. An RF power supply operating at 13.56 MHz is capacitively coupled to the floating electrode of the Reference Cell (the other is grounded and the electrode spacing is 1"). The electrode temperature is also monitored. The current and voltage waveforms are analyzed for their phase shift difference with and without the plasma. Also Fast Fourier Transforms are performed on these waveforms and the amplitude of up to the fifth harmonic is reported. The power dissipated in the plasma and the DC bias are deduced from these voltage and current measurements. These data are taken at four different pressures; 0.1, 0.25, 0.5 and 1.0 Torr. Flow rates of 2.0 and 20.0 sccm of 99.999% pure Ar are used. Performance with and without ground shielding of the electrodes is also discussed. Preliminary measurements of the optical emission of detectable plasma species is presented and their radial and longitudinal profiles are measured.

* Work partially supported by SEMATECH.

SESSION GA

8:00 AM - 9:55 AM, Wednesday, October 17

Convention Center, Chancellor Hotel - Illiniwek Room

PLASMA CHEMISTRY

Chair: J. Goree, University of Iowa

GA-1 RF Discharge Deposition of SiO_2 in N_2O-SiH_4 Mixtures, L. E. KLINE, W. D. PARTLOW, R. M. YOUNG, R. R. MITCHELL and T. V. CONGEDO, Westinghouse STC -- We used experiments and modeling to characterize the deposition process. We measured the dissociation of N_2O and the mixtures in a parallel plate reactor by downstream mass spectrometry. The gas flow direction is parallel to the electrodes. The measured amount of dissociation varies with the input energy per molecule (eV/mol) The primary downstream products are N_2, O_2, and NO in pure N_2O. In the mixtures the downstream densities of O_2 and NO are much lower, compared with pure N_2O, and SiH_4 is observed only at low eV/mol values. The film thickness (t) and index of refraction (n) were measured ellipsometrically vs. SiH_4 flow rate and input power, at 10 KHz and 13.56 MHz with total flow = 146 sccm, pressure = 0.5 Torr and dep. time = 15 min. The Si wafer substrates were placed in the center of the lower, grounded electrode. n and t were measured at several positions on the wafer. A plug flow, rate equation model was used to predict the dissociation and deposition rates vs. position on the wafer, as a function of the process settings. Rate coefficients were calculated for electron processes, taken from the, literature for gas phase processes and estimated for surface processes. SiH_3, Si_2H_X and Si_3H_X are assumed to contribute to film deposition. The major reaction pathways were identified. SiH_4 is lost primarily by reaction with O atoms. The predicted downstream product densities and film thickness variations agree with experiment.

GA-2 Diagnostics and Modeling of Reactive RF Glow Discharges in SiH_4.* T. MAKABE, F. TOCHIKUBO and S. KAKUTA, Keio University Yokohama, Japan-Diagnostics for the RF glow discharge at 13.56 MHz in pure SiH_4 and SiH_4(50%)/H_2 between 0.1 and 1 Torr has been performed by the spatiotemporally resolved optical emission spectroscopy. A new experimental evidence has been given for the plasma structure in SiH_4. The spatiotemporal net dissociation rate shows the marked profile with the three peaks in space and two peaks in time. This will be caused by the negative ions, SiH_n^- in SiH_4. Owing to the trapping of the bulk negative ions by the positive ion sheath in front of the electrode, SiH_n^- gradually accumulates and grows up to the density comparable with the positive ions. Consequently, the decrease in the sheath width, the increase of the bulk field and the double layer formation at the plasma/sheath boundary appear, as the constituent in RF discharge changes from the electron/positive ion system to the positive/negative ions system including the active minority, electrons. It is roughly confirmed theoretically by the relaxation continuum model.

*Supported in part by the Grant-in-Aid for Scientific Research on Control of Reactive Plasmas on Priority Areas.

GA-3 Modeling and Optical Diagnostics of Reactive RF Glow Discharges in CH_4 at 13.56 MHz.* T.MAKABE, N.NAKANO, A.Suzuki F.Tochikubo, Keio University, Y.Yamaguchi, Mitsubishi Kasei Corporation, Yokohama, Japan - The RF glow discharge in CH_4 at 13.56 MHz has been simulated in order to look at the physical picture characterized by a collision dominated plasma. The second-stage modeling related to the excited and radical species has been performed as well as the first-stage modeling relative to the discharge structure and electrical property by using the Relaxation Continuum Model. The model is based on the microscopic collision cross sections or the reaction rate coefficients between the electron(or ion) and molecule, and is independent of the macroscopic empirical relations. Also the space- and time- resolved optical emission spectroscopy has been executed in the same outer discharge condition. It is shown that the coincidence of the spatiotemporal behaviour of the dissociative species, CH(A), CH(B) and CH(C) is reasonably good between the theory and experiment. The radical, CH(X), CH_2(X) and CH_3(X) are characterized by the densities of 10^{11}, 10^{12} and 10^{13} cm^{-3} at 1 Torr and 26 $mWcm^{-2}$.

*Supported in part by the Grant-in-Aid for Scientific Research on Control of Reactive Plasmas on Priority Areas.

GA-4 Simulation of Remote and Direct Plasma CVD of Silicon Alloys.* Mark J. Kushner, Timothy J. Sommerer and Yilin Weng, University of Illinois, 607 E. Healey, Champaign, IL 61820. In Remoted Plasma Enhanced Chemical Vapor Deposition (RPECVD), the plasma is upstream of the substrate. A nondepositing gas is excited in the plasma zone and the deposition gas is injected downstream to produce the deposition radicals by excitation transfer reactions. We have developed a comprehensive computer model for RPECVD using rf and Electron-Cyclotron-Resonance sources. The model uses new algorithms to account for upstream diffusion in a plugflow formulation. RPECVD of SiO_2 using O_2/TEOS and rare gas/SiH_4 mixtures will be discussed and compared to direct plasma CVD in parallel plate rf discharges. We find that the upstream diffusion of feedstock gases into the plasma zone generates radicals not otherwise produced in the RPECVD process. Design constraints to prevent this occurrence will be described.

*Work supported by IBM East Fishkill and The National Science Foundation (ECS88-15781 and CBT88-03170).

GA-5 In-situ Generation of Arsine by Using Elemental Arsenic Source, T. SHENG, Z. YU, and G. J. Collins, CSU- In situ generation of the toxic polyatomic gas, AsH_3 and associated radicals AsH_x has been achieved. We employ elemental arsenic, a hydrogen gaseous feedstock source, and a plasma generated in hollow cathode discharge to form the various arsenic hydrides. Only when all those conditions are present will the desired but dangerous gas production occur thereby allowing for rapid on/off control and safer operation should an inadvertent leak occur downstream from the source. Toxic hydrides besides AsH_3 such as H_2Se, B_2H_6 and PH_3 may also be generated.

GA-6 Translationally Hot Neutrals in CF_4 Discharges for Plasma Processing.* Timothy J. Sommerer and Mark J. Kushner, University of Illinois, 607 E. Healey, Champaign, IL 61820. Models of low pressure plasmas usually assume that hot electrons drive all inelastic and dissociative processes, and that the neutral gas can be adequately described by a Maxwellian distribution of velocities having a temperature near the ambient. Translationally hot (many eV) neutral fragments, though, can be produced by dissociative excitation. At pressures significantly < 1 Torr, the fragments may not thermalize before striking the substrate. In this paper we will investigate the effects of translationally-hot neutral fragments in a CF_4 rf discharge. Electron impact rate coefficients are obtained from a self-consistent, kinetic calculation of a CF_4 discharge.[1] The source rates for hot CF_4 fragments (primarily CF_3 and F) are found from a 1-D plasma chemistry model, and the hot neutral transport is modelled using a Monte Carlo simulation. The distribution of hot radicals striking the substrate will be discussed as well as the resulting impact on etching.

[1]T.J. Sommerer, W.N.G. Hitchon and J.E. Lawler, *Phys. Rev.* A39, 6356 (1989); *Phys. Rev. Lett.* 63, 2361 (1989).

*Work supported by IBM East Fishkill Facility.

GA-7 Particle Generation in Boron Trichloride/Methane/Hydrogen RF Discharges, H.M. Anderson, J. L. Mock, Univ. of New Mexico, Albuquerque, NM. The rate of particle generation from an annular ring cathode rf plasma has been studied as a function of the discharge operating parameter space and $BCl_3/CH_4/H_2$ gas mixtures. This reactor configuration has been used previously [1] to produce bulk quantities of particles under conditions similar to SiN PECVD. In this study, an etchant feed gas (BCl_3) was mixed with a carbon source (CH_4) to gain insight into possible mechanisms for **in situ** particle generation under conditions closer to plasma etching. No particles were formed in the discharge in the absence of CH_4, but bulk quantities of a boron carbide-like powder were produced after several hours using mixtures of BCl_3 and CH_4 in a 1 to 3 ratio. Laser light scatter- was used to qualitatively determine the onset of particle presence in the gas phase. Lag times on the order of 20-30 minutes were observed between striking the discharge and the appearance of scattered light signals in the gas phase. These results are contrasted against previous studies on SiN particle generation.

1) H.M. Anderson, et. al. J. Appl. Phys. **67**, 3999(1990).

SESSION GB

8:00 AM - 10:00 AM, Wednesday, October 17

Convention Center, Chancellor Hotel - Grange Room

MODELING AND DIAGNOSTICS OF LAMP-LIKE DISCHARGES

Chair: P. Vicharelli, GTE

GB-1 Generation and Diagnostics of Surface Wave (SW) Plasmas, M. MOISAN, U. de Montréal, Québec H3C 3J7. The SW produced plasma results from the propagation of an electromagnetic wave which uses the plasma column it sustains and its enclosing dielectric vessel as its sole propagating media. The wave is launched from a localized exciter, a few cm long. There now exists a variety of wave launchers [1-3] allowing one to operate from approximately 1 MHz to 10 GHz with full coupling of the HF power from the generator. There is no limitation on the plasma column length (up to 6 m demonstrated) which grows with the HF power to the launcher. A large variety of plasma column diameters (0.5-150 mm demonstrated) and shapes using various gas compositions and pressures (10^{-4} Torr up to a few times the atmospheric pressures, depending on the discharge tube diameter) have been created. The different diagnostics employed to characterize the SW plasma will be reported together with a list of its applications.

1. Ro-Box: M. Moisan and Z. Zakrzewski, Rev. Sci. Instrum. 58, 1895 (1987)
2. Surfatron: M. Moisan, Z. Zakrzewski and R. Pantel, J. Phys. D 12, 219 (1979)
3. Waveguide-surfatron: M. Moisan, M. Chaker, Z. Zakrzewski and J. Paraszczak, J. Phys. E 20, 1356 (1987).

GB-2 Surface Wave Discharges as Fluorescent Lamps.* D. LEVY, Lawrence Berkeley Laboratory – A standard 1" (T8) discharge tube was operated at 60 Hz using its electrodes and at 200 MHz not using its electrodes. For the same amount of electric power delivered to the discharge tube, operation at 200 MHz without electrodes produced >1.35 × the 254 nm resonance radiation that operation at 60 Hz with electrodes did. The measurements were carried out in a tightly controlled thermal environment. Experimental estimates of the tube's end-voltages were made. Longitudinal and angular measurements of the 254 nm radiation were made. Potential applications to general lighting will be discussed.

* This work was supported by the Assistant Secretary for Conservation and Renewable Energy, Office of Buildings and Community Systems, Building Equipment Division of the U.S. Department of Energy under Contract No. DE-AC03-76SF00098.

GB-3 **Optical Radiation Efficiency of Surface Wave Produced Plasmas as Compared to DC Positive Columns.** **J. MARGOT-CHAKER, M. MOISAN and A. RICARD***, *Département de physique, Université de Montréal, Montréal, Québec, H3C 3J7*-- The influence of the high frequency (HF) field (200-900 MHz), gas pressure (0.05-1 Torr) and plasma density on the radial density distribution of excited atoms in a cylindrical HF sustained discharge of the surface wave type is experimentally examined through optical emission spectroscopy, using a tomography technique. These results illustrate the rôle of the radial inhomogeneity (so-called skin effect) of the wave electric field intensity on the radial density distributions of excited atoms. This set of data completed by similar measurements for the positive column of a DC discharge was further used to investigate the optical radiation efficiency as a function of the field frequency. Under certain discharges conditions, this efficiency goes through a maximum at approximately 200 MHz. The reason for such a behaviour calls on the frequency dependence of both the radial density distribution of excited atoms and the electron energy distribution function, the latter determining how the power absorbed from the HF electric field is shared between ionization and excitation processes. These various results are compared with Ferreira and co-workers' self-consistent model for DC and surface wave discharges in argon.

**Physique des Plasmas, Université Paris-XI, 91405 Orsay, France.*

GB-4 Ambipolar Diffusion Theory of the Hot Cathode Negative Glow, JOHN INGOLD, GE Lighting, Cleveland, OH 44112– Ambipolar diffusion theory of the negative glow (NG) and Faraday dark space (FDS) of a cylindrical glow discharge maintained by thermionic emission from a hot cathode is described. Electrons are divided into two groups: thermionic beam electrons and plasma electrons. Radial diffusion losses are handled by introducing the usual diffusion length. Inputs to the model include probabilities of excitation and ionization by thermionic beam electrons and by plasma electrons, electron and ion temperatures and mobilities, and discharge tube radius. The model predicts the following measured quantities[1] with good qualitative agreement: (a) combined length of NG plus FDS; (b) axial distribution of plasma electron density; and (c) ion current to cathode. The model also predicts two field reversals in axial electric field: one in the NG near the cathode where axial current is supported by ambipolar diffusion, and one near the end of the FDS at the beginning of the positive column where axial current can no longer be supported by ambipolar diffusion.

[1]J. F. Waymouth, J. Appl. Phys. **30**, 1404 (1959).

GB-5 Quantitative Spectroscopy on Hg^+. J. E. LAWLER, R. C. WAMSLEY, Univ. of Wisconsin and J. H. INGOLD, L. BIGIO, and V. D. ROBERTS, General Electric Co. --A variety of laser and classic spectroscopic techniques for ground state Hg^+ density measurements in Hg-Ar discharges are investigated. The advantages and disadvantages of various techniques such as single photon laser induced fluorescence (LIF), multiphoton LIF, and absorption will be discussed. No single technique offers high signal-to-noise ratios, excellent spatial and temporal resolution, a three dimensional mapping capability, and straightforward absolute calibration. A combination of several techniques is best. Absolute Hg^+ density measurements in Hg-Ar discharges based on a simple, inexpensive absorption experiment are reported. This experiment utilizes a 0.5m echelle monochromator and a Xe arc lamp as a continuum for absorption spectroscopy at 194 nm.

GB-6 Spatial Maps of Hg^+ and Hg^* Densities in the Cathode Region. R. C. WAMSLEY, J. E. LAWLER, Univ. of Wisconsin and J. H. INGOLD, L. BIGIO, and V. D. ROBERTS, General Electric Co.--Spatial maps of the absolute density of ground state Hg^+ ions and 6^3P^o excited Hg^* atoms extending from the hot cathode to the positive column in Hg-Ar discharges are reported. The lamps have 2.5 Torr of Ar, an inner diameter of 3.49 cm, and are operated at 200 mA and 400 mA. A combination of absorption and laser induced fluorescence techniques is used for mapping these absolute densities. Numerous features of the negative glow, Faraday dark space, and positive column are visible in these maps. The peak ion density in the negative glow at 400 mA is 5×10^{12} cm^{-3}. The minimum axial ion density in the Faraday dark space is 2.8×10^{11} cm^{-3}. An overshoot in the ionization and excitation rates exists at the beginning of the positive column. These maps are compared to earlier (Hg^+) probe measurements in the cathode region and (Hg^*) spectrosocpic measurements in the positive column.

SESSION H

10:30 AM - 11:30 AM, Wednesday, October 17

Convention Center, Chancellor Hotel - Illiniwek and Grange Rooms

ALLIS PRIZE LECTURE

Chair: J. Gerardo, Sandia Laboratories

H-1 The Diffusion of Charged Particles in Collisional Plasmas: Free to Ambipolar Diffusion and Low to High Pressures,* A.V. PHELPS, JILA, University of Colorado and NIST. - We tie together models of charged particle diffusion in quiescent, weakly ionized plasmas. The diffusion length, screening length, effective diffusion coefficient, and partially reflecting boundaries are reviewed. A map is used to correlate published models covering the complete range of the scaling parameters of the ratio of the diffusion length to the screening length and the ratio of the diffusion length to the ion mean-free-path. The description of space charge effects begins with a review of the conventional derivation of diffusion in the high pressure, ambipolar limit.[1] The results for other limiting cases, such as the very low pressure ambipolar limit[2] and the transition from free to ambipolar diffusion at high pressures,[3] are reviewed. The numerical calculations[4] covering all of the map are approximated by empirical, analytical formulas.[5-7] Finally, applications of diffusion models to electrical discharges, afterglows, etc. are illustrated.

* Work supported in part by NIST.

1. W. Schottky, Phys. Z. 25, 635 (1924).
2. L. Tonks and I. Langmuir, Phys. Rev. 34, 876 (1929).
3. W.P. Allis and D.J. Rose, Phys. Rev. 93, 84 (1954).
4. J.H. Ingold, Phys. Fluids 15, 84 (1972).
5. C.H. Muller,III and A.V. Phelps, J. Appl. Phys. 51, 6141 (1980).
6. P.J. Chantry, J. Appl. Phys. 62, 1141 (1987).
7. A.V. Phelps, J. Res. Nat. Inst. Std. Tech., (in press) (1990).

SESSION K

1:30 PM - 3:30 PM, Wednesday, October 17

Convention Center, Chancellor Hotel - Brundage and Zuppke Rooms

POSTERS

K-1 An Improved String Model for Profile Evolution With Redeposition*, T.J. DALTON**, S.C. JACKSON*** and H.H. SAWIN, Massachusetts Institute of Technology – Pattern dependencies in plasma etching processes are observed through variations in the local topography. The modeling of profile evolution in plasma etching processes is important for developing an understanding of pattern dependencies. The profile simulator is used to understand the physics of etching profile evolution, to examine the effects of mask geometry and resist sidewall profile, and to guide experiments.

Profile evolution is simulated using a string model. This model has been enhanced over previous string models to correct errors in the profile evolution caused by faulty interface movement. Including the correct physics eliminates the need for a de-looping algorithm common to other string models. The string model has been enhanced to include redeposition of sputtered materials and the subsequent passivation of surfaces by this redeposited layer. We will show how variations in physical properties (such as the sticking coefficient) and local geometry affect the etching profile. In the future, we intend to use surface kinetic data gathered at MIT to realistically model profile evolution in fluorocarbon plasmas.

*Work supported in part by SEMATECH and DuPont
**Supported by National Science Foundation
***DuPont ETL, Wilmington, Deleware.

K-2 Voltage and current characterization for measuring rf power delivered to a process chamber, JAMES F. RUPERT, KEITH J. BRANKNER, and LAWRENCE J. OVERZET†, Texas Instruments Inc., Dallas TX 75265 — We have characterized voltage and current sensors used in acquiring both the instantaneous and time averaged rf power delivered to a process chamber. Data was collected on the phase and magnitude response of these sensors using a matched 50 ohm transmission line. These measurements show significant sensor roll-off and sensor induced phase shifts, which occur as a function of frequency, and result in measurement inaccuracy of rf power at the fundamental 13.56Mhz source frequency and its associated harmonics. The induced sensor phase shift was measured by two methods. Peak waveform crossings are read directly off the oscilloscope. Comparison phase readings are obtained by calculating phase error with the following equations for power: $P=(V*I)_{avg}$ and $P= V_{rms} * I_{rms} * \cos(\theta)$. As a follow on experiment, to verify sensor robustness, various reactive components were added in parallel to the transmission line. Finally, the rf power delivered to SF_6 and Argon discharges will be shown..

† University of Texas at Dallas, Richardson, TX 75083.

K-3 Imaging of the density distribution of vibrationally excited oxygen via laser induced predissociative fluorescence.* L.M. HITCHCOCK, G. KIM, G.P. RECK, and E.W. ROTHE, Wayne State University -- We use a method described by P. Andresen et al.,[1] that yields 2-D images of state-specific molecular densities. It is based on a variant of laser induced fluorescence that eliminates the effect of collisional quenching. Molecules in a desired quantum state are excited to predissociating states that are so short-lived that they do not collide. A ribbon of narrow-band excimer-laser light passes through a medium. The laser's wavelength is tuned, in the range 193-193.8nm, to a desired transition. The fluorescence light is filtered and then recorded by an intensified CCD camera. One laser pulse yields an image. The time scale is fixed by the ≈15ns laser-pulse width. We show images of spatial distributions of O_2 in v"-2, J"=17.

1. P. Andresen, A. Bath, W. Gröger, H. W. Lülf, G. Meijer, and J. J. ter Meulen, Applied Optics 27, 365 (1988).

K-4 Two Electrons Group Model of a RF Glow Discharge in Argon. Comparison with Experimental Results, J. DEROUARD, H. DEBONTRIDE, N. SADEGHI, U. Grenoble I, France, P. BELENGUER, J.P. BOEUF, U. Paul Sabatier, Toulouse, France RF glow discharges have been studied with a numerical self consistent model based on a fluid description of the electron and ion transport coupled with Poisson's equation for the electric field[1]. The results are compared with electric and spectroscopic measurements performed in RF plasma discharges through pure Ar and Ar-K mixtures ($p < 1$ Torr, $\nu \sim 4$ - 9 MHz, $V = 40$ - 300 V). Calculation and experiments show the existence of two distinct discharge regimes ("wave riding" and "secondary electron" regimes) where the mechanism of electron energy gain are distinct : These two regimes are associated with different space and time distribution of the plasma emission, which are well reproduced by the self consistent model.

[1]P. BELENGUER and J.P. BOEUF, Phys. Rev. A 41, 4447 (1990).

K-5 Simulation of an ECR Microwave Plasma Etching Reactor. M. HUSSEIN and G. A. EMMERT, University of Wisconsin-Madison--Plasma is simulated in the source and downstream regions of an ECR microwave plasma etching reactor. The simulation is kinetic in which a Monte Carlo description for the ion dynamics, coupled with Boltzmann electrons is used to develop an iterative scheme for solution of the kinetic equation and quasi-neutrality. Collisions between ions and neutrals are included in the context of Monte Carlo techniques. In the source region, a two group electron energy model is used to describe the electron distribution function and to calculated the different interaction rates. Ionization of the neutral gas by energetic electrons is represented by a distributed ion source in the resonance cavity. The scaling of plasma density and potential with microwave power and neutral gas pressure is investigated. For the downstream region, the effect of the divergent magnetic field on the plasma potential profile, the floating potential, and the energy distribution of the ions incident on the specimen are presented. Comparison between the simulation results and experiment is also presented.

K-6 Comparison of Fluid and Particle Simulations of RF Glow Discharges. T.E. NITSCHKE, M. SURENDRA and D.B. GRAVES, U.C. Berkeley - Particle-in-cell/Monte Carlo simulations of RF parallel plate electrode glow discharges are compared to fluid model simulations in helium. The particle simulations have the advantage of being able to treat highly non-equilibrium, non-local phenomena, but they are relatively expensive computationally. For many future applications of discharge simulation, multiple spatial dimensions and neutral transport and chemistry will be important, and computational cost will become an issue. We explore the ability of a fluid model to treat discharges at pressures low enough that collisional mean free paths are not the smallest length scale. In particular, the limits of applicability of the local field approximation, the isothermal electron model and the use of the electron energy balance in general are tested by comparison with particle simulation results.

K-7 **Magnetron Plasma Transport Simulations,** J. GOREE, M.J. GOECKNER, and T.E. SHERIDAN, Dept. of Physics, Univ. of Iowa -- Molecular-dynamics simulations of electron and ion transport are carried out for a dc magnetron sputtering plasma. Individual particles are followed in 3 dimensions using prescribed dc electric and magnetic fields. We take into account elastic, excitation, and ionizing collisions by electrons; and elastic and charge exchange collisions plus low-frequency turbulence for ions. These codes predict the spatial distribution of ionization in the plasma; ionization efficiency; energy cost of operation; and the spatial, angle, and energy distribution of ion impact on the electrodes. We have tested these results against experimental measurements of the cathode erosion profile as well as in-situ Langmuir probe and LIF measurements, and found good agreement in most cases. Repeating the simulations for various pressures and magnetic fields gives insight into the physics of magnetron operation, and may offer a way to design better devices.

K-8 Dose Uniformity of Plasma Source Ion Implantation Applied to a Wedge Shaped Target*, M. SHAMIM, J. T. SCHEUER and J. R. CONRAD, Plasma Source Ion Implantation Group, Univ. of Wisc., Madison, WI 53706.

In Plasma Source Ion Implantation (PSII)[1] a target is immersed in a plasma and pulse biased to a high negative voltage (~50kV) promising better uniformity of the implanted dose than that achieved by conventional beamline implantation. We have applied PSII nitrogen implantation to a mild steel wedge shaped target. Auger electron spectrometry of the implanted nitrogen depth profile and Knoop microhardness have been performed at several locations on the target to test the uniformity of the implanted dose. Comparison of these results to theoretical predictions[2] will be presented.

* This work supported by NSF Grants ECD--8721545, ECS-8314488 and DMC-8712461, US Army Grant DAAL03-89-K-0048 and by a number of industrial grants.

1 J. R. Conrad, J. Radtke, R. A. Dodd and F. J. Worzala, J. Appl. Phys. **62**, 4951 (1987).

2 P. A. Watterson, J. Phys. D: Appl. Phys. **22**, 1300 (1989).

K-9 Measurement of Bimaxwellian Electron Distributions in rf Diffusion Plasmas Operated near ECR, R.W. BOSWELL and C. CUI, Aust.Nat.Univ. – In the WOMBAT apparatus plasmas are generated at ~ 1 mtorr in a 20 cm diameter source by a loop Prf antenna and allowed to drift into an 80 cm diameter 120 cm long diffusion region. The magnetic fields of the source and diffusion region can be controlled independently. Electron 'temperatures' are measured by the propagation of Bernstein waves across the plasma which gives a value for the average perpendicular electron energy. Single langmuir probes are used to determine the 'temperature' of electrons with energy greater than the plasma potential (i.e. the tail). These two mentods yield differences of at least a factor of two with hydrogen and argon with a factor of 9 being measured for hydrogen when the rf is at the ECR. The Bernstein measurement is always lower. Detailed analysis of the langmuir probe traces showed although the tail temperature was high, electrons collected for biases greater than the floating potential were significantly cooler. These represent greater than 90% of the electrons and they are trapped in the potential well created by the sheaths. The bulk temperature is a minimum and the tail temperature a maximum at ECR. The measurements suggest that the parallel temperature is significantly higher than the perpendicular temperature.

K-10 Investigation of Segmented Hollow Cathode Discharges, *,** D.BRUNO, H.KIRKICI, and B.R.CHEO, Polytechnic University, New York. - Hollow cathode discharges are considered as a main plasma source of gas lasers, due to their high current density capacities at lower voltages compared to planar structures. It is also known that hollow cathode operation is possible at high operating pressures[1]. The hollow cathode effect is geometry dependent, i.e. 1 torr-cm$<$pD$<$10 torr-cm, for rare gases[2]. One can achieve wider operating pressure ranges by embedding one hollow cathode geometry within another. In this work we studied a segmented hollow cathode geometry which consists of spaced segments forming a spherical hollow cathode. The spacing between the segments is one hollow cathode geometry and the spherical structure is another hollow cathode geometry. Different cathode materials such as Tungsten, Molybdenum, and Graphite segments with Nickel spacers were investigated. Experiments with these different cathode materials and different gases, Ar, He, were performed.

With this device operating pressures of 0.1 mbar to 250.0 mbar have been achieved, V-I characteristics have been obtained. Results and findings are discussed.

* Work supported by Air Force Office of Scientific Research.

** Initiated by G. SCHAEFER who passed away during proceedings of work.

1. G. Schaefer "Fast Plasma Mixing-A New Excitation Method for CW Gas Lasers," IEEE-J. Quantum Electronics, QE-22, pp.2022-2025, Oct. 1986

2. J.W. Gewartowski and H.A. Watson, Principles of Electron Tubes, Chapter 15, van Nostrand, 1965.

K-11 Particulates in Low Pressure Discharges, G.M. JELLUM, J.E. DAUGHERTY, M.D. KILGORE and D.B. GRAVES, U.C. Berkeley - The tendency of particulates in low pressure plasmas to charge negatively and remain suspended in the glow has been widely reported. However, the importance of thermal forces in influencing particle motion in low pressure glow discharges has not been as widely recognized. We have conducted a series of experiments to help test the relative importance of electrical and thermal forces on particulates in glows and in the afterglow. In addition, observations concerning the formation of various types of particle aggregates and subsequent spatial segregation of these aggregates are reported. We find that macroscopic, chain-like particle aggregates form under some conditions, with their long axis aligned with the electric field, located at the plasma-sheath interface. A fluid model of the plasma with equations for particulates added is explored to help understand and explain these and related phenomena.

K-12 Simulation of Ion Mass Measurement with Fourier Transform Mass Spectrometry in a Bounded 1D Plasma,*. J.B. Friedmann, A.T. Johnson, and J.L. Shohet, Engineering Research Center for Plasma-Aided Manufacturing, U. of Wisconsin-Madison-Fourier Transform Mass Spectrometry[1] (FTMS) is a technique which can be used to determine the mass spectrum of a plasma. The physical properties of a bounded electrostatic plasma are described with a kinetic simulation in one planar dimension including the effects of self-consistent fields. The goal of this project is to simulate the motion of ions of various species and observe the self-consistent interaction and its effects on the mass spectra of a plasma in a FTMS system through the use of the modified bounded electrostatic plasma code PDP1[2].

*Work supported by the National Science Foundation under Grant No. ECD. 8721545.

[1]A.G. Marshall, *Acc. Chem. Res.* 19, 316-322(1985).

[2]W.S. Lawson, *Jour. of Comp. Phy.* 80, 253(1989).

K-13 Negative ion measurements from modulated rf discharges,* LAWRENCE J. OVERZET AND LAIZHONG LUO, University of Texas at Dallas, Richardson, TX 75083. — We have used a new technique to examine the negative ions present in several discharges related to semiconductor processing.[1] We have observed over 15 different negative ions from a CF_4 discharge and similar numbers of negative ion peaks from fluorine-helium and chlorine-helium mixtures. Under some conditions, the expected dominant ion is not dominant. In the low power discharge through fluorine and helium, the negative ion signal at 123 amu (probably SiF_5^-) can be significantly larger than the signal from F^- at 19 amu. The 123 amu ion likely results from the slow etching of the pyrex reactor walls and is observed in CF_4 discharges too. Finally, the time dependent signals from large mass negative ions are significantly different than those obtained from light negative ions. The causes behind these differences will be presented.

* Work supported in part by the National Science Foundation under the Research Initiation Program.

[1] "Enhancement of the negative ion flux to surfaces from radio-frequency processing discharges," J. Appl. Phys. 66, 1622–1631 (1989).

K-14 Investigation of Oxygen Discharges by CARS*, C. BOISSE-LAPORTE, G. GOUSSET, A. GRANIER, M. LEFEBVRE, J. MAREC, M. PEALAT, R. SAFARI, M. TOUZEAU, M. VIALLE, LPGP (CNRS), U. Paris-Sud, 91405 Orsay and ONERA, Châtillon France -- Rotational and vibrational temperatures have been measured by CARS in low pressure oxygen discharges (0.2-10 Torr) created in a 16 mm in. diameter pyrex or quartz tube. Both a DC (discharge current, Id = 5 to 80 mA) and a surface wave (2450 MHz, Power, P = 100-800 W) discharge have been studied and compared. In the DC discharge the vibrational temperature Tv = 300-900 K is equal to the rotational temperature Tr for deposited power ranging from 0.2 to 5 W/cm, while in the surface wave discharge Tv (Tv = 900-1800 K) is slightly higher than Tr (Tr = 400-1600 K) when the deposited power ranges from 4 to 70 W/cm. These results can be explained by an efficient creation and loss of O_2 vibrational levels by collisions with oxygen atoms. The radial distribution of Tv and Tr has also been measured in the two discharges. The interpretation of all these results is in progress.

* Work supported in part by D.R.E.T.

K-15 Energy analysis of the Diffusion Plasma from an Inductively Excited Discharge. Peter Bletzinger, Propulsion and Power Laboratory, WPAFB, OH.-In this experiment, the excitation region was seperated from the diffusion space by a wire grid and terminated by a metal plate with a .3 mm opening into a retarding grid analyzer. A DC bias could then be applied to the diffusion space. Electron energy distributions over the pressure range of 0.005 to 0.5 Torr in argon show a strong increase of the high energy portion at pressures below 0.03 Torr and a shift in the distribution peak form 3 V (0.5 Torr) to 13 V (0.005 Torr). A negative bias on the end plate will shift the distribution by the bias voltage with little change in shape but an increase in n_e. With positive bias only the high energy portion of the distribution has also been observed. Below 0.1 Torr the peak energy decreases with increasing power, above that pressure it increases. Possible interpretations of the energy deposition mechanisms relating to this change will be discussed.

K-16 **Transition to the Collisional Plasma Sheath.** T. E. SHERIDAN and J. GOREE, *Dept. of Physics, The University of Iowa.* -- We include ion collisionality in a fluid model for the planar plasma sheath. In contrast to previous work, we use a collision cross section with a general power-law dependence on the ion velocity. Approximate solutions for both the collisionless and highly collisional (mobility limited) regimes are derived, and useful expressions for the amount of collisionality at which the transition between these regimes occurs are presented. These expressions are found to be in good agreement with numerical solutions of the exact equations. Additionally, we calculate the dependence on collisionality of: sheath thickness, ion energy at cathode impact, and potential variation in the sheath.

K-17 Stable operating conditions for cathode-fall dominated discharges in H_2, N_2, and Ar,* Z.Lj. PETROVIĆ** AND A.V. PHELPS, JILA, University of Colorado and NIST. - The operating conditions for diffuse, stable cathode-fall dominated discharges in parallel plate geometry were measured in H_2, N_2, and Ar for pressures from 0.3 to 3 Torr, currents from 10^{-6} to 0.1 A, and series resistances of 10^3 to 10^7 Ω. The spacing between the gold electrodes was 11 mm and their diameter was 80 mm. For H_2, oscillations were observed for a broad range of currents I and resistances R, even when the voltage-current V-I characteristic was almost constant. On the other hand, constrictions were observed only at the highest H_2 pressure and did not coincide with the oscillations. A portion of the I-R plane was not accessible because of the negative V-I characteristic. For Ar and N_2, oscillations were observed only for 0.3 and 3 Torr and the conditions for oscillations coincided with those for the onset constrictions, i.e., large negative resistance.

* Work supported in part by Wright Research and Development Laboratory.
** Permanent address: Institute of Physics, Belgrade, Yugoslavia.

K-18 Small-Angle Electron-Sodium Absolute Differential Cross Sections, 3-20 eV,* C. H. YING, F. PERALES, L. VUŠKOVIĆ, and B. BEDERSON, New York U.,- Extending previous work at 10 eV[1], we have measured 3 eV to 20 eV electron scattering by ground state sodium. Absolute differential cross sections for 3S→3P will be presented in the angular range 1° to 20° or 30° depending of impact energy. From these results partial integral cross sections are estimated. Data will be compared with two-state[2] and many-state[3] close coupling calculations. Details of deconvolution procedures used to obtain absolute (i.e., not normalized) cross sections will be presented.

* Research supported by U.S. National Science Foundation.
[1]T.Y. Jiang, C.H. Ying, L. Vušković, and B. Bederson, submitted to Phys. Rev. A (1990).
[2]D.L. Moores and D.W. Norcross, J. Phys. B 5, 1482 (1972).
[3]H.L. Zhuo, D.W. Norcross, G. Snitchler, and D.A. Staufer, Bull. Am. Phys. Soc. **35**, 1170 (1990).

K-19 Critical Evaluation of Electron Cross Sections for Molecules of Interest in Plasma Processing, W. L. MORGAN, Kinema Research, 18720 Autumn Way, Monument, CO 80132

I am performing critical evaluations of electron collision cross sections for Cl_2, HCl, F_2, CH_4, CF_4, and SiH_4 in order to provide a consistent set of cross sections for use in modeling the plasma chemistry of discharges used in plasma processing of semiconductors. The evaluation process has included computing electron swarm parameters for the various sets of cross sections that have appeared for these molecules and comparing with available measurements. The results of this survey will be presented along with recommendations for cross sections to be used in discharge modeling.

Research supported by the National Institute of Standards and Technology.

K-20 **Metastable Production Following Electron Impact Dissociation of O_2.*** L. LECLAIR, J.J. CORR and J.W. McCONKEY, University of Windsor, Canada.--We have developed a new crossed-beams apparatus to study the production of metastable fragments following electron-impact on oxygen-containing molecules. A high current, magnetically focussed electron gun is used to dissociate the target molecules. Metastable fragments drift through a differentially pumped region and form excimers on a freshly-deposited solid xenon surface. The resultant optical radiation is detected with a cooled photomultiplier. Pulsing of the electron current allows discrimination against direct electron impact fluorescence and also allows the kinetic energy of the O-fragments to be obtained from their measured flight times to the detector. Both time-of-flight and excitation function data will be presented at the Conference.

* Research supported by the Petroleum Research Fund administered by the American Chemical Society and the Natural Sciences and Engineering Research Council of Canada.

K-21 **High-Resolution V.U.V. Polarization Studies of Rare Gas Resonance Radiation Following Electron-Impact Excitation.*** C. NOREN and J.W. McCONKEY, University of Windsor, Canada.--We have developed a crossed gas and energy-selected electron beam source coupled with a single-reflection polarization analyzer to study the near-threshold excitation of the rare gas resonance lines. Conservation of angular momentum arguments predict a threshold polarization of unity for ^1P excitation and this is clearly demonstrated for the first time using a helium target. Data will be presented illustrating the effects of resonances, cascade and in the case of the heavier targets, the competition between direct and exchange excitation.

* Research supported by the Natural Sciences and Engineering Research Council of Canada.

K-22 Total Electron-Excitation Cross Sections of the $4p^5 5p$ States of Krypton and Pressure Dependence of Associated Emission Cross Sections,* JOHN E. GASTINEAU and TODD G. RUSKELL, Lawrence University—The energy dependence (10-100eV) of absolute optical emission cross sections of the ten Paschen 2p levels of krypton have been measured with the optical method. The emission cross sections vary by a factor of up to 2.5 in the range of 100 μT to 5 mT, which is a much weaker dependence compared to Paschen 2p cross sections of xenon[1]. The pressure dependence is strongest at energies above 35 eV, and cross sections below 25 eV are essentially independent of pressure effects. The higher energy cross sections for the $2p_2$, $2p_3$ and $2p_9$ levels reach low pressure limits by 200 μT and the absolute apparent cross sections have thus been determined. Estimates for the other 2p apparent cross sections are obtained by mild extrapolations. The apparent cross sections range from 0.6 to 8×10^{-18} cm^2 for the $2p_4$ and $2p_8$ levels respectively.

*Supported by a William and Flora Hewlett Foundation Grant of Research Corporation and by Lawrence University.

[1]Gastineau *et al*, 39th Gaseous Electronics Conference.

K-23 Electron Excitation of the $1s_5$ Metastable Level of Argon. R. SCOTT SCHAPPE and CHUN C. LIN, U. of Wisconsin--Since there is no emission of radiation from the $1s_5$ metastable level of the argon atom, the standard optical method for measuring electron excitation cross sections must be modified in order to determine the cross sections for the $1s_5$ level. An electron beam passes through argon atoms in a collision chamber at a pressure of about a few mTorr. The $1s_5$ metastable atoms produced by electron excitation are pumped by a laser to the $2p_2$ level. The intensity of the subsequent $2p_2 \rightarrow 1s_3$ emission as a function of the electron energy is used to determine the shape of the apparent excitation function of the $1s_5$ level. At high electron energies (above 100 eV) the direct excitation cross section of the $1s_5$ level is very small compared to the cascade cross section so that the latter can be used for absolute calibration of the apparent cross section.

K-24 Electron Impact Optical Cross Sections for Xenon,* J. D. Clark, Kim Rimkus, Wright State University, and C. A. DeJoseph, Jr., Wright-Patterson A. F. B.--- Electron impact optical excitation functions for more than 100 transitions in xenon have been measured over an electron energy range of 10 to 150 eV. These measurements were made in the spectral range of 700-4000 nm using a commercial Fourier Transform Spectrophotometer and an electron gun built in-house. Last year[1], we reported results on the lasing transitions from the 5d levels. We now report on additional transitions from more than nine manifolds of states including the 6p, 6p', 7p, 8p, 5d, 5d', 6d, 4f, and 5f levels. Many transitions lie in the i.r. region beyond the wavelength range of photomultipliers and these play an important role as cascades into lower lying levels. This cascade can be appreciable for many levels such as the 5d and 6p levels. The magnitude of the cascade and determination of level cross sections will be discussed.

* Research Supported by AFOSR

[1] DeJoseph *et al*, 42nd Gaseous Electronics Conference, p. 122.

K-25 **Electron Impact Infrared Excitation Functions in Krypton**, C. A. DeJoseph, Jr., Wright-Patterson A.F.B., J. D. Clark and Kim Rimkus, Wright State University* - Electron impact excitation functions over an electron energy range of 10 to 150eV have been measured on a number of transitions in Krypton over the spectral range of approximately 1000-4000 nm. These include transitions from the 4d, 4d', 6s, 6p, and 7s levels (Racah). Measurements were made using a low energy electron gun designed and built in-house together with a commercially built Fourier Transform Spectrophotometer. Excitation functions were measured at 1, 2, and 4 mTorr. In addition, the pressure dependence of the cross sections was investigated at 50eV over a pressure range of 0.2 to 10 mTorr. Mechanisms for the observed pressure dependence of the excitation functions will be discussed.

*Research supported by AFOSR.

K-26 **Partial and Total Electron Impact Ionization Cross Sections of CF4 from 20 to 500 eV**, * Ce Ma and Russell A. Bonham, Dept. of Chemistry, Indiana U. Partial electron impact ionization cross sections for CF3+, CF2+, CF+, F+, C+, CF3++ and CF2++ were measured from 20 to 500 eV by time-of-flight experiements. The total ionization cross sections were obtained from the charge number weighted sum of the partial ionization cross sections. The total ionization cross section increases rapidly between 20 and 65 eV and reaches a maximum 7.9 ×10E-16 (cm^2) at 140 eV. It decreases gradually to 5.2 ×10E-16 (cm^2) at 500 eV. Our results compared the measurement of Stephan et al [1] (up to 180 eV), is about a factor of 2 higher even though the cross section shapes agree. A theoretical calculation, using the Gryzinski's formula, [2] gave a maximum cross section of 9.7 ×10E-16 (cm^2) but the peak appears at lower energy.

* Work supported by the NSF through grant number PHY-8913096.

[1] K. Stephan et al, J. Chem. Phys. 83, 5712(1985).
[2] "Electron-Molecule Interaction and Their Applications", ed. Christophoron., V.1, p305, 1984.

K-27 Ionization and Attachment Cross Sections of Organophosphonates* P.J. CHANTRY and C.B. FREIDHOFF, Westinghouse STC.-- Total ion cross sections have been measured for electron beam energies 0-500 eV for dimethyl methyl- (DMMP), diisopropyl methyl- (DIMP), and diethyl methylphosphonate (DEMP), and for diethyl methyl phosphonothiolate (DEMPT). Mass resolved relative ion signals have also been measured, and normalized to the totals. In all cases the parent positive ion is a minor product above threshold, and there are typically ten or more fragment ions of significant magnitude. Positive ion thresholds for the listed molecules are 10.4, 9.8, 9.4, and 10.4 eV respectively, corresponding to the appearances of 124^+, 139^+, 152^+, and 168^+ amu. ions. The total dissociative ionization cross sections peak near 90 eV with values of 0.91, 2.05, 1.28, and 0.79 x 10^{-15} cm^2 respectively. The major negative ion products are 16^-, 137^-, 123^-, and 17^-, with peak cross sections of 0.7, 8.8, 1.4, and 1.6 x 10^{-19} cm^2 occurring at 7.1, 3.1, 3.1, and 8.9 eV respectively.

*Supported by Aero Propulsion and Power Laboratory, Wright Research and Development Center, WPAFB, Ohio.

K-28 **Total Electron Scattering and Dissociative Attachment Cross Sections of SF_6-Discharge By-products.*** J. K. OLTHOFF, R. J. VAN BRUNT, *NIST*, H.-X. WAN, J. H. MOORE, and J. A. TOSSELL, *U. of MD* — A full understanding of the physical processes occurring in SF_6 discharges requires a detailed knowledge of the interaction of free electrons with SF_6 and its by-products. Using an electron transmission spectrometer, absolute total electron scattering cross sections for SF_6, SO_2, SOF_2, SO_2F_2, SOF_4, SF_4, and S_2F_{10} have been measured as a function of electron energy over the range of 0.2 eV to 12 eV. Absolute cross sections for negative ion formation through electron attachment have been measured from 0.2 eV to 5 eV. These results are compared with previous data where available and, for example, agree well with the mass spectrometric studies of Sauers *et al.*[1] Calculations have been carried out to identify the negative ion states involved in the electron attachment processes.

[1]I. Sauers, L. G. Christophorou, and S. M. Spyrou, in *Gaseous Dielectrics IV*, Pergamon Press, New York, pp. 261–272 (1984).

*This work supported by NSF Grant No. CHE-87-21744 and the U.S. Department of Energy.

K-29 Dissociative Electron Attachment Cross section of Ozone, S.Kajita, Y.Kondo and S.Ushiroda, Toyota College of Technology, Toyota, Japan 471- Electron attachment coefficients have been measured for the dissociative attachment process of ozone by moderate energy electrons in the oxygen containing a small amount of ozone using a drift tube. Through the self consistent analysis of the Boltzmann equation using a set of cross sections of oxygen, the experimental results of the attachment coefficient and the contents of ozone, we obtained the dissociative electron attachment cross sections of ozone. The results are shown in Fig.1. Curve (A) is the result of Stelman et al.

Fig.1

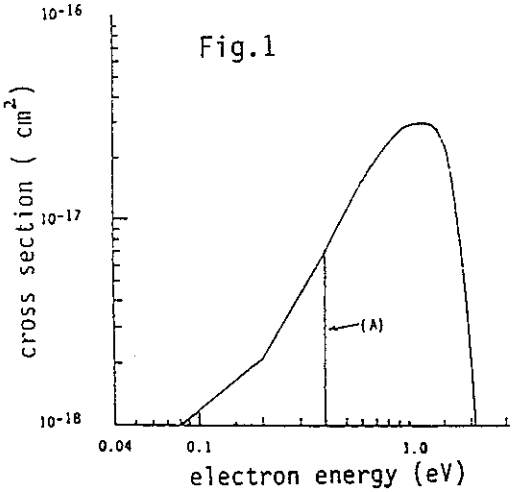

Stelman D., Morruzi J. and Phelps A., J.Chem. Phys., 56, 89(1972)

K-30 The Effects of Oxide Doping on Barium Evaporation, R.D. GROVES and B.A. SMEDLEY, GE Lighting – Fluorescent lamp emission mix consists of oxides of Ba-Sr-Ca to enhance electron emission at low temperatures (1350 K). The lifetime of a fluorescent lamp depends primarily on the evaporation rate of the free barium formed when the triple oxide reacts with the tungsten face of the coil. Past work has shown that the addition of zirconium oxide reduces this rate by a factor of two to three and thus increases lamp life. This work investigates the addition of alternate oxides of the Lanthanides as well as selected oxides of Groups III, IV and V to the emission mix and studies their effects on the evaporation rate. Resonance radiation absorption as well as temperature profile measurements of the cathode have allowed us to present the first quantitative study of these additives and their effect on barium evaporation. This work finds that the addition of some Lanthanides can accelerate this evaporation rate by up to a factor of 30 and addition of the others have reduced or maintained the rate of the control. In addition, these rare earths have a decided effect on the work function as the operating temperature of the electrodes at a given current density change as these are added. It is hypothesized that these additives are causing a distortion in the triple oxide crystal structure thus affecting the work function.

K-31 Thermionic Emission from Oxide Coated Electrodes in Low Pressure Discharge: P. HLAHOL, A.S. AWADALLAH, and A.K. BHATTACHARYA, GE Lighting, Cleveland, OH - The zero-field electron emission from Ba-Sr-Ca oxide coated tungsten ribbons in a rare gas plus Hg filled diode measured using the techniques described earlier will be reported (1). The zero-field electron emission and the work function were found to be dependent upon the nature and pressure of the fill gas in the temperature range of 1000--1200 K, in agreement with Waymouth (2). The dependence of the 'work function' on the gas pressure is determined by Ba coverage on the electrode. Barium content on the electrode surface is determined by the balance between the evaporation of Ba from and back diffusion onto the surface, which are dependent on the surface temperature, gas composition and pressure.

(1) P. Hlahol and J. DeLuca, Proc. Symp. High Temp. Chemistry, ed. E. Zubler, 88-4, Electro. Chem. Soc. (1988); (2) J.F. Waymouth, Electric Discharge Lamps, The M.I.T. Press, Cambridge, Mass, 1979.

K-32 A Diode Array System for Measuring the Temperature of Discharge Lamp Electrodes, A. AWADALLAH and A. BHATTACHARYA, GE LIGHTING

A tool to measure discharge lamp electrode temperature using two color pyrometry and absolute intensity is described. An optical system consisting of a diode array, a spectrometer and a data acquisition system was used to collect and manipulate the spectral data. This technique provides a one shot measurement of the temperature profile along an operating lamp electrode. A diode array (1024 elements) provides a very high spatial resolution (0.025 mm). A fully automated system provides a quick and repeatable temperature measurement. Applications of such an instrument for measuring the temperature distribution on electrodes of an operating fluorescent lamp are demonstrated. Electrode temperature is found to depend on the electrode design, manufacturing processes and discharge current. Temperature of test lamp electrodes in 40 W rapid start and 96 W slimline lamps were measured in the range of 1350-1400 K and 1425-1475 K respectively.

K-33 Optogalvanic Spectroscopy of Ground State Scandium Ions in a High Pressure Metal Halide Discharge, JERRY KRAMER, GTE Labs - Pulsed laser irradiation of ground state scandium ions in a vertically burning 60 Hz high pressure metal halide discharge decreased the voltage required to sustain the discharge. The scandium ions were excited at 363.1 nm from the a^3D_2 spin-orbit component of the ground state (68 cm^{-1} above the ground state) to the $z^3F_3^0$ state. The optogalvanic Sc^+ signals were compared with the optogalvanic signals from excitation of an excited state of neutral Hg at 365.0 nm ($6^3P_2 \rightarrow 6^3D_3$). The Sc^+ and Hg optogalvanic signals had the same polarity and very similar temporal response. The optogalvanic signals from Sc^+ and Hg had a similar non-linear dependence on laser energy. The comparison between Sc^+ and Hg suggests that a common mechanism produces the optogalvanic signal for ions and neutral atoms in this high pressure discharge. The radial and axial dependences of the Sc^+ optogalvanic signals were compared with laser induced fluorescence (LIF) measurements. The radial optogalvanic profiles were compressed relative to the LIF profiles, but the axial optogalvanic profiles showed good agreement with the LIF values. From 355 to 370 nm there was a good correspondence between the optogalvanic and emission spectra. The transitions in this wavelength range are from Sc^+ and Hg.

K-34 Effects of rotation and magnetic field on a high pressure Hg arc, P.Y. Chang and J.T. Dakin, GE Lighting, Cleveland, OH 44112–A numerical model is used to study the combined impact of gravity, arctube rotation, and magnetic field on convection in a high pressure arc. The model solves the Navier Stokes equations for laminar compressible flow combined with the electric current continuity equation in a three-dimensional curvilinear coordinate system. Temperature dependent fluid properties are taken from a separate discharge model which assumes local thermodynamic equilibrium, and includes rigorous treatment of radiation trapping. Model calculations are presented for a 1 atm, 400 W Hg arc in a 3.33 cm i.d. arctube with 15.5 cm electrode separation. The model results are compared with those obtained experimentally for the same conditions by Kenty.[1] Convection patterns predicted by the model for various values of the rotation rate, magnetic field, and orientation relative to vertical are presented. Different approaches to creating a straight horizontal arc are shown to involve significantly different convections.

[1]C. Kenty, J. Appl. Phys., **9**, 53 (1938).

K-35 Validation of a 3-dimensional computer model of a high pressure discharge lamp. L. CIFUENTES, Thorn Lighting Ltd., Lamp Research. A 3-dimensional model which includes the fluid flow, heat transfer and current continuity equations and implements a finite volumes method, has been validated against measurements carried out on a horizontal burning, commercially available metal halide lamp (MBIL). Inputs to the model include the lamp geometry, arc tube and electrode material properties, the transport properties of the plasma and the current. The model predicts the arc bowing and the position of cool and hot spots; it also predicts the voltage drop across the arc gap and the wall temperatures within 20% of the measured values. Plots for temperature distribution, electric field and velocity vectors are presented.

K-36 Measurement of the Power Density Distribution within an Operating Surface Wave Discharge Lamp, A. T. ROWLEY, THORN Lighting Ltd., Leicester, U.K. - A thermal imaging camera has been used to measure the variation of power density, $\emptyset$, along the length of a surface wave discharge sustained in a mercury-argon environment. At low powers, $\emptyset$ falls away linearly from a maximum value near the launcher to zero at the end of the discharge. At higher powers, when the surface wave has been reflected from the end of the discharge tube, different distributions of $\emptyset$ are seen. A simultaneous measurement of the light output along the discharge enables the variation of light production efficiency to be calculated and the dependence of efficiency on power density to be determined. In this example, the optimum power density is about 0.25 W/cm^3.

K-37 Surface Waves in Highly Collisional Plasmas.* G.G. LISTER, THORN EMI Central Research Laboratories.UK and T. ROBINSON, University of Leicester, UK.-The theory of surface waves in cases where the electron-atom collision frequency, ν, is large compared to the applied frequency ω is discussed. Analytic solutions are found for the case where the axial electron density profile is linear, and numerical solutions for the dispersion relation are presented. This is an extension of the formalism of Gradov and Stenflo[1] for collisionless, electro-static surface waves with large density gradients. Results are compared with those obtained using the standard WKB approximation for the weak collisional limit ($\nu/\omega \ll 1$).

*Part of this work was completed at THORN Lighting, Leicester

[1]O.M. Gradov and L. Stenflo, Plasma Phys. and Contr. Fusion 26, 759 (1984)

SESSION LA

3:30 PM - 5:35 PM, Wednesday, October 17

Convention Center, Chancellor Hotel - Illiniwek Room

ALTERNATIVE CONFIGURATIONS FOR PLASMA PROCESSING

Chair: A. Garscadden, Wright-Patterson Air Force Base

LA-1 RF Diffusion Plasma Etching Systems, R.W. BOSWELL and A.J. PERRY, Aust.Nat.Univ. – Low pressure plasmas have been generated for some decades using external coupling. Resonant circuits used can involve tapped capacitors or inductors, slow wave structures and auto-resonant circuits (1/4 and 1/2 λ coupling). Our experimental and theoretical work has concentrated on a form of resonant slow-wave structure which, in the presence of a magnetic field, excites a Helicon wave. At low rf powers, the discharge is capacitive with a high Q resulting in high undesirable antenna voltages and rf plasma potentials. Depending on gas pressure, rf power and magnetic field, a mode change occurs, and the discharge becomes inductive with a significant decrease in Q and increase in plasma density.
In this mode, high density diffusion plasmas of 30 cm diameter have been achieved using both multipole and solenoidal confinement. Excellent etch rates of Si, SiO_2, resist and $GaAs$ have been achieved at pressures up to 1 Pascal.
The performance of this source will be compared with other low pressure systems (MIE, DECR, Microwave, ECR, helical resonator).

LA-2 Multipolar Confined Reactor Configurations, T.D. MANTEI, U. of Cincinnati - This paper will describe recent progress in the use of multipolar magnetic field plasma confinement geometries for dry processing applications. Multipolar confinement was first described by Sadowski[1] and by Limpaecher and MacKenzie.[2] The principal advantages include increased plasma densities, better plasma parameter uniformity and reduced operating pressures. A short summary will be given of multipolar configurations and early confinement studies. Then electrical probe measurements and etch results will be presented for a microwave electron cyclotron resonance (ECR) multipolar discharge. Plasma densities at the substrate in excess of 10^{11} cm^{-3} are routinely achieved at sub-millitorr pressures. Radial plasma uniformities of 2-4% are measured at one millitorr over a 20 cm diameter, becoming less uniform at lower pressures. Vertical etch rates in Si of 300 to 1100 nm/min are obtained with SF_6 at 0.3 to 1.0 mT. A new multipolar ECR reactor with a permanent magnet axial field source will also be described.

1. M. Sadowski, Phys. Lett. 25A, 695 (1967).

2. R. Limpaecher and K.R. MacKenzie, Rev. Sci. Instrum. 44, 726 (1973).

LA-3 Magnetron Etch Reactor Configurations. S. BOBBIO, MCNC Center for Microelectronics

There are currently a number of excitation methods which are capable of producing high plasma density for high rate wafer-at-a-time etching. Ultimately, however, the discharge must be coupled to the semiconductor wafer in a way to promote the most efficient etching for a given etch chemistry. In this presentation, the subject of plasma/wafer coupling will first be discussed generally, and then focused to a remote source magnetron configuration which optimizes the ion energy across the wafer sheath and which has been developed at MCNC. Two very different examples will illustrate the effect of the ion energy on the activated etch chemistry: polymer etching in Oxygen and polysilicon etching in Bromine.

LA-4 Studies of volume and surface reactions in low pressure reactors by modulated excitation. J. DEROUARD, J.P. BOOTH+, A. BOUCHOULE*, P. RANSON*, N. SADEGHI, Univ. Grenoble I, France.--The kinetics of H, O and F atoms in plasma reactors has been studied by time resolved optical emission spectroscopy (actinometry) in modulated plasmas. The experiments were performed in both inductively coupled RF (13.56 MHz) and microwave (2.54 GHz) DECR, low pressure (1-10 mTorr) reactors. In some experiments we observed the transient emission following the switching on of the plasma. In other cases the time evolution of the different species in the afterglow was monitored using the emission induced by a short (~ 50 μs) RF probe pulse. This enabled us firstly to determine the relative importance of dissociative excitation processes compared to direct excitation in the formation of the radiating atomic states. Secondly this enabled us to measure the reaction probability of radicals on the chamber surfaces. For example, the recombination probability of H on Si is found to be large, about 0.5. On the other hand we found that F atoms inhibit the reaction of O on stainless steel.

+ CNET Meylan, France.
* GREMI, Univ. Orléans, France.

LA-5 "Electron Cyclotron Resonance Sources for Plasma Processing", Richard C. Myer, Applied Science and Technology, Inc., 35 Cabot Road, Woburn MA 01801. Electron cyclotron resonance (ECR) plasma sources are being used in an increasing number of applications for semiconductor processing and hard coatings. The ECR is an ideal source of ions for many applications as it provides a high flux (J_i > 10 mA/cm^2) of low energy ions (E_i ~ 20 eV). This talk will deal with some of the physics issues associated with ECR source operation, including microwave coupling and absorption, power balance, ion and radical fluxes, and the relationship between the electron energy, ion energy, and plasma potential. Engineering issues such as choice of wall materials, the effects associated with pumping, and scaling to larger areas will also be discussed. Data taken from sources including plasma measurements and examples of deposited films will be presented.

SESSION LB

3:30 PM - 5:15 PM, Wednesday, October 17

Convention Center, Chancellor Hotel - Grange Room

LAMPS AND HIGH PRESSURE DISCHARGES

Chair: J. Dakin, GE Lighting

LB-1 Near-Resonance Electronic Raman Scattering Measurements of $Hg(6^3P_1)$ in a Low-Pressure Hg-Ar Discharge, L. BIGIO, General Electric Corporate Research and Development Center ---Use is made of near-resonance electronic Raman scattering as a pinpoint spatially resolved diagnostic to measure the radial density distribution of $Hg(6^3P_1)$ in the positive column of a low-pressure Hg-Ar discharge. The discharge tube has an inner diameter of 34 mm, is filled with 2.52 Torr argon, and is operated at 400 mA dc. The intermediate and final states used are the 7^3S_1 and 6^3P_2, respectively. The absolute on-axis density is determined by calibrating with a known amount of H_2, given the relative Raman cross-sections for the two systems. This yields a density of $1.9\pm0.3\times10^{11}$ cm^{-3} which is ~43% lower than that measured earlier using a different method.[1] Radial distribution results compare well with those from the earlier measurements.[1] The depolarization ratio, $\rho=\sigma_{zx}/\sigma_{zz}$, is also measured and found to agree with theory.

[1]L. Bigio, J. Appl. Phys. 63, 5259, (1988).

LB-2 *Optically-Thick Diagnostics of Arc Lamps Using a Retroreflective Array*, S. COURIS, T. FOHL, and P. A. VICHARELLI, *GTE Laboratories Incorporated, Waltham, MA*— Emission and absorption coefficients have been measured in optically thick regions of the spectrum of an axisymmetric high intensity Hg arc lamp. First, the spatial distribution of the absorption coefficient as a function wavelength is determined. This is accomplished by using a retroreflective array (RRA) to reflect arc radiation back upon itself. The idea of using the arc emission as an external source for absorption measurements is not new,[1] but optical distortion due to the arc tube walls makes it very difficult to insure alignment of the paths of the emitted and absorbed light if a conventional mirror is used. The use of an RRA to reduce the effects of such distortions in flames has been studied by Peck and Morris.[2] We have confirmed that the RRA is effective in limiting such aberrations in quartz arc tubes. Once the absorption coefficient as a function of radial position is known, a series of measurements of the integrated intensity for various chordal line-of-sight offsets may be Abel inverted to yield local emission coefficients. Values for the absorption/emission coefficients and the optical depth as functions of position and wavelength for several optically-thick Hg lines will be presented.

[1]W. Lochte-Holtgreven, *Plasma Diagnostics* (North-Holland, Amsterdam, 1968).

[2]K. Peck and M. D. Morris, Rev. Sci. Instrum. **58**, 189 (1987).

LB-3 The Detection of Ground State Scandium Ions in a High Pressure Metal Halide Discharge by Saturated Laser Induced Fluorescence, JERRY KRAMER, GTE Labs - Ground state scandium ions in a vertically burning 60 Hz high pressure metal halide discharge were detected by saturated laser induced fluorescence (LIF).[1] Scandium ions were excited with a pulsed dye laser at 363.1 nm from the a^3D_2 spin-orbit component of the ground state (68 cm^{-1} above the ground state) to the $z^3F_3^0$ state. The LIF, observed at 440.0 nm ($z^3F_3^0 \rightarrow a^3F_3$), was optically thin. The Sc^+ LIF profiles along a diameter were asymmetric about the center, with a local minimum near the axis, and maxima at about ± 2 mm (radius = 6.5 mm). The profiles varied with axial position and lamp power. The LIF Sc^+ signals are modulated during the ac phase angle. At the discharge axis the maximum signals occur just after the current zero crossings (near the voltage reignition spikes) and the minima just after the current maxima. LIF was also observed from other nearby excited electronic states of Sc^+, populated by collisions. From the positional dependence of the ratio of the fluorescence at 437.5 ($z^3F_4^0 \rightarrow a^3F_4$) to 440.0 nm we suggest that neutral scandium atoms are responsible for the collisional energy transfer.

[1]J. Kramer, J. Appl. Phys. 67, 2289 (1990).

LB-4 Dielectric-Barrier Discharges as a Source of narrow-band VUV, UV or Visible Excimer Radiation, B. GELLERT, B. ELIASSON, and U. KOGELSCHATZ, ASEA BROWN BOVERI, Corporate Research, 5405 Baden, Switzerland - More than 20 different excimers could be generated in dielectric-barrier discharges (silent discharges). The excited species include rare gas dimers, halogen dimers, rare gas halogen excimers, rare gas mercury excimers and mercury halogen excimers. Their emission spectra range from 126 nm (Ar_2^*) to 558 nm (HgCl*). In many cases selective narrow-band radiation of typically 1-17 nm half width and efficiencies up to 10% were observed. Detailed model calculations of the VUV output from Xe_2^* dimers (λ = 172 nm) in such discharges predict an optimum range for the parameters electron energy, electron density and xenon pressure.

LB-5 Electronic Quenching Effects of Atom-Molecule Interactions in a Non-Equilibrium Plasma at Atmospheric Pressure. M. GORDON and C. H. KRUGER, Stanford University -- Emission measurements of temperature and electron density have been made downstream of a 50 kW induction plasma torch at temperatures and electron densities near 7000 K and 10^{20} m^{-3}, respectively. Absolute and relative atomic line intensities, absolute recombination continuum, Stark-broadening of the hydrogen Balmer lines, and the relative rotational line intensities of the N_2^+ (0,0) band were interpreted for several plasma powers and gas compositions in order to investigate the electronic quenching effect of atom-molecule interactions. The data indicate that for all conditions, non-equilibrium exists in the form of an over-population of free electrons due to finite recombination rates and diffusion of electrons to the cold plasma edges. For purely atomic plasmas, we find that the excited electronic states are similarly over-populated with partial equilibrium between the bound and free electrons typically observed. However, when a diatomic species is present - either an argon plasma seeded with nitrogen and/or hydrogen, or an air plasma - the excited electronic states remain approximately in equilibrium with the ground state irrespective of an over-population of free electrons.

LB-6 Breakdown of a wire-to-plane discharge

M.A. JOG, I.M. COHEN, and P.S. AYYASWAMY, Dept. of Mech. Engg. and App. Mech., U. of Penn., Philadelphia, PA 19104-6315

A wire-to-plane discharge during the early phases of breakdown has been studied. Such discharges are used, for example, in melting a wire in ball bonding of semiconductor chips. Here,the discharge has been modelled in a prolate spheroidal coordinate system with the wire shape taken as a hyperboloid of revolution. Four simultaneous coupled nonlinear partial differential equations describe the electrical discharge. These are: the conservation equations for ion and electron densities, the energy equation for electron temperature, and Poisson's equation for the self-consistent electric field. By solving this formulation subject to appropriate boundary conditions, charged particle densities and temperature variations have been obtained as the ionization progresses outwards from the wire tip. The results show that both the electron temperature and the charged particle densities increase with the progress of ionization. The effect of different wire polarities is also examined. With a positive wire polarity, the increases in electron temperature and charged particle densities are confined to regions of the discharge in the vicinity of the wire tip. With a negative wire polarity, the breakdown occurs in the entire gap at a faster rate than with a positive wire polarity.

LB-7 Comparison of the AWA Lumped-Circuit Model OF Electrical Discharges with Empirical Data W. B. MAIER II, A. KADISH, (Los Alamos National Laboratory), and R. T. ROBISCOE (Montana State University). We compare experimental data for transient electrical discharges with an AWA lumped-circuit discharge model in which the arc resistance is taken to be $R_a = V^*/|I|$, where V^* is a positive parameter and I is the discharge current. We first examine three 1.7-m-long underdamped discharges and suppose that in addition to the arc resistance, there is a series resistance, R, arising from the external circuit. R and V^* are deduced from one discharge, and these values are applied to all three discharges. We find good agreement with the experimental data; for example, we predict the observed abrupt discharge termination and the proper number of current reversals for each discharge. We also compare experimental arc resistances from overdamped arcs with our model and with other models. We show that the AWA lumped circuit model represents the empirical data at least as well as other theories and provides a conceptually improved picture of threshold behavior and abrupt termination of discharges.

SESSION NA

8:00 AM - 9:45 AM, Thursday, October 18

Convention Center, Chancellor Hotel - Illiniwek Room

HIGH DENSITY PLASMA PROCESSING

Chair: M. S. Barnes, IBM - East Fishkill

NA-1 High Etch Rate Modes in Microwave Plasma Etching of Silicon in High Magnetic Fields, Y.HORIIKE and H.SHINDO, Hiroshima University-High etch rate modes in microwave plasma etching were studied in high magnetic field regime. The Si etch rate showed clearly two modes in which the local maxima appeared in the magnetic fields around B_c=875 G and $2B_c$, and the second maximum at $2B_c$ attained as high as 1500 A/min at 5×10^{-5} Torr of NF_3 with 600 W input power. In two modes, the plasma attained high density, as confirmed by the measurements of plasma light emission and ion saturation current, the electron density in the second mode was three times larger than the ECR cutoff density. The first mode was ascribed to the ECR, but exactly to the upper hybrid resonance because the magnetic field at which the ion current showed the maximum lowered at higher electron density. A measurement of the microwave field inside the plasma demonstrated that the phase velocity of microwave changed continuously with the magnetic field centered on $2B_c$. Since this was consistent with the dispersion of the Whistler wave, the second mode was ascribed to the Whistler mode resonance. An energy analysis by the retarding method revealed that the ion energy was about the floating potential even in the second mode.

NA-2 Investigation of Limiters in ECR Plasmas for Applications in Plasma Processing. B. G. LANE, D. L. SMATLAK, G. GIBSON, H. H. SAWIN,* L. BOURGET,** R. S. POST,** Plasma Fusion Center, M.I.T., * Dept. of Chem. Eng., M.I.T., ** Applied Science and Technology, Inc., Woburn, MA - Although limiters have often been used to define a plasma edge in fusion plasmas, their use in plasmas for microelectronic processing applications is not common. We report here on results in which two quartz annular limiters are placed in the source region of a commercially available microwave source (ASTeX). Two beneficial effects are noted: (a) the plasma in the source region decays rapidly in the limiter "shadow" and (b) the presence of the limiters can be seen in well defined "corners" in the radial ion saturation current profiles downstream. The first effect suggests limiters will be useful in avoiding plasma induced damage problems to source inner walls, while the second suggests that radial diffusion is not excessive and thus plasma can be guided along field lines allowing great flexibility in source design. It was also found that the radial ion saturation current profile was significantly more uniform when using limiters for the conditions of the experiment.

NA-3 Modeling Remote Plasma Sources for Materials Processing using a Hybrid Monte Carlo-Fluid Simulation.* Yilin Weng and Mark J. Kushner, University of Illinois, 607 E. Healey, Champaign, IL 61820. Remote Electron Cyclotron Resonance (ECR) plasma sources are being developed for use in etching and deposition of semiconductor materials. At the gas pressures (<<10's mTorr) and power deposition (many W-cm^{-3}) of interest, the fractional ionization in the plasma zone is high and longitudinal transport along the magnetic field is rapid. We have developed a hybrid Monte Carlo-fluid model for such devices and the results will be discussed in this paper. A Monte Carlo Simulation, which employs special techniques to account for electron-electron collisions, is used to generate transport coefficients as a function of position in an ECR reactor. The coefficients are used in an iterative matrix solution of the fluid conservation equations and Poisson's equation for electron, ion and excited state densities, and the longitudinal electric field. Electron temperature and species densities as a function of position and plasma parameters will be presented.

*Work supported by the National Science Foundation (ECS88-15781 and CBT88-03170).

NA-4 Laminar Plasma Production with ECR. R.ITATANI and A. HATTA Dept. of Electronics,Kyoto U.--The method to generate a thin laminar ECR plasma for a new type of plasma reactor has been demonstrated. In very low pressure, ionization occurs in the region where ECR condition is satisfied. Supurposition of dipole magnetic fields of permanent magnets to a uniform one can provide line shaped ECR zones. The plasma produced there flows along magnetic lines of force and forms a laminar plasma. Number of sheets is equal to the number of the resonance zones in the plasma vessel. The thickness of the plasma is controlled by changing the shape of the resonance zone. The shape of the plasma were measured by optical method across the plasma. The minimum thickness obtained is about 5mm. Electron density estimated by probe measurement is about in the order of $10^{10}/cm^3$ and almost proportional to input microwave power.

In this plasma reator, working gas is fed across the laminar plasma, and is decomposed into radicals, the production rate of which depends strongly upon the effective residence time of the gas in the plasma, proportional to electron density and plasma thickness, and is easily controlled by this method.

NA-5 Low Pressure High Density Inductive Plasma for Plasma Processing-Theory and Experiment, John H. Keller, Michael S. Barnes, John C. Forster, IBM E. Fishkill, B/300, Z/48A, Hopewell Junction, NY.

High plasma densities and low ion bombardment energies, which result in high rates and low substrate damage, are desirable for plasma processing to achieve ULSI dimensions and device quality. RF plasmas can be produced by capacitive and inductive coupling. It is extremely difficult to obtain both high densities and low ion energies using capacitive coupling. Inductive coupling, however, can produce very high plasma densities, e.g., 7E10 and higher, with floating potentials on the order of 10-15 volts. Capacitively coupled bias of the subtrate of an inductively coupled system then allows independent control of bombarding ion energies.

In inductively coupled systems, the plasma acts as a one turn transformer where the degree of coupling is affected by gas pressure, coil Q and skin depth. This paper will discuss different coil designs in both theory and experiment. Experimental etch results will be discussed.

SESSION NB

8:00 AM - 9:40 AM, Thursday, October 18

Convention Center, Chancellor Hotel - Grange Room

ELECTRON EXCITATION AND DISSOCIATION

Chair: B. Bederson, New York University

NB-1 Theory of Electron–Molecule Collisions. B. I. SCHNEIDER, Los Alamos National Laboratory, Los Alamos, NM and National Science Foundation, Washington, D.C.—Collisions of electrons with neutral molecules, molecular ions and radicals play a fundamental role in many areas of technological importance. Recent theoretical and computational developments[1,2] have enabled detailed, *ab–initio* calculations to be performed on a number of small diatomic and polyatomic molecules of interest to these technologies. The two key developments which have paced these recent advances are the full integration into the scattering theory of the methods of bound state quantum chemistry and the discovery of anomaly free, variational methods using analytic or numerical basis set expansions of the scattering wavefunction. It is now possible to perform multi–channel calculations, including exchange and polarization on systems as "simple" as H_2 or O_2 and as "complex" as H_2CO, CH_4, and C_2H_4. The effect of resonant vibrational excitation has been included using the "Boomerang" model. I will illustrate the theory using examples chosen from the calculations of Schneider, Rescigno, McCurdy and Lengsfield using the complex Kohn variational method and those of McKoy et. al. using the Schwinger variational principle.

[1]B. I. Schneider and L. A. Collins, Phys. Rev. A27, 2847 (1983)

[2]T. N. Rescigno and B. I. Schneider ibid A37, 1044 (1987); T.N. Rescigno, C. W. McCurdy and B. I. Schneider Phys. Rev. Lett. 64, 248 (1989)

NB-2 Range of Validity of Second Order Perturbation Series for Electron-Hydrogen Collisions, *D. H. MADISON, LAMR, U. of Missouri-Rolla -- One of the fundamental scattering problems in atomic physics is the electron-hydrogen problem. Over the years this has been one of the most often studied processes, since it represents the basis for almost all collision work. There have been several highly sophisticated calculations for this problem, but surprisingly, experiment and theory were not in accord. We recently demonstrated[1], however, that an exact second order distorted wave Born calculation (DWB2), which included second order exchange, predicted reliable results for the magnitude of the scattering amplitude at an incident electron energy of 54 eV. We have now performed a detailed comparison with all experimental and theoretical results in the intermediate energy range, and have found that the DWB2 is reliable for elastic scattering for energies of 30 eV and above and reliable for 2s and 2p excitation for energies of 50 eV and above.

*Work supported by the NSF.

[1]D. H. Madison, I. Bray, and I. E. McCarthy, Phys. Rev. Lett. 64, 2265, 1990.

NB-3 **Electron–H_2O Collisions in an Exact Exchange Plus Parameter–Free Polarization Model, A. Jain, Phys. Dept., Florida A&M Univ., Tallahassee, Fl 32307, D. G. Thompson, The Queen's University, Belfast and F A Gianturco, Univ. of Rome, Italy** – The low–energy e–H_2O scattering is treated in the static–exchange plus paremeter–free polarization model. The exchange effects are included exactly by solving the inhomogeneous coupled differential equations iteratively. The convergence of scattering parameters with respect to the number of iterations is checked for each symmetry and energy. We found significant differences between the previous results using model exchange (like the free electron gas exchange) and the present one with exact exchange. We compare our calculations (differential, integral and momentum transfer cross sections) with recent measurements and other calculations where exchange effects are considered properly.

NB-4 Cross Sections for the Electron-Impact Dominated Processes in Etching Plasmas*. K. BECKER, Physics Dept., City College of New York - We report recent results of our ongoing studies[1] of dissociative and ionizing electron collisions with the molecules SF_6, CF_4, NF_3, CCl_2F_2 and BCl_3 which are frequently used as constituents of etching plasmas. We discuss (i) the production of fluorine resonance radiation in the VUV and its potential for photochemical processes in the plasma, (ii) the role of partial fragmentation processes of CCl_2F_2 and (iii) the dissociative excitation of BCl_3 and the presence of two break-up mechanisms, a "neutral" channel and a "ionic" channel. Preliminary results will be presented on the ionization and dissociative ionization of these molecules using the fast neutral beam method[2] and on the formation of neutral ground state fragments using LIF techniques.

[1]P.G. Gilbert, R.B. Siegel and K. Becker, Phys. Rev. A 41, 5594 (1990) and references therein to earlier work
[2]T.R. Hayes et al. Phys. Rev. A 35, 559 (1987)

* Supported by the NSF (Grant Nos. CBT-8896249 and CTS-8902405) and by PSC-CUNY (Grant Nos. 669370 and 661402)

NB-5 Measurements of Electron-Impact Cross Section for Dissociation from CH_4 into CH_3 and CH_2,* H. SUGAI, T. NAKANO and H. TOYODA, Nagoya University, Japan -- In order to model a methane plasma, there has been a great need to obtain the data set of partial cross sections for neutral dissociation by electron methane collisions. Here we report studies on the partial dissociation cross sections for neutral radical CH_3 and CH_2. The radical species is detected by threshold ionization mass spectrometry which has been successfully used to measure the radical densities in a methane plasma.[1,2] The gas is introduced into the dissociation region and irradiated by an electron beam (5-100 eV). The neutral species are extracted and ionized by the second beam at the energy below the ionization threshold for the parent gas. The energy dependences of the cross sections for CH_3 and CH_2 are measured. A comparison will be made with a few previous reports on the total dissociation cross section.

*Work supported by a Grant-in-Aid for Scientific Research from the Ministry of Education, Science & Culture, Japan.

[1]H. Toyoda, H. Kojima and H. Sugai, Appl. Phys. Lett. 54, 1507(1989).

[2]H. Kojima, H. Toyoda and H. Sugai, Appl. Phys. Lett. 55, 1292(1989).

SESSION PA

10:05 AM - 12:00 Noon, Thursday, October 18

Convention Center, Chancellor Hotel - Illiniwek Room

HIGH DENSITY PLASMA PROCESSING AND DIAGNOSTICS

Chair: J. Keller, IBM - E. Fishkill

PA-1 Low Pressure Etching Using Helical Resonator Discharges*, DALE E. IBBOTSON, AT&T Bell Laboratories – Submicron, anisotropic polysilicon etching has been performed on a single-wafer etcher using a simple helical resonator (HR) structure that sustains an intense radio frequency discharge at low pressure ($\lesssim 10^{-3}$ torr). Etched profiles of polysilicon, material selectivity, polysilicon etch rates and etch uniformity were used to test the performance of the discharge source with Cl_2 and Cl_2/O_2 mixtures. In initial experiments with small HR's polysilicon etch rates were low (< 200 Å/min) and were limited by the integral ion flux these HR's could produce[1]. Scaled HR's yield polysilicon etch rates from 250 – 850 Å/min for discharge powers from 300 – 1400 W at 0.3 mtorr. Selectivities for polysilicon over gate oxide and trilevel resist were 70 : 1 and 4 : 1, respectively. Improved HR sources for single wafer etching, design considerations, and processing variables will be discussed.

*In collaboration with J. M. Cook and C. P. Chang.

[1]J. M. Cook, D. E. Ibbotson, and D. L. Flamm, J. Vac. Sci. Technol. B8, 1 (1990).

PA-2 RF or microwave plasma reactors? Factors determining the optimum frequency of operation. M. MOISAN, C. BARBEAU, R. CLAUDE, C.M. FERREIRA*, J. MARGOT-CHAKER, J. PARASZCZAK**, A.B. SA*, G. SAUVE AND M.R. WERTHEIMER***, U.Montréal, Québec H3C 3J7. It is now accepted that the frequency $\omega/2\pi$ at which a high frequency (HF) discharge is sustained has considerable influence on the properties of the plasma. For example, the electron density obtained for a given HF power density deposited into the plasma is usually higher at microwave than at radio frequencies (RF). We review a series of experiments that we performed regarding the influence of ω on the power balance between the HF field and the plasma, and regarding plasma processing of materials: on the two particular etching and deposition processes we describe, the "optimum" frequency (at which the process is most efficient) happens to be in the range between 50 and 100 MHz. This suggests that converting a plasma process from 13.56 to 2450 MHz does not necessarily lead to the greatest possible process enhancement and that optimization may require some flexibility in the operating frequency of the plasma reactor. To provide insight into these results, the most recent models dealing with the influence of ω on the electron energy distribution are reviewed.

* Instituto Superior Técnico, Lisboa, Portugal.
** IBM-Yorktown Heights, NY 10598.
*** Ecole Polytechnique, Montréal, Québec H3C 3A7

PA-3 Experiment and Modeling of Helicon RF Diffusion Plasmas,* C. CHARLES and R.W. BOSWELL, PRL, ANU, AUSTRALIA. P. RANSON, C. LAURE, A. BOUCHOULE, GREMI, U. of Orleans, FRANCE - The application of high density diffusion plasmas to processing in the microelectronics industry is of great current interest. One promising technique for producing these plasmas is the Helicon rf source which produces high electron densities over a wide range of filling pressures. In our experiments two electrostatic probes (Langmuir probe and energy analyser) were used to make a detailed study of the spatial plasma diffusion for an Argon plasma. We have developed a simple analytical model of the plasma diffusion on axis based on these results which explains the evolution of density, plasma potential and ion energy distribution function at low pressure (1mTorr). The experimental results, the range of applications of the model and the interest of such a work for etching and deposition applications are discussed.

* Work supported in part by Alcatel-CIT, Annecy, FRANCE.

PA-4 EEDF Evolution in a Low Pressure Capacitive Argon rf Discharges at 13.56 MHz, V.A. GODYAK, R.B. PIEJAK AND B. M. ALEXANDROVICH, GTE Laboratories Incorporated, Waltham MA -- Probe measurements of the electron energy distribution function (eedf) have been made in argon rf discharges using a newly developed technique to minimize the problems of probe contamination, rf plasma potential oscillation and low frequency noise which are typically found in these discharges. Measurements were performed over a wide range of discharge current (0.3-10 mA/cm^2) and gas pressure ($3x10^{-3}$ - 3 Torr) covering different modes of discharge operation: stochastic heating mode, collisional heating mode and the γ-regime. Essentially different eedf shapes have been observed and from these eedf's the plasma density and mean electron energy have been determined. The behavior of the eedf and the plasma parameters versus gas pressure and discharge current will be discussed.

PA-5 Langmuir Probe Studies of He, O_2 and Cl_2 in a 13.56 MHz Plasma Reactor. K.F. Al-Assadi & N.M.D. Brown, The Joint Ceramic Res. Centre, University of Ulster, Coleraine, N.Ireland--This paper describes the results obtained by a self-R.F. compensated Langmuir probe from which the plasma potential, Vp, together with the electron densities, Ne, and electron temperature, Te, have been determined. Also reported is the positive ion current, I_+, which flows to a small cylindrical Langmuir probe for He, O_2 and Cl_2 gas discharges at a pressure of 30 mtorr and at rf powers in the 10-150 watt range. It is shown that within a predictable restricted range of charge density linear plots of I_+^2, versus the probe-plasma potential difference could be obtained for a negatively- and positively-biased probe, in agreement with the Langmuir theory of orbital-limited-current-collection. However, the values of the above positive ion densities deduced from the slopes of the plots were not equal and always exceeded the electron densities. In the case of the O_2 and Cl_2 gas discharges where the negatively charged ions exist, the positive ion densities obtained are found to be considerably larger than those produced, for similar pressure and input powers in He. A calculation of the sheath width of the discharge gases on these measurements is also presented.

1. Cox, T. I., Dishmukh, T.G. et al., J. Phys.D. 20, 82-89 (1987)
2. Al-Assadi, K.F., Chatterton, P.A. et al., IPAT 87, 296-301 May 1987.
3. _____. Vacuum 38, No. (8-10), 633-638 (1988).

SESSION PB

10:10 AM - 11:50 AM, Thursday, October 18

Convention Center, Chancellor Hotel - Grange Room

ELECTRON IMPACT AND HEAVY PARTICLE COLLISIONS

Chair: S. Chung, University of Wisconsin

PB-1 Metal Atom Differential Cross Sections,* L. VUŠKOVIĆ, New York U,- We report on differential cross section measurements of electron scattering by metal atoms, employing atom recoil technique or electron spectroscopy. The strength of the first method,[1] appropriate for absolute measurements, is demonstrated on sodium as a test of various close coupling calculations.[2] Cadmium serves as an example of the second method. We performed[3] wide-range angular distribution measurements of several s-, p-, and d-states for singlet and triplet excitations as test of distorted wave approximation calculations.[4] Both experimental approaches include energy ranges where inelastic channel threshold calculations do not generally converge.

* Research supported by U.S. National Science Foundation.
[1]T.Y. Jiang, C.H. Ying, L. Vušković, and B. Bederson, submitted to Phys. Rev. A (1990) and contribution in this meeting.
[2]D.L. Moores and D.W. Norcross, J. Phys. B **5**, 1482 (1972); H.L. Zhuo at al., BAPS **35**, 1170 (1990).
[3]B. Marinković, V. Pejčev, D. Filipović, and L. Vušković, XV ICPEAC, Brighton (1987) p. 186.
[4]D.H. Madison at al., BAPS **35**, 1171 (1990).

PB-2 Electron-Polarized Photon Coincidence Study of the Heavy Noble Gases,* K. MARTUS**, S. ZHENG and K. BECKER, City College of CUNY- The electron-polarized photon coincidence technique has been used to study the electron impact excitation of the heavy noble gases. The resulting coherence parameters yield information about the excitation amplitudes and their interference. A P_1 of unity has been measured in the forward direction at impact energies ranging from 30-100eV for the $(^2P_{3/2})ns[3/2]_1$ and $(^2P_{1/2})n's[1/2]_1$ states in Krypton in addition to the $(^2P_{1/2})n's[1/2]_1$ state in Neon and Argon. The measured values agrees with the DWBA calculation of Bartschat and Madision[1] as well as physical intuition. Measurements at small scattering angles of both linear coherence parameters perpendicular to the scattering plane for Argon and Krypton at an impact energy of 50eV reproduce the general features of the curves predicted by theory.

*Work supported by NSF through Grant No. PHY-8910369

**Present Address: Univ. of Idaho

[1] K. Bartschat and D.H. Madision, J. Phys. B **20**, 5839 (1987)

PB-3 Rates for the Vibrational Excitation of O_3, CO_2 and N_2O by Electron Impact, K. HOLTZCLAW, B.L. UPSCHULTE, B.D. GREEN, Physical Sciences Inc., W.A.M. BLUMBERG, and S.J. LIPSON, Geophysics Laboratory (AFSC)* -- Rates for the vibrational excitation of O_3, CO_2, and N_2O by electron impact have been measured. IR fluorescence from electron-irradiated O_3, CO_2, and N_2O was observed in the GL LABCEDE facility in which O_3/N_2, O_3/Ar, CO_2/N_2, N_2O/N_2, and N_2O/Ar mixtures at mT pressures were irradiated with a pulsed 4.5 keV electron beam. Experiments were performed over a range of pressures so that both primary and secondary electron excitation were separately observed. Time-resolved spectra were obtained over the wavelength range 2.5-15 microns using a circular variable filter. The populations of the vibrational levels of the O_3, CO_2, CO, N_2O, and NO IR bands observed were determined by synthetic spectral fitting. Relative vibrational level excitation rates were determined. In addition, absolute excitation rates were inferred. These results are important for characterizing IR emissions from O_3, CO_2, and N_2O in the electron-disturbed atmosphere.

* Supported by the Air Force Office of Scientific Research and the Defense Nuclear Agency.

PB-4 Electron Energy Distribution Functions and Kinetics of Excited Electronic States in Nitrogen Afterglow*, RAJESH NAGPAL and P. K. GHOSH, Department of Chemistry, Indian Institute of Technology Kanpur, Kanpur 208016 INDIA - The relaxation of vibrational populations and electron energy distribution functions (EEDF) in a nitrogen afterglow are followed theoretically as a function of the vibrational distribution of excited electronic states (EES) (determined by collisional-radiative processes in the discharge[1]) by solving the vibrational master equations coupled to the Boltzmann transport equation without the field term. Earlier work[2] had seen only the effect of the $A^3\Sigma_u^+$ and the $B^3\Pi_g$ states; the present results show that superelastic collisions from all the EES considered ($A^3\Sigma_u^+$, $B^3\Pi_g$, $W^3\Delta_u$, $B'^3\Sigma_u^-$, $C^3\Pi_u$, $a'^1\Sigma_u^-$, $a^1\Pi_g$, and $w^1\Delta_u$) are reflected on the EEDF at their respective thresholds along with a correlation between the vibrational temperature and the average energy of electrons. Energy balance and relaxation mechanisms of the above EES coupled to the electron kinetics are discussed.

* Work supported by the Aeronautics Research and Development Board.

[1] R. Nagpal and P. K. Ghosh, J. Phys. D, to be published.

[2] C. Gorse et al, Chemical Physics, 119, 63 (1988).

PB-5 Calculations of fine-structure changing collisions of excited Xe.* A. P. HICKMAN, D. L. HUESTIS, and R. P. SAXON, SRI International-Calculations of cross sections for mixing of $Xe(5p^5\ nl)$ (nl = 6s,6p,5d) by thermal collisions with He Ar, and Ne are underway. *Ab initio* structure calculations are being performed using the COLUMBUS codes[1] that include spin orbit effects and treat the heavy atom core effects using relativistic effective potentials. An analytic model has been developed that allows the necessary nonadiabatic coupling matrix elements to be determined by fitting the *ab initio* adiabatic potential curves with a small set of parameters. The dynamics equations are solved using the coupled channel method. Preliminary results have been obtained for Xe ($5p^5$ 6p) collisions with He. The largest calculated cross section is for the $6p[3/2]_1$ to $6p[5/2]_3$ transition; the calculated potentials reveal a curve crossing of the diabatic states of $\Omega=0^-$ symmetry corresponding to these states, and show no other such crossings. The calculated rate agrees with experimental measurements (preceding abstract) within a factor of two.

1. R. M. Pitzer and N. W. Winter, J. Phys. Chem. **92**, 3061 (1988).

*Supported by Sandia National Laboratories.

PB-6 State-to-State Quenching of Xenon 6p Levels by Rare Gases,* W. J. ALFORD, Sandia National Laboratories -- Neutral quenching of the xenon 6p levels is important in understanding the kinetics of high-pressure xenon lasers. Measured state-to-state quenching rates are presented for many 6p levels quenched by helium, argon, and xenon. The fluorescence from collisionally populated 6p levels following excitation of a specific 6p level is used to determine quenching rates. Some new measurements of total quenching rates are also presented. Quenching of the $6p[3/2]_1$ level by helium goes almost entirely to the $6p[5/2]_3$ level with a rather large rate. Quenching of the $6p[3/2]_1$ level by argon, however appears to be less selective with a much lower rate. Implications for xenon lasers will be discussed.

*This work performed at Sandia National Laboratories, supported by the U.S. Department of Energy under Contract Number DE-AC04-76DP00789.

SESSION QA

1:30 PM - 3:30 PM, Thursday, October 18

Convention Center, Chancellor Hotel - Illiniwek Room

PLASMA DIAGNOSTICS

Chair: B. G. Lane, MIT

QA-1 Computer-Controlled Langmuir Probe and Optical Emission Spectrometer for a DC Discharge, ISAAC D. SUDIT and R. CLAUDE WOODS, Department of Chemistry, University of Wisconsin-Madison--Computer Controlled Langmuir probe and optical emission spectroscopy (OES) diagnostics have been developed and used in our DC discharges. These discharges, which are contained in glass tubes 15 cm in diameter and approximately 3 m in length with cylindrical electrodes at the ends, are used to produce molecular ions for study by microwave spectroscopy. The system developed allows us to measure electron and ion densities, electron and ion temperatures, electron energy distribution functions (EEDFs), and plasma and floating potentials, as functions of discharge current, neutral gas pressure and temperature, axial magnetic field intensity, and position along the discharge in the radial and axial directions. Both cylindrical and planar probes have been used to obtain I-V curves, which were analyzed using software developed to work with the data-acquisition technique. Results for nitrogen, argon, oxygen and other gases will be presented.

QA-2 Diagnostics and Modeling of Radical Density Profiles in a Methane rf Discharge,* H. SUGAI, H. TOYODA and Y. HIKOSAKA, Nagoya University, Japan -- We have measured the spatial distributions of neutral radical CH_3 and CH_2 in a parallel plate rf discharge in methane, using threshold ionization mass spectrometry.[1] The discharge conditions are varied in a wide range of methane pressure (0.01 $\sim$ 1 Torr) and the rf electrode separation (3 $\sim$ 6 cm). In comparison with CH_3, the CH_2 species has a lower density with the inhomogeneous profile. In order to use as inputs to theoretical modeling of radicals in the plasma, comprehensive measurements are made for electron energy distribution, ionic composition, and radical sticking coefficient. The modeling have revealed the main channels of radical source and sink: (i) CH_3 radicals are produced by ion-molecule reactions at a high pressure and lost by recombination, (ii) CH_2 radicals are produced by electron impact dissociation, while they are lost by surface sticking at a low pressure and by radical molecule reaction at a high pressure.

*Work supported by a Grant-in-Aid for Scientific Research from the Ministry of Education, Science & Culture, Japan.
[1]H. Sugai, H. Kojima, A. Ishida and H. Toyoda, Appl. Phys. Lett. 56, 2616(1990).

QA-3 Photodetachment Measurement of D^- Density In a Hot Cathode Triode Discharge, B.N. Ganguly and Alan Garscadden, Aero Propulsion and Power Laboratory, WPAFB, OH -- The D^- density variation with the screen grid (2mm from cathode) bias voltage change has been measured by optogalvanic detection of photodetachment, using pulsed (5ns) laser excitation, in a hot cathode low current ($\leq$ 30mA) discharge with gas pressure ranging from 30 mtorr up to 200 mtorr. At pressures below 60 mtorr, the D^- density increased with the positive bias voltage increase up to 22.5 volts and almost linearly with the discharge current, whereas, a ten percent further increase of the bias voltage decreased the photodetachment signal by nearly two orders of magnitude possibly due to the onset of fast electron collection at the grid. At pressures above 100 mtorr, the grid bias control becomes less effective, and totally ineffective above 150 mtorr, due to the plasma shielding of the applied field, although the photodetachment signal increased with the current at constant bias voltage.

QA-4 Determination of negative ion densities in a CF_4 RF plasma, F.J. DE HOOG, J.L. JAUBERTEAU, G.J. MEEUSEN, M. HAVERLAG, G.M.W. KROESEN, Dept. of Phys., Eindhoven Univ. of Techn., Netherlands– Experiments to study negative ion densities in an RF plasma in CF_4 have been carried out using photodetachment of these ions by the pulse of a Nd–Yag laser at the tripled (355nm) and quadrupled (266nm) frequency. The photodetached electrons are detected as a sudden increase of the electron density in the quasi–parallel plate reactor by a microwave method. The negative ion density consists mainly of F^-. At typical conditions (pressure of 13 Pa, RF power density of 0.12 W/cm^2, CF_4 flow of 15 sccm) the negative ion density is (4±1) times higher than the volume averaged electron density of 1.2×10^{15} m^{-3}. The decay of the detached electrons after the laser pulse has been interpreted in terms of attachment and diffusion. At an RF power density of 0.12 W/cm^2 the electron attachment rate constant is found to be $(7\pm1) \times 10^{-17}$ m^{3}s^{-1} and the electron diffusion coefficient is (0.13±0.12) m^2 s^{-1} at standard conditions.

*Submitted by H.L. HAGEDOORN

QA-5 Calibrated Spatial and Temporal Profiles of H-atoms in Hydrogen Discharges,* B.L. PREPPERNAU, T.M. CERNY, J.R. DUNLOP, A.D. TSEREPI, and T.A. MILLER, The Ohio State University - Refined measurements of H-atom spatial and temporal concentration distributions in hydrogen discharges using two-photon allowed laser induced fluorescence (TALIF) detection have been obtained over a range of frequency, power, and pressure conditions. Calibration of H-atom concentrations is obtained by use of a novel discharge reactor titration technique. Particular attention is paid to measurements of concentration gradients very near electrode surfaces.

*Work support by Air Force Wright Research and Development Center.

QA-6 **Time Dependent Processes in an Argon rf Glow Discharge,** M. Colgan, N. Kwon, Y. Li,* and D.E. Murnick. **Department of Physics, Rutgers University - Newark, New Jersey 07102.** - New results on time and space resolved plasma induced emission (PIE) from 10 MHz Argon glow discharges, with applied rf power between 1 and 10 watts at pressures from 0.3 to 5 torr, are presented. Nanosecond resolution was obtained for $2p \rightarrow 1s$ and $3p \rightarrow 1s$ transitions at 750.4 and 425.9 nm respectively. The observed 3p state lifetime is shorter than its tabulated radiative value and comparable to that of the 2p (21nsec) state. Excitation functions were obtained from PIE data deconvoluted with the *measured* lifetimes. Comparision of excitation rates to 2p and 3p levels provides data on the instantaneous electron "temperature" if a Maxwellian distribution is assumed for the electron velocity. The data are essentially consistent with the continuum model[1] but differ from some previously published experimental results[2].

1 D.B.Graves, J.Appl.Phys., **62**,88 (1987).
2 E.Gogolides, J-P Nicolai, and H.H.Sawin, J.Vac.Sci.Tech. **A7**, 1001, (1989).

*Supported in part by the Rutgers Research Council.

QA-7 Lineshape Measurements in Processing Gas Discharges,* J.R. DUNLOP, T.M. CERNY, B.L. PREPPERNAU, A.D. TSEREPI, and T.A. MILLER, The Ohio State University - We have performed Doppler shift measurements on TALIF-detected lineshapes to determine translational temperatures of hydrogen atoms in plasma environments. We use photodissociation of hydrogen-containing molecules by the laser probe beam followed by TALIF to characterize gases present in plasma environments. Doppler profiles of hydrogen atoms generated by the photodissociation of parent molecules (NH_3, H_2S, C_2H_2) indicate translationally hot atoms which hold the potential for the identification of parent molecules. Results of lineshape measurements of H-atoms generated by hydrogen RF and microwave discharges are also compared.

*Work support by Air Force Wright Research and Development Center.

QA-8 **Experimental Studies of Plasma Dynamics and Emissions in Dense Pinch Plasma.** M. YOKOYAMA, Y. KITAGAWA and Y. YAMADA, ILE, Osaka University, JAPAN -

The plasma dynamics of dense pinch D_2 and H_2 plasmas were optically investigated by ruby laser shadowgraphy and holographic interferometry. The energetic protons and deuterons were measured by CN film track detection technique and nuclear activation method. X-ray and ion pinhole cameras were also used. The deuteron temperature and kinetic energy were measured by using a D_2-^3He mixture gas.

In the optimum D_2 gas pressure, high energy deuterons up to 3 MeV was observed. It is found that high energy ions are accelerated by high induced voltage across the plasma diode formed above anode surface. The generation efficiency of high energy ion beam (> 330 keV) was below 1 % of the discharge current. The D-D neutron yield scaling law with current will be considered.

SESSION QB

1:30 PM - 3:15 PM, Thursday, October 18

Convention Center, Chancellor Hotel - Grange Room

ATOMIC Xe AND OTHER LASERS

Chair: J. Crane, Lawrence Livermore Laboratory

QB-1 Gain Measurements in Fission-Fragment Excited Xenon Gas Mixtures,* G. A. HEBNER and G. N. HAYS, Sandia National Laboratories -- The results of recent CW probed measurements of the small signal gain at 2.03, 2.65 and 3.51 μm in fission-fragment excited Ar/Xe, Ne/Ar/Xe and He/Ar/Xe gas mixtures will be discussed. Time dependent gain measurements demonstrate that for pump rates from 5 to 700 W/cm^3, the 2.03 μm peak gain can vary from 1.1 to 6.0%/cm. For pump rates above 70 W/cm^3, the gain in Ar/Xe prematurely terminates and becomes absorptive. The termination is thought to be due to the effects of excessive gas heating since changing the buffer gas to Ne/Ar/Xe reduces the premature termination without detrimentally affecting the peak gain. Gas impurities such as N_2 and "air" in concentrations of less than 0.1 percent were observed to decrease the gain by up to 30 percent. For pump rates of 50 to 200 W/cm^3, the 2.65 μm gain can vary between approximately 5 to 8%/cm in Ar/Xe, Ne/Ar/Xe and He/Ar/Xe gas mixtures. Measurements conducted at 3.51 μm indicated only net absorption for all buffer gases and pump rates examined. Gain scaling laws as well the influence of Ne/Ar ratio and Xe concentration on the peak 2.03 μm gain will also be discussed.

*This work was performed at Sandia National Laboratories, supported by the U.S. Department of Energy under Contract Number DE-AC04-76DP00789.

QB-2 Gain at 2.03 μm in the Fission Fragment Excited Xe Laser: Model Comparisons with Experiments.* Jong W. Shon and Mark J. Kushner, University of Illinois, 607 E. Healey, Champaign, IL 61820; Gregory A. Hebner and Gerald N. Hays, Sandia National Laboratory, Albuquerque, NM 87185. Using fission fragment excitation, low pressure (<1 atm), low power (<100 W-cm^{-3}), long pulse (1-10 ms) and high energy deposition (≤0.5-1.0 kJ/ℓ) operation of the atomic xenon laser can be achieved. Experimental measurements of gain at 2.03 μm have recently been made for a fission fragment excited laser having these characteristics. The results have been analyzed using a comprehensive computer model, which accounts for the pertinent electron kinetics and heavy particle reactions while allowing laser oscillation on five infrared transitions (1.73 μm - 3.51 μm) between the 5d and 6p manifolds. By comparing the model's results with the experiment, we derived a broadening coefficient for the 2.03 μm transition by collisions with argon of $k \simeq 2 \times 10^{-9}$ cm^{3}s^{-1}. We also found sharp decreases in gain can be attributed to increases in gas temperture of 100-200°K.

*Work supported by Sandia National Laboratory.

QB-3 Long Pulse, 100 μs Flat Top, Electron Beam Pumped, Ar/Xe Laser,* T.T. PERKINS, X. CHEN, S.M. FRESHMAN, J.H. JACOB, Science Research Laboratory, Inc. — Measurements of output energy, temporal profile, and intrinsic efficiency from a long pulsed electron beam pumped Ar/Xe laser have been obtained. The laser cavity optics were optimized for the 1.73 μm transition with a gain length of 50 cm. The electron beam was generated by a thermionic cathode fabricated with tungsten filaments and operated at 200 - 220 kV. A 100 μs pulse was generated by switching a high voltage cable to the cathode and terminating it 100μs later with a crowbar switch. Current densities varied from 5 to 10 mA-cm^{-2} corresponding to an electron beam power deposition of 100-200 W-cm^{-3}. Output energy and temporal profile were measured as a function of output coupling, Xe concentration and total gas pressure. From this data, estimates of the small signal gain, saturation flux, and non-saturable loss have been made of the active medium.

*This work was sponsored by Sandia National Laboratory under Document #56-5433.

QB-4 Vibrational Autoionization in Ne_2* Near the Adiabatic Ionization Threshold. S.B.Kim, D.J.Kane, J.G.Eden, Everitt Laboratory, University of Illinois.* Inter-Rydberg excitation spectrum of the diatomic neon beyond the first ionization limit shows a series of suppressions superimposed over an envelope of predissociating continuum. We believe this effect is due to the Δv=-1 vibrational Autoionization(AI) of the $np^3\Pi_g$(A $^2\Sigma^+_{1/2u}$ ion core) Rydberg state of Ne_2*. The small Frank-Condon shift between the lower state($3s^3\Sigma_u$) and the upper state($np^3\Pi_g$) makes it possibe to access low vibrational states of the high Rydbergs near the adiabatic ionization threshold. allowing AI with Δv=-1, which is favored by the "propensity rule", to be possible. The progression traces out the $np^3\Pi_g(v'=1)$ - $3s^3\Sigma_u(v''=0)$ Rydberg transitions for n=15 to n=25, and its limit is in excellent agreement with the previously known ionization potential($np^3\Pi_g$,v=0) and its vibrational constant. Futhermore, isotopic studies confirmed the vibrational assignment. The suppressions indicate that this perturbation is in direct competition with the predissociation of these high-lying Rydberg states. From the transition linewidth considerations we are able to predict the lower and the upper limits of the vibrational AI rate.

*Work supported by AFOSR and NSF

QB-5 Rotationally Resolved Excitation Spectroscopy of $nf(^3\Sigma_g^+,^3\Pi_g)$ and $np^1\Pi_g$ of Ne_2*, S.B. Kim, D.J.Kane, J.G.Eden, Everitt Laboratory, University of Illinois.*

High resolution Inter-Rydberg spectra of Ne_2, originating from the $a^3\Sigma_u^+$ metastable state, have been obtained using Laser-Induced-Fluorescence technique. Comparison was made of these results with theoretical calculations and with expected properties of similar Rydberg states in other molecules to determine the specific electronic state assignments. The rotationally resolved spectra involving the $np^1\Pi_g$ - $^3\Sigma_u^+$ (n=4 to 8) inter-Rydberg trasitions have been identified and analyzed. The spectra acquired in the ~27270-27500 cm^{-1}, ~29830-30030 cm^{-1} and ~31180-31380 cm^{-1} regions at a resolution of ~0.04 cm^{-1} show rotational structure that is attributed to the strongly *l*-uncoupled $nf(^3\Sigma_g^+,^3\Pi_g)$, n=4, 5, 6 states of the molecule. Effective molecular constants B_v, D_v, H_v and F(0) have been determined and will be presented for the states $a^3\Sigma_u^+$, $nf(^3\Sigma_g^+,^3\Pi_g)$, and $np^1\Pi_g$.

*Work supported by AFOSR and NSF

QB-6 Observation and Simulation of Bound→Free Emission From Zn_2 and Cd_2 Excimers*, G. RODRIGUEZ and J.G. EDEN, University of Illinois,— Laser excitation of Zn and Cd metal vapors has produced molecular oscillatory emission continua in the ultraviolet (Zn: 230 nm $\leq \lambda \leq$ 315 nm; Cd: 250 nm $\leq \lambda \leq$ 310 nm) characteristic of Condon internal diffraction bands. For both Zn_2 and Cd_2, the emission has been ascribed to the $0_u^+(^1\Sigma_u^+) \rightarrow X0_g^+(^1\Sigma_g^+)$ molecular transition associated (in the separated atom limit) with the $^1P_1 \rightarrow {}^1S_0$ atomic resonance line. Excitation at several wavelengths has allowed for computer simulation of the emission patterns. Quantum mechanical calculations of the continuous Franck Condon factors have yielded the spectroscopic constants for Zn_2 and Cd_2.

*Work supported by AFOSR and the NSF

QB-7 Spectroscopy and Kinetics of Photodissociated PbI_2*, G. RODRIGUEZ and J.G. EDEN, University of Illinois,— The relative yields of the $A^2\Delta$ and $X^2\Pi$ states of diatomic PbI have been studied by the ultraviolet photodissociation of its parent molecule PbI_2. Using standard excimer laser wavelengths (λ=193 nm, 248 nm, 308 nm, and 351 nm), the production of PbI(A) is found to be preferred under λ=248 nm pumping, producing a strong A→X emssion spectrum (435 nm $\leq \lambda \leq$ 700 nm). The PbI(X) absorption spectrum has been measured from 220 nm to 700 nm upon probing the photodissociated PbI_2 molecules with a pulsed Xe flashlamp continuum. By monitoring the PbI(B,A←X) absorption, the PbI(X) state production efficiency is maximum for λ=351 nm. Also, the PbI(A→X) spontaneous lifetime, and the collisional quenching rate of the PbI(A) state by PbI_2, have both been measured.*

Work supported by AFOSR and the NSF

SESSION R

3:30 PM - 5:30 PM, Thursday, October 18

Convention Center, Chancellor Hotel - Brundage and Zuppke Rooms

POSTERS

R-1 Ion-Surface Interactions in Reactive Ion Etching
S. Mouncey and W.G. Graham Queen's University, Belfast, N. Ireland and A. McKinley University of Ulster, Coleraine, N. Ireland - It is difficult, in the complex plasma environment, to identify important processes occurring at the plasma-surface interface. We are using an ion-surface apparatus to study the interactions of ion species, produced in typical plasma etching environments, with known surfaces and under ultra-high vacuum conditions. A low energy (<1keV), monoenergetic, single species ion beam is used to bombard a surface. Ions sputtered, back-scattered or desorbed from the surface are energy and mass analysed, as a function of incident and exit angles. The preliminary results for Ar^+, CF_x^+ and $SiCL_x^+$ (where x = 1 to 4) incident on Al and Cu surfaces show evidence for the matrix effect when fluorine and chlorine are present. A wide range of negative ions, but a surprising small production rate for molecular ions, is found.

R-2 POWER DEPOSITION IN PARALLEL PLATE DISCHARGES,[1] J. P. Verboncoeur, V. Vahedi, and C. K. Birdsall, University of California, Berkeley - The fields applied to the parallel plates of an RF discharge deposit power into the plasma. The power is deposited in each charged species non-uniformly at a rate given by **J.E.** This phenomenon is studied using the Particle-in-Cell code PDP1[2], which includes collisional processes via a Monte-Carlo collision model[3]. RF discharge simulations exhibit ohmic heating in the bulk plasma and stochastic heating at the plasma sheath edge for electrons, and ohmic heating in the sheath region for ions.

---

1. This work was supported in part by ONR contract N00014-90-J-1198, and DOE contract DE-FG03-90ER54079.

2. Codes available from Industial Liaison Program, EECS Dept. UC Berkeley, 94720.

3. M. Surendra and D. B. Graves, "Particle Simulation of Frequency Effects in a Parallel Plate Discharge", 36th National Symposium of the American Vacuum Society (1989).

R-3 Standing wave discharge (SWD) in a mixture of Helium-Neon gas and at 433 MHz frequency. Z. RAKEM and P. LEPRINCE*, Centre de Developpement des Technologies Avancees (HCR) -2 Bd F. Fanon, Algiers, ALGERIA

The plasma discharge created by standing waves has been studied for argon in capillary tubes at low pressures, and at a frequency of 2450 MHz[1,2]. In a He-Ne gas mixture (using different composition values), and under 433 MHz frequency with the same pressure, power, and dimension conditions of the tube (p=0.1 Torr, P=45 W, ϕ_{inside}=2 mm) as in argon SWD at 2450 MHz, we find also the axial modulation phenomenon of the discharge and wave parameters (electric and magnetic components of the field E, and H, emission line intensities, ...), and where the mean values are quite flat. The longitudinal measures show that the 632.8 mm Neon line intensity has no phase difference with H, but is in opposite phase with E.

*Lab. Phys. Gaz et Plasma (Univ. Paris XI, FRANCE)

[1]Z. Rakem *et al.*, XXXIX GEC-Madison 89
[2]Z. Rakem *et al.*, Revue Phys. Appl. 25 (1990)

R-4 Chaos in Electrical Discharges in Gases

D. F. HUDSON NAVSWC/WO - A selection of inert atomic, non reactive and electronegative molecular gases has been examined for evidence of chaotic behavior in dc discharges. Evidence in the form of discrete oscillations of the current ranging in frequency from 10's of kHz in Ne to 350 kHz in N_2 plus harmonics has been obtained. Thus far, chaos has only been seen in gases with electronic metastable states. The most important control parameter is the current, except in O_2, where temperature is also important. A minimal model consisting of a coupled set of nonlinear rate equations has been formulated. Results from the experiments, numerical solutions to the model and an attempt to correlate with existing data will be given.

R-5 Hybrid fluid-particle model of transient hollow cathode discharges: L.C. Pitchford and J.-P. Boeuf, CNRS, Centre de Physique Atomique, Toulouse, FRANCE - We have developed a hybrid fluid-particle model of pseudospark discharges in which we find that the large and localized source of ionization which results from a transient hollow cathode is responsible for the onset of the pseudospark discharge mode. The large increase in the electron multiplication in the hollow cathode is due to two effects. The first is that the electrons emitted from the inside surfaces of the hollow cathode are confined and thus the probability that an electron undergoes ionization in this region is enhanced. The second effect is the increase in multiplication due to the creation and subsequent acceleration of secondary electrons in the high field sheaths of the hollow cathode. We will show that the multiplication can reach a maximum of several hundred for conditions typical of pseudospark discharges when the high field sheaths cover a large fraction of the volume of the hollow cathode cavity.

R-6 Characterisation of a pulsed multicusp ion source. A.A. Mullan University of Ulster, Coleraine, N. Ireland, W.G. Graham Queen's Univesity, Belfast N. Ireland and M.B. Hopkins, Dublin City University, Dublin, Ireland - Recently the development of negative hydrogen ion sources has reached a stage where they can be deployed in the neutral beam heating systems of nuclear fusion devices. This requires plasma sources capable of operating with plasma densities of above 10^{12} cm^{-3}. We have used a digital Langmuir probe technique to characterize a typical multicusp ion source, operating in a pulsed mode to achieve discharge currents of 100A. Measurements of the plasma parameters, including the electron energy distribution function, in different regions of the source and at different times during the discharge current pulse and in the afterglow will be presented and used to access how negative ion production may be optimized in such sources. The plasma parameters are generally found to scale as predicted from previous measurements with discharge currents of less than 20A.

[1] M.B. Hopkins and W.G. Graham. Vacuum, 36, 873 (1986)

R-7 Cylindrical Magnetron Employing a Non-homogeneous Periodic Magnetic Field for Depositing Hermetic Coatings on Fluoride Glass Fibers, *Z. YU, G. J. COLLINS, CSU, B. HARIBSON and I. AGGARWAL, NRL-A multilayer hermetic seal has been sputter coated on fluoride glass fibers by a cylindrical magnetron. The magnetron uses a non-homogeneous periodic magnetic field, 40 cm in length along with a coaxially positioned anode. A series of donut shaped permanent magnets are placed outside of the target tube with alternative magnetization between the adjacent magnets. This combination of a baseline B field with a superimposed periodic non-homogeneous magnetic field component acts to segment the plasma into a series of annular rings, thereby stabilizing glow to arc transitions and better confining the discharge plasma on the target surface away from the center of the discharge column. This configuration reduces undesired heating or charge particle bombardment of glass fibers being coated. Deposition rates of 1 μ/min are obtained for pure Aℓ. The stress of Aℓ/Aℓ_2O_3 multilayer coatings on fluoride glass have also been studied.

*Work supported by Naval Research Laboratory, Contract #N00014-89-C-2470.

R-8 Generation of Electron Beams by a Helicon Antenna, R.W. BOSWELL and PEIYUAN ZHU, Aust.Nat.Univ. – During the first millisecond of an argon discharge excited by a Helicon antenna strong electron beams with energy ~ five times the thermal energy have been observed. The beams are restricted to the central 1 cm of the 5 cm diameter discharge and appear when a threshold power of 2 KW at 7 MHz is surpassed. The energy of the beam increases and the density decreases with time; 1 msec into the discharge, the electron distribution becomes thermal at ~ 5 eV. Spectroscopic measurement of AII lines and microwave interferometry density measurements are consistent with the temporal evolution of the fast electrons. The beam intensity has a maximum when the applied magnetic field is near the lower hybrid frequency for the exciting rf. Although the behaviour is suggestive of a resonance phenomenon, the particular mechanism responsible for accelerating the electrons is not known.

R-9 Helical Resonator Plasma Source* M.A. LIEBERMAN, A.J. LICHTENBERG, D.L. FLAMM, and K. NIAZI, EECS Dept., U. of Calif, Berkeley -- A theory has been developed for a helical resonator plasma source consisting of a cylindrical plasma surrounded by a slow wave helical structure in a grounded coaxial cylinder. Such sources can be efficiently matched to an external power source and can operate at low gas pressures. A developed sheath helix model is employed, to obtain the dispersion characteristics, the electric and magnetic fields, and the scaling of the dispersion and fields with source parameters and geometry. A quasistatic approximation is used to obtain the fields in a cylindrical structure including plasma collisions. These results are then used to calculate the stochastic heating, which dominates at low pressures, and the ohmic heating, which dominates at high pressures. We determine the resulting plasma density, loaded resonator Q, and source coupling. The theory is compared to some preliminary experimental results.

*Work supported in part by DOE Grant DE-FG03-87ER13727

R-10 Measurement of the Density and Translational Temperature of Si($3p^2\ {}^1D_2$) Atoms in RF Silane Plasma Using UV Laser Absorption Spectroscopy, T. GOTO. M. SAKAKIBARA and M. HIRAMATSU, Department of Electronics, Nagoya Univerisity- We need quantitative measurements of various radicals in actual rf silane plasma to clarify formation mechanisms of amorphous silicon thin film. In this work, using uv absorption spectroscopy with the SHG (line width of 1MHz) of a ring dye laser excited by a cw argon ion laser as a light source, first we could measure the absorption profile of the 288.2 nm line transititing to the $3p^2\ {}^1D_2$ level in the rf (13.56 MHz) Ar/SiH_4 plasma. The rf chamber had plane parallel electrodes of 10 cm diameter and 3 cm separation, and the White type multireflection system for getting an absorption length enough. The Si($^1D_2$) atom density and Si translational temperature were obtained from the measured absorption intensity and line width of the 288.2 nm line, respectively, as a function of total pressure and SiH_4 concentration.

R-11 RF Discharge Modeling,* R. T. MCGRATH, Sandia National Laboratories -- A new collision algorithm applicable to electron interactions with the neutral gas of an RF driven plasma processing discharge has been developed. The algorithm greatly reduces the computational time required to evaluate the collision term in the Boltzmann equation, yet maintains the necessary multi-dimensional aspects of the velocity space distribution, f(z,v,t). The collision operator is simplified by assuming that the transverse portion of f(z,v,t) can be represented by a Maxwellian characterized by a local temperature, $T_\perp(z,t)$. Introduction of a polynomial expansion for $\sigma(v)v/(v^2 - 2E/m_e)^{1/2}$, where E = energy loss during an inelastic collision, allows for analytic evaluation of the transverse velocity space integrals which appear in the collision term. In the Boltzmann-Poisson solver, the particle motion algorithm need follow the evolution of only the one-dimensional distribution, $f(z,v_z,t)$, and one additional variable, $T_\perp(z,t)$. Reduced computational time compensates for any loss of accuracy associated with the assumed Maxwellian form for the transverse portion of the distribution. Overall accuracy of the model will be assessed by comparison with experimental measurements and comparison to models which calculate the full, multi-dimensional distribution function.

*This work performed at Sandia National Laboratories, supported by the U.S. Department of Energy under Contract Number DE-AC04-76DP00789.

R-12 Examination of Temporal Relaxations of Transport Parameters and Rate Coefficients,* P. HUI, E. KUNHARDT, Weber Research Institute, Polytechnic University, - Temporal relaxations of transport parameters and rate coefficients after a stepwise change of reduced electric field E/N have been examined using the concept of macro-kinetic distributions.[1] The Monte Carlo flux method[2] has been used to obtain macro-kinetic distributions with varying degrees of temporal resolution and to calculate the transport parameters and rate coefficients. It is observed that the relaxations of the drift velocity, the mean energy, and the rate coefficients are related. Moreover, the mean energy and all the rate coefficients have the same adjustment time. The effect of the temporal resolution of the distribution on calculation of the transient transport parameters and rate coefficients are discussed.

*Work supported by the National Science Foundation.

[1]E. E. Kunhardt, J. Wu and B. Penetrante, Phys. Rev. A37, 1654 (1988).

[2]G. Schaefer and P. Hui, J. Comput. Phys. (1990).

R-13 Electron Macrokinetics,* E. E. KUNHARDT, Weber Research Institute, Polytechnic University, - In earlier papers,[1,2] closed macroscopic descriptions of the dynamics of an assembly of electrons under the influence of space-time varying fields have been presented by assuming a functional ansatz for the dependence of the distribution function on the macroscopic variables. In this paper, the macroscopic description is accomplished by approximating the phase-space distribution function in an equivalent space whose coordinates are the infinite set of moments, $\{m_j; j=1,\cdots,\infty\}$. This approximation corresponds to projections in $\{m_j\}$ space, in contrast to projections in $\underset{\sim}{v}$-space in which a finite subset of a complete set of $\underset{\sim}{v}$-space functions are used to represent the distribution. Expressions for the approximate distribution function and transport parameters are obtained for a scale of resolution corresponding to the energy relaxation time.

*Work supported by ONR.

[1]E. E. Kunhardt, J. Wu, and B. Penetrante, Phys. Rev. A37, 1654 (1988).

[2]E. E. Kunhardt, Phys. Rev. A July (1990).

R-14 Modeling of Magnetic Multicusp Hydrogen Plasmas for Negative Ion Production: an Improvement, C. GORSE, R. CELIBERTO, M. CACCIATORE, M. BACAL+ and M. CAPITELLI, University of Bari and Centro Studio Chimica Plasmi (CNR) Italy and Ecole Polytechnique+ France- Different experimental situations for the volume production of negative ions in magnetic multicusp sources have been simulated. Our previous self-consistent model[1] has been improved by using both a new set of cross-sections for electronic excitation, dissociation and ionization of H_2 ground vibrational levels and a complete set of V-T (vibration-translation) rate coefficients for H_2-$H_2(v)$ and H-$H_2(v)$ processes. It is worth noting that the H-$H_2(v)$ relaxation involves hot H atoms (T=4000K) and cold H_2 molecules (T=500K). Both molecular vibrational distributions and electronic quantities (number density, mean energy, temperature) are reported, the effect of varying the gas pressure and the current intensity are discussed. Such a model will be extended to describe the D^- volume production.

[1]C. Gorse, M. Capitelli, M. Bacal, J. Bretagne and A. Laganà, Chem. Phys. 117 (1987) 177.

R-15 Influence of electron-electron collisions on electron distribution function in N2 discharges from Monte Carlo method. M. YOUSFI, A. ALKAA, O. LAMROUS, A. HIMOUDI, Univ. Paul Sabatier, CPAT, CNRS, Toulouse, FRANCE.- The effects of coulomb collisions are far to be negligible in the case of several kinds of gas discharges. Such effects have been already considered in the literature with the help of various two-term solutions of Boltzmann equation. However, in the case these methods, a stationary and unbounded system without in particular space gradients is generally assumed. This means that non-equilibrium effects due to the presence of walls, sources, etc... are not taken into account. Under these conditions, a lot of informations useful for discharge modeling are completely lost. Meanwhile, from Monte Carlo methods it is much easier than Boltzmann equation solutions to take into account non-equilibrium effects. However, to the author's knowledge, electron-electron collisions have not been yet considered in the literature in Monte Carlo treatments. Therefore, the aim of this communication is to treat the effect of electron-electron collisions from Monte Carlo calculations. The Monte Carlo method used is a classical null collision method. As it is well known, in the case of the Monte Carlo method, the initial electrons are treated one by one. During an electron-electron impact, the problem is to know a priori the angular and energy distribution of the electron targets.This distribution is assumed known during the first electron treatment, and during the i^{th} electron treatment, the chosen electron target distribution corresponds to the distribution of the $(i-1)^{th}$ electron. It is clear that when the number i of treated electrons increases, the electron target distribution becomes more and more closer than the final electron distribution. This means that our approximation of electron target distribution is improved little by little number i increases. Finally, the Monte Carlo equilibrium distribution functions are very well compared to distributions calculated from a classical two-term Boltzmann solution in the case of N_2 discharges under influence of relatively low uniform electric fields.

R-16 Deposition of Diamondlike Carbon Film Using Lisitano Coil Excited Electron Cyclotron Resonance Plasma.* S. C. KUO, A. R. SRIVATSA,** E. E. KUNHARDT, Weber Research Institute, Polytechnic University, - Hard diamondlike carbon films were deposited through Electron Cyclotron Resonance (ECR) microwave plasma decomposition of CH_4 gas. This ECR plasma was excited by a Lisitano coil. Ion species gained energy from a magnetic beach configuration in the plasma column and a negative DC bias on the substrate. High energy ion species played an important role on the growth of diamondlike carbon film. The deposited films were characterized by Raman spectroscopy, Fourier-Transform Infrared Spectroscopy (FTIR) and Near Edge X-ray Absorption Fine Structure (NEXAFS) analysis.

*Work supported by Grumman Aerospace Corporation.

**Moltech Corporation, Chemistry Dept., SUNY at Stony Brook, Stony Brook, NY 11794.

R-17 In Situ Particle Generation in Fluorocarbon Based Etching Discharges. P.J. Resnick, H. M. Anderson, Univ. of New Mexico, N.E. Brown, Sandia National Laboratories-- A High Yield Technologies (HYT) Particle Flux Monitor has been used to study **in situ** generation of particles during reactive ion etching of oxide on Si substrates using C_2F_6 and C_2F_6/CHF_3 feed gases. Installing the particle flux monitor sensor downstream in a pump line port below the etch chamber allowed counts to be made of particulate matter generated during the etch cycle. Particles in the 0.38 - 0.70 μm size range were observed often in bursts during the 2-3 min. single wafer etch cycle. Using OES endpoint detection, it is shown that a significant correlation exists between the detection of particles and the breakthrough of the oxide layer. Generally, a lag time on the order of 10-20 sec. existed between oxide breakthrough and the detection of particles downstream. Other factors such as the particular etchant chemistry, electrode composition, and stability of the discharge were also observed to have a significant impact particle production, but these factors were independent of the oxide breakthrough effect. Based on these observations, the potential importance of plasma/surface interactions to **in situ** particle generation is discussed.

R-18 Plasma Etching of Ceramic Oxide Thin Films, M. R. POOR and C. B. FLEDDERMANN, Center for High Technology Materials, University of New Mexico- Plasma etching of ceramic thin films, specifically ferroelectric and high-T_c superconducting thin films, has been studied. A dc hollow cathode reactor using HCl and CF_4 as the process gases was used to etch Cr masked PLZT and Y-Ba-Cu-Oxide thin films. The etch rates and stoichiometry variations were found to be highly dependent upon the substrate temperature, reactor pressure, gas mixture, and film preparation techniques. For both materials, elevated substrate temperatures were required for etching. The minimum temperature required to etch PLZT films is 200°C. Solution-deposited PLZT films etched at approximately 1500 Å/min at 275°C and 200 mTorr, while the etch rate for sputter-deposited films was about 2000 Å/hr under the same conditions. The minimum temperature required for etching the superconducting films was 300°C. The etch rate for unannealed films at 500°C and 200 mTorr was 1 μm/min. This was more than an order of magnitude faster than the etch rate of for annealed films under the same conditions. Four-point probe measurements were used to determine the critical temperature of the superconducting films and capacitance-voltage measurements were performed on the ferroelectric films prior to and after etching to indicate degradation which occurred due to the etching process. For all films, the anisotropy of the etch was determined using a scanning electron microscope (SEM).

R-19 Etching of GaAs in a Helicon Reactor, R.W. BOSWELL, M.A. JARNYK, J.S. WILLIAMS Aust.Nat.Univ. and M.W. AUSTIN, RMIT – High etch rates of *GaAs* have been measured in an inductively coupled radio frequency diffusion plasma confined by a weak magnetic field. Etch rates have been measured as a function of the three operating parameters: $SiCl_4$ pressure, source power and the rf-bias voltage. A peak etch rate of 3.2 μm min^{-1} was measured at 9.3 mTorr, with a source power of 500 W and an rf-bias of 80 volts. Etch profiles were highly anisotropic except at high rf-bias voltages where sputtering of the photoresist mask led to sloped profiles.

R-20 The Causes of SiH_4 Dissociation in Silane DC Discharges,* D.A. DOUGHTY** and A. GALLAGHER, JILA, U. of Colorado and NIST - Film growth on glass fibers strung between discharge electrodes is used to measure the distribution of a-Si:H film-producing radicals in a silane dc discharge. The measured distribution, as well as film deposition rates on the electrodes, show that typically >80% of the depositing radicals are produced in the cathode sheath. The spatial distribution of optical emission from the discharge rules out the possibility that this dissociation in the sheath is due to electron-impact. Collisions of energetic ions and neutrals with silane are clearly implicated as the cause of this sheath dissociation. In contrast almost all dissociation is due to electron collisions in the low-power rf discharges most commonly used for film production. In addition, the ratio of the number of Si atoms deposited on the surfaces to the total number of ions collected at the cathode is measured to be 30, which demonstrates the dominance of neutral radical deposition in these discharges.

* Work supported by the Solar Energy Research Institute

** Present Address: General Electric Co., PO Box 8, Bldg. K1-4C28, Schenectady, NY 12301

R-21 Monte Carlo calculations of distribution functions and swarm parameters of H^+ ions in Helium discharges. A. HIMOUDI, M. YOUSFI, Univ. Paul Sabatier, CPAT, CNRS Toulouse, FRANCE.- The motion of H^+ ions in He background gas under uniform electric field influence has been studied, from a Monte Carlo simulation method, in order to show the presence of non-equilibrium phenomena already observed, for example, in the case of electron motion in He. The effects of background gas temperature on ion distribution functions and swarm parameters (ion mean energy, drift velocity,...) have been also analyzed. The Monte Carlo procedure is based on the classical null collision method in which energy exchange and thermal motion of background gas during elastic collisions are properly taken into account. The momentum transfer cross section used are taken from Lin et al[1] and scattering is assumed isotropic. Calculations have been done with (T_{gas}=300K) and without (Tgas=0K) considering gas temperature. Following results are obtained for reduced electric field E/N varying between around 5Td to 40Td and for 0.2 Torr gas pressure:
- the time evolution of ion mean energy and drift velocity shows a well prononciated transient phase before to reach an equilibrium phase which is stable because, under the relatively low E/N values considered, there are not yet runaway phenomena .
- the space variation (along electric field axis) of ion mean energy and drift velocity shows two non-equilibrium regions due to the presence of the electrodes.Calculations are done for a few cm (1 to 10cm) gap distance between two plane parallel electrodes.
- the equilibrium energy distribution function of H^+ ions is not maxwellian, more particularly the distribution tail (i.e. for ion kinetic energy $\varepsilon > 0.2$eV).
- the influence of He temperature on ion distribution function and swarm parameters is far to be negligible, more particularly at lower E/N values.

[1]Lin SL, Gatland IR, Mason EA, 1979, J. Phys.B:At. Mol. Phys. 12, 4179-88

R-22 Diffusion in an Electronegative Plasma with a Longitudinal Magnetic Field, D.E. BELL and WM. F. BAILEY, Air Force Institute of Technology, WPAFB OH.-- A one dimensional, quasi-neutral theory of an electronegative discharge in a longitudinal magnetic field is developed. The resulting continuity and momentum transfer equations are solved numerically using a relaxation technique. The two eigenvalues of the on-axis ratio of negative ions to electrons and the normalized ionization rate are calculated, the resulting density and flux profiles are also obtained. The implications of the presence of a magnetic field on the wall boundary conditions for the negative ion flux and density are explored. At a pressure of 1 Torr, with B-fields ranging from 0-1000 Gauss, density profiles are essentially unaltered; however, the normalized ionization rate is reduced by 0-20% in comparison to the electropositive case.

R-23 Swarm Parameters in Gases and Plasmas, S. TAKEDA, Chubu University

In spite of the different energy distribution of electrons, which determine the swarm parameters in gases and plasmas, both parameters are frequently thought to be same. Since such confusion is seen sometimes in recent publications, the problem is here discussed.

Even though the distribution in plasmas somewhat deviates from a strict Maxwellian one, the electron temperature can be defined as an equivalent value. As several exsamples are shown the collision frequency, the drift velocity and the ionization frequency in plasmas. These values shown as a function of the electron temperature are somewhat different from that in gases based on the cross-section data.

R-24 Approach to Drift Equilibrium in a Steady, Uniform Electric Field. JOHN INGOLD, GE Lighting, Cleveland, OH 44112—Five-moment equations for conservation of electron density, average momentum, and average energy are solved numerically to give the motion of electrons subjected to a steady, uniform electric field, similar to conditions found in drift tube measurements of electron drift velocity and characteristic energy. The solutions predict a region near each electrode where electrons are not in equilibrium with the electric field. The length of the equilibration region is predicted to be the same for both drift velocity and average energy; it varies linearly with electric field and inversely as the square of the gas pressure. Based on comparison of results predicted by five-moment theory with those predicted by density gradient expansion theory, it is concluded that the latter method is unsuitable for dealing with problems of the sort described in this paper because proper convergence can not be established.

R-25 Transport Coefficients of SF_5^- and SF_6^- in SF_6, *J.DE URQUIJO, I.ALVAREZ, H.MARTINEZ and C. CISNEROS, Instituto de Física, UNAM, México- The mobility and longitudinal diffusion coefficients of SF_5^- and SF_6^- in SF_6 have been measured using a drift tube-mass spectrometer over a wide E/N range from 17.5 to 440×10^{-21} V m^2. The mobilities compare well with those of Patterson[1] up to $E/N = 70 \times 10^{-21}$ V m^2, thereafter his data being systematically higher by about 4% up to $E/N = 140 \times 10^{-21}$ V m^2. Above this value, we are not aware of any published mass-analyzed mobility or longitudinal diffusion data for comparison. However, a comparison with other data from experiments without mass analysis is presented. Both mobility curves show clear maxima around 300×10^{-21} V m^2, which are 4-9% lower than those calculated by Brand and Jungblut[2].

*Work supported in part by DGAPA, Project No. IN-014889 and by CONACyT.

[1] P.L. Patterson, J.Chem.Phys. 53 696 (1970)

[2] K.P. Brand and H. Jungblut, J. Chem. Phys. 78 1999 (1983)

R-26 Transport Parameters for Electrons in Carbon Dioxide W.ROZNERSKI, J.MECHLIŃSKA-DREWKO and K.LEJA. Dept.Phys. and Math., Technical University of Gdańsk, Gdańsk, Poland - By means of Townsend-Huxley technique the characteristic energy /D/μ/, the ratio of longitudinal diffusion coefficient to mobility /D_L/μ/ and the attachment coefficient /η/N/ in CO_2 have been measured for $40 \leq E/N \leq 2000$ Td at ambient temperature. The present D_L/μ results agree well with those by Saelee et.al.[1] as our η/N data are in good agreement with the results of Alger and Rees[2], and Risbud and Naidu[3] although are slightly lower than those of latter work. As to the D/μ coefficient the agreement between our results and the data of other investigators is, generally, worse.

Work supported in part under project CPBP 01.06.

1 H.T.Saelee, J.Lucas and J.W.Limbeek, IEE J.Solid State Electron Devices 1,111 /1977/.
2 S.R.Alger and J.A.Rees, J.Phys.D 9,2359 /1976/.
3 A.V.Risbud and M.S.Naidu, Indian J.Pure Appl.Phys. 16,32 /1978/.

R-27 Multidimensional Imaging of Species in Plasma-Etching Discharges*, P. J. HARGIS, JR. and K. E. GREENBERG, Sandia National Laboratories -- Laser-induced fluorescence (LIF) and discharge optical emission can be imaged onto diode or CCD arrays to obtain spatially resolved profiles of plasma species. In the simplest configuration, two-dimensional, time-averaged emission profiles can be obtained by imaging the optical emission onto a CCD camera through a narrowband optical filter. The camera can also be gated to obtain time-resolved emission profiles during a 13.56-MHz rf cycle. Representative emission profiles, obtained using a Hamamatsu CCD camera system, will be shown for an argon discharge in the GEC reference cell. Spatially-resolved (1-dimensional) optical emission spectra can be obtained using the CCD camera in conjunction with a spectrometer. The camera can also be used in the gated mode to determine spatial profiles of plasma species using laser-induced fluorescence spectroscopy. LIF from a static fill of a gas that fluoresces strongly in the absence of a discharge is used to correct the measured spatial profiles for nonuniformities in the laser beam and optical detection system.

*This work performed at Sandia National Laboratories, supported by the U. S. Department of Energy under Contract Number DE-AC04-76DP00789.

R-28 Diagnostics of Chlorine Densities in Glow Discharges with Low or High Frequency Excitation,* M.RÖMHELD and R.J. SEEBÖCK, Siemens Research Laboratories, Erlangen, F.R. Germany- Low pressure chlorine plasmas have been studied in a parallel plate etching reactor with low (≈60 kHz) or high (13.56 MHz) frequency excitation. We have used mainly plasma emission and laser induced fluorescence spectroscopy (LIF) to obtain information on the pressure and power dependence of relative particle densities in the bulk of the plasma. For increasing power the densities of the Cl_2^+ ions and electronically excited Cl_2^* molecules increase, too. When plotted against pressure, the densities of $Cl_2^+(X)$ and Cl_2^* show a maximum which lies in the range between 10 and 30 Pa. Using two-photon LIF, we have measured a linear increase of the atomic Cl density between 5 and 50 Pa. For Cl, we have also compared optical emission actinometry with LIF.

*Work supported by BMFT under NT 2702B2

R-29 **LIF Characterization of a dc Multidipole Discharge,** M.J. GOECKNER, J. GOREE, and T.E. SHERIDAN, Dept. of Physics, Univ. of Iowa, -- Using sub-Doppler laser-induced fluorescence (LIF) and Langmuir probe measurements, we have characterized a multidipole filament discharge. LIF measurements in the center of the discharge, using the $(^1D)3d\ ^2G_{9/2} \rightarrow (^1D)4p\ ^2F_{7/2}$ argon ion transition, reveal that the ions are at room temperature over a wide range of pressures, discharge currents and discharge voltages. By scanning the discharge current, we found that the metastable ion density n_i^* scales linearly with n_e. The discharge parameters were: $20 \leq P_{Ar} \leq 150$ Pa, $0.12 \leq I_{dis} \leq 6$ A, $20 \leq V_{dis} \leq 80$ V. Langmuir probe measurements at the center of the discharge indicate that $0.5 \leq V_p \leq 3$ V, $1 \leq T_e \leq 1.5$ eV, and $0.4 \leq n_e \leq 6 \times 10^9$ cm^{-3} over these parameter ranges.

R-30 Plasma Characterization of a Downstream Microwave Source, D.L. SMATLAK and C.C. PAO, MIT Plasma Fusion Center - Oxygen plasmas from downstream microwave plasma sources are finding increasingly wide use in the dry stripping of photoresist. However, little is known about the plasma parameters produced by these sources. We have characterized the plasma density and electron temperature as a function of microwave power, gas pressure and position for a commercially available 2.45 GHz source. For argon discharges, the electron temperature ranged from 4 eV at 60 mTorr and 200 W to 0.6 eV at 1.6 Torr and 200 W. The electron density ranged from 4×10^{10} cm^{-3} for a 60 mTorr, 900 W discharge to 2×10^7 cm^{-3} for a 1.6 Torr, 200 W discharge.

R-31 Thickness of the Ion Sheath Around a Cylindrical Electrode Immersed in a Plasma, M. NACHMAN and J. MONTREUIL, Ecole Polytechnique of Montreal - Results of a theoretical and experimental study are presented concerning the size of the ion sheath around a floating or negatively biased cylindrical electrode in a low-pressure plasma. A numerical analysis is carried out on the radial dependence of the change Δn_e in the electron density n_e within the sheath, induced by a small variation in the electrode bias V. It is found that the plots of Δn_e vs radial distance x from the electrode surface exhibit a pronounced peak in the region where n_e presents a steep increase with x. It is proposed to define the sheath edge as the surface where this maximum of Δn_e occurs. The existence of the maximum is confirmed experimentally by exploring the sheath with a point-like cold probe, and a linear dependence of the sheath thickness on $|V|^{1/2}$ is found over a wide range of electrode biases, plasma densities and gas pressures.

R-32 Ion Kinetics in Low Pressure RF Modulated Sheaths, MICHAEL S. BARNES, JOHN C. FORSTER, and JOHN H. KELLER, IBM E. Fishkill, B/300, Z/48A, Hopewell Junction, NY, 12533-0999--Ion kinetics in low pressure (e.g., 1 mTorr) electropositive rf glow discharge sheaths are studied using a Monte Carlo based computer simulation. The numerical model integrates particle trajectories using a spatially-nonlinear time-varying model of the electric field in the rf sheath (1). A scaling relationship will be discussed, relating a normalized ion energy spread to a scaled parameter R, which is the ratio of an analytically determined ion transit time to the rf period. The scaled numerical data shows good agreement with existing numerical and experimental data. Four regimes of ion transport through an rf modulated sheath will be identified.

(1) M. A. Lieberman, IEEE Trans. Plasma Sci., 16 (6), 638 (1988).

SESSION S

7:00 PM - 9:00 PM, Thursday, October 18

Convention Center, Chancellor Hotel - Illiniwek and Grange Rooms

CROSS SECTION WORKSHOP

Chair: K. H. Becker, CCNY

S-1 MCHF Atomic Structure Calculations,* C. FROESE FISCHER, Vanderbilt University -- An atomic structure package, called MCHF-ASP[1], has been developed for determining non-relativistic wave functions for bound states, based on the multiconfiguration Hartree-Fock approximation. From these wave functions a number of properties can be determined. This approximation is suitable for cases where correlation is the most important Hartree-Fock correction and relativistic effects can be included in the LSJ Breit-Pauli approximation. Some transition probability calculations will be described.

*Work supported by the U.S. Department of Energy, Office of Basic Energy Sciences

[1]C. Froese Fischer, A. Hibbert, M. Godefroid, et al, (submitted to Comput. Phys. Commun.) (1990).

S-2 Electron Excitation of Excited Target Atoms, CHUN C. LIN, U. of Wisconsin--In recent years experiments on electron-impact excitation of excited target atoms have been reported by several groups. Although cross sections for electron excitation out of excited levels in many cases are of great importance for modeling discharge systems, measurements of such cross sections so far have been limited to only a few atoms because of the experimental difficulties. Aside from the application to gaseous discharge, experiments on excitation of excited target atoms reveal important features of the basic physics of electron excitation processes. For instance the behaviors of the cross sections for exciting He atoms out of the 2^3S metastable level are quite different from those for exciting ground-level He atoms.

S-3 Studies of Electron-Molecule Collisions on Highly Parallel Computers* C. WINSTEAD, Q. SUN, P. G. HIPES, and V. McKOY, Caltech, M. A. P. LIMA, Unicamp—We will report on the results of applications of the Schwinger Multichannel (SMC) method to obtain low-energy electron scattering cross sections for polyatomic gases including SiH_4, Si_2H_6, SiF_4, GeH_4, PH_3, C_3H_8, C_4H_{10}, and $C_2F_2H_2$. We report cross sections for elastic scattering, momentum transfer, and, for some molecules, vibrational excitation. These studies made use of a recently developed parallel implementation of our computer codes on a highly parallel machine of the multiple-instruction, mulitple-data stream (MIMD) type. Our experience indicates that such machines are well suited for carrying out the computationally intensive step of these calculations.

* Work supported by grants from the National Science Foundation and the Innovative Science and Technology Program of SDIO through the Army Research Office.

S-4 Electron-Impact Dissociation of Molecules.* P. C. COSBY, SRI International--At electron energies above a few eV, dissociative excitation of molecules becomes an important process that can substantially change the chemical composition in a plasma. Since the products are generally ground state atoms or molecules that are difficult to detect, quantative measurements of electron impact dissociation cross sections have been few in number. We have developed a relatively general technique for measureing these cross sections at SRI, wherein a fast (keV) molecular beam is intersected by an electron beam. The high velocity of the parent molecule produces high velocity dissociation products that are constrained to a narrow cone in the laboratory frame and can be uniformly detected by secondary emission, independent of internal energy state. Dissociation cross sections have been measured for such molecules as O_2, N_2, CO, CO_2, etc. together with product state distributions. Selected cross sections will be presented and compared with other measurments to illustrate the advantages and disadvantages of this technique.

* Research supported by USAF Wright Research and Development Center, Wright-Patterson AFB, OH under Contract F33615-85-C-2560

S-5 Future Opportunities for Research. Ronald A. Phaneuf, ORNL*--Cross sections for electron-molecule reactions are important in the modelling of nearly all low-temperature plasma environments. For example, in magnetically confined fusion reactors, the cooler edge plasma near the vacuum vessel is now recognized to play a critical role in insulating the hot central plasma core from the container walls, which are lined with a low-Z material such as graphite. Cross sections for reactions involving hydrocarbon molecules and molecular ions are needed to properly characterize the behavior of this edge plasma. A brief overview will be presented of these and some other practical needs for cross-section data for modelling of low-temperature plasmas.

*Operated by Martin Marietta Energy Systems, Inc. under contract No. DE-AC05-84OR21400 with the U.S. Department of Energy.

SESSION TA

8:00 AM - 9:40 AM, Friday, October 19

Convention Center, Chancellor Hotel - Illiniwek Room

SHEATHS, GLOWS AND CHEMISTRY

Chair: K. Greenberg, Sandia National Laboratory

TA-1 The Bohm Criterion and Sheath Formation, K.-U. RIEMANN, Institut für Theoretische Pysik, Ruhr-Universität Bochum, D 4630 Bochum 1, West-Germany. In the limit of a small Debye length ($\lambda_D \to 0$) the analysis of the plasma boundary layer leads to a two scale problem of a collision free sheath and of a quasineutral presheath. Bohm's criterion expresses a necessary condition for the formation of a stationary sheath in front of a negative absorbing wall. The basic features of the plasma-sheath transition and their relation to the Bohm criterion are discussed and illustrated from a simple cold-ion fluid model. A rigorous kinetic analysis of the vicinity of the sheath edge allows to generalize Bohm's criterion acounting not only for arbitrary ion- and electron distributions, but also for general boundary conditions at the wall. It is shown that the generalized sheath condition is (apart from special exceptions) fulfilled marginally and related to a sheath edge field singularity. Due to this singularity a smooth matching of the presheath and sheath solutions requires an additional transition layer. Previous investigation concerning special problems of the plasma-sheath transition (including magnetic field effects) are reviewed in the light of the general relations.

TA-2 Studies of Temperature Profiles of N_2 in a Low-Pressure, DC Glow Discharge Using High Resolution CARS. P. P. YANEY, J. Cirillo,* and M. Millard, U. of Dayton**; -- Raman spectra of the nitrogen Q-branch were recorded using scanning, folded-BOXCARS with a of 0.08 cm^{-1} resolution at axial and radial positions. The spatial resolution element was about 50 m dia. by 1 mm long. A normal-glow, parallel plate discharge was set up between molybdenum electrodes spaced 14 mm with a current of 30 mA and at a pressure of 30 Torr. The nearly wall-less discharge was constrained by an insulating electrode cap machined from Micro y with a 9-mm hole and mounted on the cathode. A nitrogen flow rate of 80 SCCM was maintained. Theoretical spectra were fit to experimental data by fitting separate rotational and vibrational temperatures. The results show equal rotational temperatures within experimental error and large ranges of vibrational temperatures in the axial profiles.

* In partial fulfillment of the requirements for the M.S. degree in Electro-Optics.

** Supported by USAF Contract F33615-81-C-2012.

TA-3 Excitation of Balmer Alpha in H_2 - Ar Mixtures at Low Voltages and High E/n,* B.M. JELENKOVIĆ,** Z.Lj. PETROVIĆ,** AND A.V. PHELPS, JILA, University of Colorado and NIST. - The addition of 10% Ar to low current H_2 discharges operating at 190 V and 0.15 Torr (E/n = 1 kTd) produces a 600% increase in Hα emission near the cathode. Replacement of H_2 with 50 to 90% Ar produces factors of 30 to 50 increases in Hα emission near the cathode without similar large increases in current multiplication. In order to determine the dominant excitation processes, Hα emission was measured for H_2 and for H_2-Ar mixtures for E/n from 300 to 3000 Td at pressures from 1.3 to 0.1 Torr. Using published ion-molecule cross sections[1] and the large H-Ar excitation cross section,[2] the calculated excitation is much too small. We suggest that rates of processes such as $H_3^+ + H_2 \rightarrow H^+ + 2H_2$ are underestimated.

* Work supported in part by NSF and US-Jugoslavia Joint Board Project 924 (NIST).

** Permanent address: Institute of Physics, Belgrade.

1. A.V. Phelps, J. Phys. Chem. Ref. Data 19, 653 (1990).
2. B. Van Zyl, H. Neumann, H.L. Rothwell, and R.C. Amme, Phys. Rev. A 21, 716 (1980).

TA-4 Energy Balance of Cold Negative Glow Electrons. J. E. LAWLER, T. J. SOMMERER, and W. N. G. HITCHON, Univ. of Wisconsin, Madison, WI--Recently laser techniques have been used to study the negative glow of dc He glow discharges. Collisional effects from a high density of cold electrons were observed. By combining information from the observed suppression of singlet metastables due to superelastic spin exchange electron collisions, and information from transfer between low Rydberg levels due to inelastic electron collisions, a density (5×10^{11} cm^{-3}) and a temperature ($k_B T_e$=0.12 eV) was determined. Heating from from superelastic collisions on metastable atoms is a minor term in the energy balance of the cold electrons. Self-consistent kinetic calculations based on the Convective Scheme indicate that a field reversal, and thus a potential energy well for cold electrons, develops in the negative glow. The temperature of the cold trapped electrons is determined by a balance between cooling due to elastic collisions with neutrals and heating due to Coulomb collisions with energetic "beam" electrons injected into the negative glow from the cathode fall.

TA-5 Removal of Sulfur Dioxide from Gas Streams Using Dielectric Barrier Discharge, M.B. CHANG, J. BALBACH, M.J. KUSHNER, and M.J. ROOD, UNIVERSITY of ILLINOIS at CHAMPAIGN-URBANA-The concept of using a dielectric barrier discharge to remove $SO_{2(g)}$ from gas streams has been tested experimentally in a laboratory-scale reactor. This gas phase reaction process has the potential to simultaneously remove acid rain precursors from gas streams at lower cost than existing devices. This coaxial reactor is made of a cylindrical quartz tube and electrodes consisting of stainless steel wire mesh and tungsten rod. The air stream contained 2% by volume $H_2O_{(g)}$ and an initial $SO_{2(g)}$ concentration of 1000 ppmv at approximately 25°C. This gas stream was exposed to energetic electrons produced by dielectric barrier discharge. Experimental results show that the $SO_{2(g)}$ removal efficiency increased with increasing voltage up to a removal efficiency of 71% at 25 kV. The gas residence time was 5 seconds. Further experimental tests are planned to evaluate the ability of the system to simultaneously remove $SO_{2(g)}$ and $NO_{(g)}$ from gas streams.

TA-6 Processing Flue Gases to Remove SO_2 and NO_x Using 60 Hz Plasma Excitation and Photolysis.* Jeanne H. Balbach, Moo Been Chang, Mark J. Rood and Mark J. Kushner. University of Illinois, 607 E. Healey, Champaign, IL 61820. Combined Plasma Photolysis (CPP) is a process which removes SO_2 and NO_x from flue gases ($Air/H_2O/CO_2/SO_2/NO_x$) using a pulsed discharge followed by irradiation with ultraviolet photons. This method has the potential of removing SO_2 and NO_x at lower capital and operating costs than current methods. The basis of CPP is the efficient production of hydroxyl radicals which react with SO_2 and NO_x to produce H_2SO_4 and HNO_3 droplets, respectively, which are easily removed with filters or electrostatic precipitators. We have modeled the electron kinetics, photo-physics, and plasma chemistry of CPP removal of SO_2 and NO_x, and validated the model by comparison with experimental data. We find that optimum removal efficiency is obtained with a series of short discharge pulses as obtained with a 60 Hz dielectric barrier discharge, as opposed to a single high energy pulse. SO_2 removal generally increases with increasing O_2 fraction due to the higher production of OH radicals.

*Work supported by Advanced Environmental Control Technology Research Center and the National Science Foundation (CBT88-03170).

SESSION TB

8:00 AM - 9:40 AM, Friday, October 19

Convention Center, Chancellor Hotel - Grange Room

NOVEL TECHNIQUES IN COLLISION PHYSICS

Chair: T. W. Shyn, University of Michigan

TB-1 Atomic Oxygen and Nitrogen Sources.* J. P. DOERING, Johns Hopkins U. -- The study of electronic collisions with unstable atoms such as H, O, N, and S requires simple, reliable continuous sources for these species. For most applications, pure beams are not required so flow-through discharge sources can be used. The useable flux from such sources can be greatly enhanced by placing the discharge as close as possible to the collision center (< 5 mm). In the sources we have developed, an extended 3.5 wavelength microwave cavity allows tuning the source from outside the vacuum system and fulfils the requirement of having the actual discharge close to the collision center. The products of the discharge expand in a jet which is crossed by the electron beam just outside the discharge tube orifice. Operating parameters of such sources will be discussed as will alternate designs.

*Work supported by NSF Grant ATM-8915375.

TB-2 Fast Oxygen Atom Studies, G.E. CALEDONIA, B.L. UPSCHULTE, R.H. KRECH, and K.W. HOLTZCLAW, Physical Sciences Inc. - We have used the technique of laser-induced gas breakdown to develop a high flux pulsed source of fast oxygen atoms (v=5-12 km/s). The technique has also been used to produce high velocity beams of hydrogen atoms and mixtures of N/N_2, and can be extended to produce beams of other atomic species. The fast oxygen atom source has proven extremely versatile and has been used to study a variety of gas-surface and gas-gas collision phenomena. The present paper will review results from several of the investigations including fast oxygen atom surface studies involving material etching, surface glows, and energy accommodation as well as high velocity oxygen atom-target gas interactions which result in ultraviolet/infrared emissions.

TB-3 **Laser Induced Fluorescence Detection of Ground-State Molecular Fragments Following Electron-Impact Dissociation of Cooled Targets.*** M. DARRACH and J.W. McCONKEY, University of Windsor, Canada.--As part of a program to measure electron-impact cross sections for dissociation of molecules into ground state fragments we have developed a pulsed crossed-beams apparatus consisting of electron, supersonically-cooled gas and laser beams. Using this we have investigated the production of ground state CN fragments following the break-up of CH_3CN. We find that the CN fragments are rotationally cool and that the cross section for their production reaches a maximum at an incident electron energy of 70 eV. The shape of the excitation function is indicative of the original dissociation process being optically allowed. Additional data on this and other molecules will be presented at the Conference.

* Research supported by the Natural Sciences and Engineering Research Council of Canada.

TB-4 The Use of Electron Cyclotron Resonance Ion Sources for Multicharged Ion Collision Studies, F. W. MEYER, ORNL*--The availability of high charge state, high intensity beams from ECR multicharged ion sources has opened up many previously inaccessible areas of research focusing on the atomic collision physics of multicharged ions. Examples are crossed-beams and merged-beams experiments, which, due to very low inherent signal rates, become possible only if sufficiently intense ion beams are available. Other classes of experiments include high resolution optical or electron spectroscopy measurements, which have characteristically low detection efficiencies. Such classes of experiments are presently being carried out at Oak Ridge and other laboratories, where ECR sources have been built and are available for use in atomic physics studies. Specific applications to be discussed include crossed-beams and merged-beams measurements of electron impact ionization and excitation, respectively, of high charge state ions; merged-beams measurements of very low energy electron capture collisions involving multicharged ions, and high resolution measurements of electrons emitted during collisions of multicharged ions with neutral atoms and surfaces.

*Operated by Martin Marietta Energy Systems, Inc., for the U.S. Department of Energy under contract No. DE-AC05-84OR21400.

SESSION VA

10:00 AM - 12:00 Noon, Friday, October 19

Convention Center, Chancellor Hotel - Illiniwek Room

LASERS AND PHOTOPHYSICS

Chair: G. Hebner, Sandia National Laboratory

VA-1 Vacuum Ultraviolet Time-Resolved Laser-Induced Fluorescence for Radiative Lifetime Measurements. T. R. O'BRIAN and J. E. LAWLER, Univ. of Wisconsin, --Accurate (±5%) radiative lifetimes for atoms and ions are measured in the vacuum ultraviolet (VUV) using time-resolved laser-induced fluorescence on a slow atomic or ionic beam. A low pressure, large bore hollow cathode discharge beam source has produced atomic and/or ionic beams for more than 25 elements. Continuously tunable pulsed VUV laser radiation in the region 160-200 nm is generated by anti-Stokes Raman shifting in cooled H_2 gas of the 2nd harmonic of a Nd:YAG-pumped dye laser. The laser-induced fluorescence is detected with a fast PMT and transient digitizer, permitting lifetime measurements in the range 2ns to 2μs which are free from systematic error. Accurate level lifetimes, combined with precise branching ratios, provide the best determination of absolute atomic transition probabilities. Such data are needed for absolute density measurements in gaseous electronics and astrophysics. Results on SiI will be presented and future plans will be discussed.

VA-2 Measurement of Collisional Broadening of the Intercombination Resonant Transitions in Sr and Ca* J. CRANE, R. PRESTA, J. CHRISTENSEN, J. COOKE, and M. SHAW, Lawrence Livermore National Laboratory—We report measurements of collisional broadening of the $4^1S_0 \rightarrow 4^3P_1$ transition in Ca and the $5^1S_0 \rightarrow 5^3P_1$ transition in Sr by collisions with Ne and Ar as well as collisions with the ground state of Ca or Sr. Measurements were made in a one-meter-long heat pipe using two different laser diagnostics to independently measure linewidth and neutral density. We compare our results with a theoretical model for collisional broadening.

*Work performed under the auspices of the U. S. Department of Energy by the Lawrence Livermore National Laboratory under contract no. W-7405-Eng-48.

VA-3 Optical Gain in Hg at 5461Å via Recombination Pumping*, R.L. RHOADES and J.T. VERDEYEN, U of Illinois. We have observed evidence for gain on the 5461Å transition of mercury in the afterglow of a pulsed discharge using various buffer gases. Helium or neon was the majority buffer gas (p=10-80 Torr) with nitrogen or hydrogen added as a minority molecular gas (p=0.5-5 Torr). While the gain is small for the conditions of the present experiment ($\gamma_o l_g$=0.03), the system appears to be ideally suited for nuclear or e-beam pumping where the presence of a minority molecular gas does not affect the electron-ion pair production process to a significant degree. The upper state appears to be pumped by recombination [1] of electrons with Hg_2^+ with the gain tracking the decay of the spontaneous emission in the afterglow. It also appears that the majority of the Hg_2^+ is formed [2] by associative ionization.

[1] V.E. Jog and M.A. Biondi, J. Phys B, 14, 4719, (1981).

[2] S. Majetich, E.M. Boczar and J.R. Wiesenfeld, J. Appl. Phys., 66, 475, (1989).

* Work supported by Sandia National Laboratory.

VA-4 The Effect of CF_4 Impurities on Operation of the Electron-Beam Excited KrF Laser.* Roger Hui, Helen Hwang, Kris James and Mark J. Kushner, University of Illinois, 607 E. Healey, Champaign, IL 61820. The performance of electron beam excited KrF lasers (248 nm) is known to be sensitive to fluorocarbon impurities, especially CF_4. The observed degradation in laser performance with impurities may result from absorption by plasma generated fragments (CF_4 is virtually transparent at the laser wavelength), interception of the kinetics leading to the upper laser level by CF_4 and its fragments, or quenching of KrF(B) by CF_4. In this paper, we report on results from a computer model for the KrF laser in which we account for the presence of CF_4 and its plasma generated fragments. For typical pumping conditions ($Ar/Kr/F_2$ = 90/10/0.5, 150 kW-cm^{-3}), we find that CF_4 becomes an important impurity when its mole fraction is a few to 10% that of the F_2 density. At this level of impurity, optical absorption by CF_2 and interception of Kr^+ by neutralization with CF_3^- combine to lower laser efficiency by as much as 30%.

*Work supported by Los Alamos National Laboratory.

VA-5 Photoassociation of Krypton–Fluorine Collision Pairs.* R. B. JONES, J. S. SCHLOSS, J. G. EDEN, University of Illinois, Urbana–Champaign.—The KrF ion pair states have been formed by photoabsorption of Kr and atomic fluorine collision pairs. An excitation spectrum of the B (1/2)←X (1/2) transition from 207 nm to 250 nm has been obtained. The effect of the D (1/2) excited state and the influence of non thermalized collision pairs on the excitation spectrum will also be discussed.

*Work supported by the National Science Foundation

VA-6 Kinetics and Spectroscopy of $ArKr^+$ and Kr_2^+. R. B. JONES and J. G. EDEN, University of Illinois, Urbana–Champaign.— The $2(1/2)_g \leftarrow 1(1/2)_u$ transition in Kr_2^+ and the $4(1/2) \leftarrow 1(1/2)$ transition in $ArKr^+$ have been studied by the fluorescence suppression technique. Photoexcitation of the ground state diatomic ion of interest with a frequency doubled, pulsed dye laser is detected by the transient suppression of atomic Kr $5p \rightarrow 5s$ recombination fluorescence. The production of the ions is initiated by the multiphoton ionization of Kr with an ArF laser. Spectra and absolute cross sections have been measured. A detailed kinetics model has been used to assess the effects of population refeeding, 5p photoionization, and transitions from the Kr_2 5s $(1_u, 0_u^-)$ state on the results. Application to KrF laser modeling of these results will be discussed.

*Work supported by the Los Alamos National Laboratory and the National Science Foundation.

VA-7 **UV XeBr($^2\Sigma \rightarrow ^2\Sigma$) Pulsed Flashlamp and Breakdown Voltage Characteristics of Xe/Br_2 Mixtures**† P. B. KEATING‡, G. BLACK, and L. A. SCHLIE, Advanced Laser Technology Division (WL/ARDK), Kirtland AFB, NM 87117–6008. Xe/Br_2 mixtures are under investigation for potential use in high–intensity flashlamps for pumping the photolytic iodine laser. Currently, mercury lamps (both cw and pulsed) are used to photodissociate the C_3F_7I gas fuel to produce the lasing species $[I(5^2P_{1/2})]$. The absorption band peak of the C_3F_7I is at 270nm. Electrically discharged Xe/Br_2 produces ultraviolet emission peaked at 282nm from the $(^2\Sigma \rightarrow ^2\Sigma)$ band of XeBr which may be a more efficient alternative for pumping C_3F_7I. Voltage breakdown (V_b) characteristics, emission spectra, and transient behavior of the discharged Xe/Br_2 mixtures will be discussed. The V_b characteristics of the system were measured at room temperature in the pressure range of 10^{-2} to 10^2 torr. For a given total pressure beyond the breakdown minimum, the breakdown voltage increased with the Br_2/Xe ratio. Preliminary time–resolved emission spectra for various Br_2 concentrations in Xe will be shown and compared with the spectra of the mercury lamps. A preliminary assessment of the Xe/Br_2 system for use as a pump source for the photolytic iodine laser will follow.

† Funded by the Air Force Office of Scientific Research
‡ Dept. of Physics, UNM, Albuquerque, NM 87131.

VA-8 **Transverse Excitation of Large Volume Hydrogen Azide (HN_3) Gas Mixtures**†. M. W. WRIGHT‡, L. A. SCHLIE, and E. A. DUNKLE, Advanced Laser Technology Division (WL/ARDK) Kirtland AFB, NM 87117–6008.–Recent plasma and chemical kinetic studies of hydrogen azide gas mixtures have indicated their potential use as hybrid electro–chemical flashlamps or visible/UV laser systems. Initial results of a UV pre–ionized, transversely excited discharge (5 x 7 x 50 cm^3) in these HN_3 gas mixtures are presented. Gas mixtures of hydrogen azide and inert gases along with boron trichloride(BCl_3) have been tested. As in the breakdown discharge studies, strong NH(A – X) ultraviolet emission from the discharge initiated chain reaction in the HN_3 decomposition was observed. With the addition of BCl_3, the characteristic 270 nm BCl(A – X) intense bands were also evident. The attraction of this system lies in the possibility for lasing, with the HN_3 pumping the BCl, and the potential use as a photolytic pumping source for the atomic iodine laser due to the near coincidence of the 272 nm BCl band with the peak of the C_3F_7I absorption band. A kinetic model incorporating the various reaction mechanisms for the breakdown of the HN_3 and the effect of diluents will be discussed.

† Funded by the Air Force Office of Scientific Research.
‡ Dept. of Physics, UNM, Albuquerque, NM 87131.

SESSION VB

10:00 AM - 12:00 Noon, Friday, October 19

Convention Center, Chancellor Hotel - Grange Room

SIMULATIONS

Chair: J. Scheuer, University of Wisconsin

VB-1 Particle-In-Cell Combined with Monte Carlo Collisions-In Living Color C. K. BIRDSALL Univ of Calif. Berkeley - PIC codes have been in use for decades as have MCC codes. In PIC all of the charged particles are moved at the same time, Δt by Δt. In MCC each particle is moved with its own Δt, according to a collision probability, hence, incompatible with PIC. However, a marriage of PIC and MCC has been made for uniform Δt's by changing the interpretation of the collision probability, colliding only a few ions and electrons with neutrals each uniform Δt.[1,2] An interactive implementation of MCC-PIC in 1d3v on fast PC's has been made[3] and applied to a variety of low pressure collisional plasmas: RF discharges (planar, cylindrical, spherical, magnetized and not) implantation (PIII, PSII), particulate accumulation (floating probles of radius a $<\lambda_D$), ECR source. Some of these applications will be demonstrated, with a variety of physics diagnostics and direct measurements in t, x.

1. R. W. Boswell and I. J. Morey, Appl. Phys. Lett. 52 21 (1988).
2. M. Surendra, D. B. Graves, I. J. Morey, Appl. Phys. Lett. 56 1022 (1990).
3. I. J. Morey, V. Vahedi, J. Verboncoeur, Bull. Am. Phys. Soc. 34, 2028 (1989).

VB-2 Particle Simulations of RF Glow Discharges: Electron Power Deposition and Electron Energy Distribution Functions, M. SURENDRA and D.B. GRAVES, U.C. Berkeley - Self-consistent, kinetic level particle-in-cell/Monte Carlo simulations of RF glow discharges have revealed that the relative importance of electron power deposition due to sheath oscillation and ohmic heating in the bulk of the plasma depends on the magnitude of the applied voltage. At low voltages, a larger fraction of the electron power deposition occurs in the bulk of the plasma. When sheath oscillation heating dominates, electron conduction current in the body of the plasma can be carried predominately by electrons accelerated by the advancing sheath front. This appears to have implications for the electron energy distribution function in the body of the plasma. Simulation results are compared to the available experimental data for rf discharges in helium.

VB-3 PIC Modelling of Electropositive and Electronegative RIE Systems with Varying Area Ratios, R.W. BOSWELL, D.S. VENDER and H.B. SMITH, Aust.Nat.Univ. – In order to model low neutral pressure (< 100 mtorr) parallel plate plasma reactors, we have devised electrostatic particle in cell (PIC) codes to study the rf plasma and its interaction with the non periodic boundaries. The method uses a time stepping algorithm to obtain the electric fields and the particle motions self consistently. Time dependent phenomena such as breakdown and decay in pulsed plasmas, or the dynamics of the rf sheath are easily modelled.

Important results include the observation of a two temperature electron distribution, ions entering the sheath at the sound speed and energy distribution of ions arriving at the electrodes. Charge exchange collisions increase the plasma density and spread the ion energies at the electrodes. Variable area ratios are simulated using spherically symetric geometry. Self bias of the smaller electrode has been measured as a function of area ratio and blocking capacitor size. Electronegative plasmas have been simulated with electron densities between 1 to 10% of the positive ion density. Loss rates for the negative ions have been measured in a pulsed discharge.

VB-4 Modeling and Simulation of Magnetically Confined, Low Pressure Plasmas in Two Dimensions,* R. K. PORTEOUS and D.B. GRAVES, U.C. Berkeley - A model of a cylindrical, uniformly magnetized, ECR source plasma has been developed. The ions in an ECR reactor are weakly magnetized and their velocity distribution is strongly non-Maxwellian and anisotropic. They are modeled using a 2D3V particle-in-cell technique. The ions may have both elastic and charge exchange collisions with neutrals. Multiple time and length scales are used to efficiently handle the narrow boundary sheath layers. By contrast, electrons are strongly magnetized and cross-field diffusion is strongly inhibited. Electrons are modeled as an assembly of one dimensional (along the magnetic field) Maxwellian fluids. ECR heating power is assumed uniform along the axis but is non-uniform radially. Plasma density, potential, electron temperature and ion flux are presented for different radial power profiles and operating conditions. Ion flux to the walls is shown to be sensitive to the nature of the radial power profile chosen.

* Work supported in part by IBM T.J. Watson Research Center.

VB-5 Stability of Particulate-Contaminated Low Pressure Electric Discharges.* Michael J. McCaughey and Mark J. Kushner, University of Illinois, 607 E. Healey, Champaign, IL 61820. The stability glow discharges can be strongly affected by gas phase particulates which result from electrode sputtering or gas phase chemical reactions. If sufficiently large, these particles charge negatively and act as a Coulomb-like scatterers of electrons. This causes a shift of the electron energy distribution to lower energies, and a reduction in rate coefficients for high threshold processes. As these rates diverge at different locations in the plasma due to nonuniform contamination, instabilities such as arcing and streamers can develop. We will report on a theoretical study of the stability of dust contaminated glow discharges using a two dimensional plasma chemistry model. Transport coefficients for the dusty plasma were obtained from a hydrid Monte Carlo/Molecular Dynamics simulation previously developed.[1] Using these models, the effects of dust on the spatial variation of current density, a key factor in the formation of arcs and streamers, will be discussed. Tolerances on the density and distribution of dust will be presented.

[1]M. McCaughey and M. Kushner, *Appl. Phys. Lett.* 55, 951 (1989).

*Work supported by the National Science Foundation (CBT88-03170 and ECS88-15781).

VB-6 Simulation of Nanocrystal Particle Generation in Sputter Deposition Discharges.* Seung J. Choi, Robert S. Averback and Mark J. Kushner, University of Illinois, 607 E. Healey, Champaign, IL 61820. Moderate pressure (≈0.5-1.0 Torr) sputter deposition discharges are currently being used as a source to nucleate nanocrystalline gas phase particulates having sizes of 10's nm. We have developed a computer model for the production of such nanocrystals in dc discharges. The Monte Carlo method is employed to model the trajectories of energetic sputtered atoms in an Ar buffer gas. Collisions of energetic and thermalized sputtered atoms with other sputtered atoms constitute the first step in the nucleation. The transport of higher order clusters are simulated using continuum drift diffusion equations. In this paper, spatial profiles of clusters in sputter discharges will be presented and the criteria required for their growth discussed. In order to grow particles of the observed sizes, the residence time in the plasma must be longer than available for neutral particles. The electric potential in low pressure glow discharges, though, provides a trap for negatively charged particles. We have found that large clusters which are negatively charged can have the required residence time and, in fact, may be a requirement for growth.

*Work supported by the Army Research Office.

VB-7 The Influence of Non-Linear Volumetric Processes on the Diffusion of Charged Particles in an Electronegative Discharge. D.E. BELL and WM. F. BAILEY, Air Force Institute of Technology, WPAFB OH.-- A radial segregation of plasma constituents into positive ion-negative ion and electron-positive ion regions occurs in non-equilibrium electronegative plasmas. Because negative ions are trapped by the ambipolar field, their density is determined by volumetric processes, rather than diffusive transport. A discharge model is considered with both linear and non-linear volumetric processes: one-step and two-step ionization, collisional detachment by both electron and neutral particle impact, mutual neutralization of ions, and electron-positive ion recombination. The parametric behavior of the discharge with respect to these processes is presented. An off-axis peak in the ratio of negative ions to electrons results in some cases. Analytic expressions for the on-axis ratio of negative ions to electrons and the location of the regional boundary are obtained.

43rd Annual Gaseous Electronics Conference

OCTOBER 16 – 19, 1990

CHANCELLOR CONVENTION CENTER
CHAMPAIGN, ILLINOIS

Tuesday, October 16		Wednesday, October 17		Thursday, October 18		Friday, October 19	
AA. 0800–0940 Discharge Models — Illiniwek	AB. 0800–0930 Novel Sources — Grange	GA. 0800–0955 Plasma Chemistry — Illiniwek	GB. 0800–1000 Lamp-like Discharges — Grange	NA. 0800–0945 High Density Plasma Processing — Illiniwek	NB. 0800–0940 Excitation and Dissociation — Grange	TA. 0800–0940 Sheaths, Glows and Chemistry — Illiniwek	TB. 0800–0940 Novel Techniques for Collisions — Grange
Break 0940 – 1005		Break 1000 – 1020		Break 0945 –1005		Break 0940 – 1000	
BA. 1005–1150 RF and μwave Models — Illiniwek	BB. 1005–1155 Collision Physics — Grange	Welcome H. 1030 –1130 Allis Prize Lecture J. Business Meeting 1130 –1200		PA. 1005–1200 Processing and Diagnostics — Illiniwek	PB. 1005–1200 Electron and Heavy Particle Collisions — Grange	VA. 1000–1200 Lasers and Photophysics — Illiniwek	VB. 1000–1200 Simulations — Grange
Lunch 1200 – 1330						Adjourn	
CA. 1330–1535 Heavy Particle Collisions — Illiniwek	CB. 1130–1535 Plasma Surface Interactions — Grange	K. 1330–1530 Posters (Glows, Electron Collisions, Lamp Related Phenomena) — Zuppke-Brundage Room		QA. 1330–1530 Diagnostics — Illiniwek	QB. 1330–1515 Atomic Xe and Other Lasers — Grange		
D. 1535–1730 Posters (Lasers, Electron and Heavy Particle Collisions, DC and RF Glows) — Zuppke-Brundage Room		LA. 1530–1735 Alternative Configurations — Illiniwek	LB. 1530–1715 Lamps and High Pressure Discharges — Grange	R. 1530–1730 Posters (Discharges, Transport Calc. Plasma Chemistry, Transport of Ions and Electrons, Etching) — Zuppke-Brundage Room			
E. 1900–2100 Posters (Lamps, Atomic Properties, Laser Produced Plasmas and High Pressure Discharges)		Social Hour 1830 – 1930 Alumni Room		S. 1900 – 2100 Workshop on Cross Sections — Illiniwek–Grange			
F. 2000–2100 Workshop GEC Cell	Zuppke Brundage	Banquet 1930 –2130 — Midwest Ballroom					